



This work is licensed under a Creative Commons Attribution License (CC BY 4.0).

Monograph

[urn:lsid:zoobank.org:pub:6AD0082E-7349-48DE-AFCA-1EE0BFBB3887](https://zoobank.org/pub:6AD0082E-7349-48DE-AFCA-1EE0BFBB3887)

From a pair to a dozen: the piscivorous species of *Haplochromis* (Cichlidae) from the Lake Edward system

Nathan VRANKEN^{1,*}, Maarten VAN STEENBERGE², Annelies HEYLEN³,
Eva DECRU⁴ & Jos SNOEKS⁵

¹⁻⁵KU Leuven, Laboratory of Biodiversity and Evolutionary Genomics,
Department of Biology, Charles Deberiotstraat 32, 3000 Leuven, Belgium.

^{1,5}Royal Museum for Central Africa, Biology department, Section Vertebrates,
Leuvensesteenweg 13, 3080 Tervuren, Belgium.

²Royal Belgian Institute of Natural Sciences, Operational Directorate Taxonomy and Phylogeny,
Vautierstraat 29, 1000 Brussels, Belgium.

²Masaryk University, Department of Botany and Zoology, Kotlářská 2, 611 37 Brno, Czech Republic.

*Corresponding author: nathan.vranken@kuleuven.be

²Email: mvansteenberge@naturalsciences.be

³Email: annelies.heylen@hotmail.com

⁴Email: eva.decru.icht@gmail.com

⁵Email: jos.snoeks@africamuseum.be

¹[urn:lsid:zoobank.org:author:0F8A0E8B-8BE3-458F-8BB8-D5BA0B489A0D](https://zoobank.org/author:0F8A0E8B-8BE3-458F-8BB8-D5BA0B489A0D)

²[urn:lsid:zoobank.org:author:57C714E0-F233-4B3E-960E-17A7863FBF6F](https://zoobank.org/author:57C714E0-F233-4B3E-960E-17A7863FBF6F)

³[urn:lsid:zoobank.org:author:559336E6-F710-45F2-9116-775C59874D70](https://zoobank.org/author:559336E6-F710-45F2-9116-775C59874D70)

⁴[urn:lsid:zoobank.org:author:1AEB7EED-C939-4702-8590-B3FCA7076324](https://zoobank.org/author:1AEB7EED-C939-4702-8590-B3FCA7076324)

⁵[urn:lsid:zoobank.org:author:13A8AB26-FF46-437C-9806-D49E11C5E15D](https://zoobank.org/author:13A8AB26-FF46-437C-9806-D49E11C5E15D)

Abstract. Piscivory is a common trophic niche among cichlids of the East African Great Lakes, including Lakes Edward and George. From these two lakes, we examined the taxonomic diversity of cichlid species with a piscivorous morphology. Prior to this study, two piscivorous species were formally described, *Haplochromis squamipinnis* and *H. mentatus*. We redescribe both species and describe an additional ten new species of *Haplochromis* with a piscivorous morphology: *H. latifrons* sp. nov., *H. rex* sp. nov., *H. simba* sp. nov., *H. glaucus* sp. nov., *H. aquila* sp. nov., *H. kimondo* sp. nov., *H. falcatus* sp. nov., *H. curvidens* sp. nov., *H. pardus* sp. nov., and *H. quasimodo* sp. nov. All twelve species differ in dominant male colour pattern (unknown for *H. latifrons* sp. nov. and *H. curvidens* sp. nov.) and morphological traits. The species can be divided into two morphological groups: the macrodontic piscivores and the microdontic piscivores. This division potentially reflects an ecological differentiation in habitat use, hunting technique, prey species, and prey size. We conclude that some 12–20% of the species from the cichlid assemblage of Lake Edward have a piscivorous morphology.

Keywords. Adaptive radiation, haplochromines, *Harpagochromis*, *Prognathochromis*, new species.

Vranken N., Van Steeberge M., Heylen A., Decru E. & Snoeks J. 2022. From a pair to a dozen: the piscivorous species of *Haplochromis* (Cichlidae) from the Lake Edward system. *European Journal of Taxonomy* 815: 1–94. <https://doi.org/10.5852/ejt.2022.815.1749>

Introduction

The East African Lakes Albert, Edward, Kivu, and Victoria and associated water bodies are inhabited by an estimated 700 species of *Haplochromis* Hilgendorf, 1888 (Genner *et al.* 2007). Nearly all these species belong to the Lake Victoria region superclade (LVRS), an assemblage of cichlids that evolved rapidly over the last 100–200 ka, which constitutes a model of adaptive radiation in evolutionary biology (Verheyen *et al.* 2003; Genner *et al.* 2007; Meier *et al.* 2017; Salzburger 2018; McGee *et al.* 2020; Svardal *et al.* 2021). The LVRS displays a high degree of endemism: each lake harbours a unique species assemblage that exploits the ecological opportunities present in the lake. The species of the LVRS display a large diversity in trophic morphology and ecology and contain, a.o., molluscivores, algae scrapers, parasite eaters, paedophages, scale scrapers, and piscivores. While the LVRS is morphologically and ecologically very diverse, its genetic variation is extremely small due to its young age, so much so that established molecular markers fail to differentiate between species (Verheyen *et al.* 2003; Wagner *et al.* 2013; Salzburger 2018; McGee *et al.* 2020; Svardal *et al.* 2021).

In *Haplochromis*, piscivores s. str. (hereafter referred to as piscivores) are species that prey mostly on whole fishes of all post-buccal stages, hereby excluding paedophages and scale scrapers (Witte & van Oijen 1990). Lake Victoria harboured at least 100 species of piscivores before the collapse of its haplochromine cichlids during the 1980s (van Oijen *et al.* 1981; Witte & van Oijen 1990; Witte *et al.* 2013). Lakes Kivu and Albert each harbour only one piscivorous species of *Haplochromis* (Trewavas 1938; Snoeks 1994), and those from the Lake Edward system (i.e., the drainages of Lakes Edward and George) remained poorly known until now (Greenwood 1973). Hitherto, two piscivorous species from the Lake Edward system had been formally described, *H. squamipinnis* Regan, 1921 and *H. mentatus* Regan, 1925, both based on a single specimen from Lake Edward. During later expeditions, more specimens with a piscivorous morphology were collected from Lake Edward, all initially identified as *H. squamipinnis*, *H. mentatus* or *H. guiarti* (Pellegrin, 1904) (a Lake Victoria species) (Trewavas 1933; Poll 1939; Hulot 1956). Greenwood (1973) suspected at least three undescribed piscivorous species to be present in Lake Edward but did not provide further details. Greenwood (1973) did perform a taxonomic revision of all *Haplochromis* species from Lake George and identified all specimens with a piscivorous morphology as *H. squamipinnis*. He questioned the validity of *H. mentatus* and regarded it as a putative synonym of *H. squamipinnis*.

Species of *Haplochromis* with similar feeding habits often have, besides a similar feeding apparatus, also similar head and body shapes. Species of piscivores, however, display a large variation in body size and depth (Greenwood 1974; van Oijen 1982). Yet, they all share a piscivorous morphology, i.e., having a long head (mean > 36% SL) and a long lower jaw (mean > 45% HL) set with slender tooth bands that consist of unicuspid, conical, and acutely pointed teeth (Greenwood 1974; Witte & van Oijen 1990; van Oijen 1991). Both the high species richness and the large morphological variation of piscivores has been attributed to a large ecological differentiation in habitat use, hunting technique, prey species, and prey size (Fryer & Iles 1972; van Oijen 1982). This can be exemplified by the following three species from Lake Victoria: (1) *Haplochromis mento* Regan, 1922, a pelagic species with a shallow body and large oral teeth that presumably pursues and captures the fast swimming *Rastrineobola argentea* Pellegrin, 1904 by biting; (2) *Haplochromis macrognathus* Regan, 1922, a benthic species with a deeper body and small oral teeth that, by suction feeding, ambushes and captures unsuspecting small *Haplochromis* specimens (van Oijen 1982; Barel 1983); (3) *Haplochromis longirostris* (Hilgendorf, 1888), a pelagic species with a shallow body and small oral teeth that feeds on both fishes and insects (van Oijen 1982).

Greenwood (1979, 1980) placed all species of the LVRS into 22 genera. In this classification, most piscivorous species were classified in ‘*Harpagochromis*’ Greenwood 1980 and ‘*Prognathochromis*’ Greenwood 1980, including both *H. squamipinnis* and *H. mentatus* in ‘*Harpagochromis*’. ‘*Harpagochromis*’ differs from ‘*Prognathochromis*’ by a broader and deeper neurocranium with a high vs low supraoccipital crest (Greenwood 1980). Van Oijen (1991) re-examined both genera and concluded that all synapomorphic traits overlapped considerably and represented continuous morphoclines. Hoogerhoud (1984), Witte & Witte-Maas (1987), Snoeks (1994), de Zeeuw *et al.* (2012), and Vranken *et al.* (2019, 2020b) found that not all species of *Haplochromis* could be classified unambiguously into one of Greenwood’s (1979, 1980) genera. Furthermore, most of these genera seemed to be polyphyletic (Meier *et al.* 2017; McGee *et al.* 2020). Therefore, we follow Hoogerhoud (1984) and van Oijen (1996) who suggested to retain all species of the LVRS in *Haplochromis*, as prior to Greenwood’s revision. When referring to the genera sensu Greenwood (1980), we will place them between quotation marks to indicate that we do not consider them to be valid.

During four expeditions conducted between 2016 and 2019 within the framework of the HIPE project (Human impacts on ecosystem health and resources of Lake Edward), the Ugandan part of the Lake Edward system was extensively sampled (see Decru *et al.* 2020 for an overview of the sampling localities). This system includes Lakes Edward and George that are connected by the Kazinga Channel, and their associated river systems. Lake Edward is a relatively large (2325 km²) and deep (~117 m maximum) lake with various habitats, while Lake George is smaller (250 km²) and very shallow (~4 m maximum) with almost only muddy substrates (Greenwood 1973; Lehman 2002). The sampling led to the discovery of many new species of *Haplochromis*. Specimens were classified into eco-morphological groups and then revised. Following the revisions of the paedophages (Vranken *et al.* 2019), lobed-lipped insectivores (Vranken *et al.* 2020a), oral mollusc shellers (Vranken *et al.* 2020b), and *H. pharyngalis* Poll & Damas, 1939 (Vranken *et al.* 2020c), we here present a taxonomic revision of the species of *Haplochromis* with a piscivorous morphology from the lacustrine part of the Lake Edward system (i.e., Lakes Edward and George and the Kazinga Channel). We formally (re)describe all species with a piscivorous morphology and provide an identification key.

Material and methods

Museum abbreviations

IRSNB	=	Royal Belgian Institute of Natural Sciences, Brussels
MCZ	=	Museum of Comparative Zoology, Boston
NHMUK	=	Natural History Museum, London
RMCA	=	Royal Museum for Central Africa, Tervuren

A total of 185 specimens of *Haplochromis* with a piscivorous morphology from the Lake Edward system were examined. These included 158 specimens from the RMCA and five from the IRSNB, which were all recently collected in Uganda by the HIPE project during four expeditions (HIPE1–4; 2016–2019). These recent specimens were mostly collected with gill nets with various mesh sizes (8–40 mm) and occasionally bought from fishermen. Photographs were made of freshly collected specimens, both dry and in a cuvette. Specimens were euthanised by an anaesthetic overdose (clove oil), fixed in 10% formalin, and preserved in 70% ethanol. In addition, we examined 20 specimens from a historical collection (KEA exped.: Exploration hydrobiologique des lacs Kivu, Édouard et Albert; 1952–1954) of the IRSNB from the Democratic Republic of the Congo; and the holotypes of *H. squamipinnis* (NHMUK 1914.4.8.32) and *H. mentatus* (MCZ 31523).

To exclude conspecific status with other species, all examined specimens were also compared to descriptions of species from Lake Victoria (Greenwood 1962 ; van Oijen 1991) and Lake Kivu (Snoeks

1994), and to specimens of *H. avium* (Regan, 1929) (RMCA 1989.059.P.0295 to 97 and 2002.063.P.0012), the only known piscivorous species from Lake Albert.

From all specimens, a total of 56 morphometrics were taken by a single person (NV). These include 27 measurements, taken with a pair of callipers (± 0.1 mm), and 23 counts that were taken under a binocular microscope ($6.5\text{--}50\times$) following Vranken *et al.* (2019): standard (SL) and head lengths (HL); body depth (BD); predorsal (PrD), preanal (PrA), prepectoral (PrP) and prepelvic distances (PrV); pectoral- (PL) and pelvic-fin lengths (VL); dorsal- (DFB) and anal-fin base lengths (AFB); caudal peduncle length (CPL) and depth (CPD); head width (HW); eye diameter (ED); interorbital width (IOW); snout length (SnL); lacrimal (LaD) and cheek depths (ChD); premaxillary pedicel length (PPL); upper jaw length (UJL); lower jaw length (LJL) and width (LJW); lower pharyngeal length (LPL, $n=24$) and width (LPW; $n=24$); dentigerous area length (DAL, $n=24$) and width (DAW, $n=24$); number of upper (UOT) and lower (LOT) outer teeth; number of upper and lower inner tooth rows (UTR/LTR); dorsal- (DFR: DFRs/DFRr), anal- (AFR: AFRs/AFRr), and pectoral-fin formulas (PFR), consisting of spine and branched-ray counts; gill-raker formula (GR: GRc/1/GRc), consisting of cerato- and epibranchial gill-raker counts; abdominal and caudal vertebrae (V: Va/Vc; taken from X-rays); longitudinal line scales (LongL); lateral line scales (LatL: LatLu/LatLl), consisting of upper and lower lateral line scale counts; upper (D-UUL) and lower transverse line scales (ULL-A); scales around the caudal peduncle (CPS); scales between pectoral and pelvic fins (P-V); infraorbital and postorbital cheek scales (ChS: ChSi/ChSp); and lower pharyngeal teeth in the posterior row (LPTp; $n=24$) and the median longitudinal row (LPTm; $n=24$). Lower jaw side inclination (i.e., lower jaw side obliqueness sensu van Oijen 1991) ($n=60$) was measured using a protractor. Gape and snout inclinations ($n=60$) were taken following Barel (1983), with the parasphenoid used as a reference line from X-ray scans made by the VisiX X-ray system (Medex Loncin SA) with a DeReO WA detector and a GemX-160 generator in ImageJ (Rasband 2018). Following Greenwood (1980), neurocranial length (NL; $n=51$), preorbital depth (PrOD; $n=51$), and orbital depth (OD; $n=51$) were measured from X-ray scans in ImageJ.

All qualitative characteristics were described following Barel *et al.* (1977) and included: the lateral outline of the neurocranium (observed from X-rays), the dorsal outlines of the head and snout, the lateral outline of the snout, the premaxillary pedicel prominence, the maxillary bullation, the maxillary posterior extension (in reference to a line perpendicular to the body axis instead of to the anterior margin of the vertical preoperculum limb), the caudal- and pelvic-fin outlines, the gill-raker shape, and the colour patterns in live specimens (from photographs of freshly caught specimens) and specimens fixed in formalin and preserved in alcohol (hereby excluding the ethanol-fixed holotypes of *H. mentatus* and *H. squamipinnis*). Here, we describe conspicuously coloured males as dominant and less-conspicuously coloured males as non-dominant (Fernald 2017). The shape and dentition of the oral jaws were described based on the investigation of intact specimens and X-ray scans (dissection of the oral jaws was not allowed for curatorial reasons). Those of the lower pharyngeal jaw were described based on direct investigation of dissected lower pharyngeal elements. All characteristics were described in reference to the generalised *Haplochromis* morphology sensu Barel *et al.* (1976), which was based on *H. elegans* Trewavas, 1933, an insectivorous species from the Lake Edward system. A distinction was made between terms that describe the size of structures in the dorso-ventral axis, i.e., shallow and deep, in the antero-posterior axis, i.e., short and long, and in the medial-lateral axis, i.e., narrow and broad. The shape of the dentigerous arms of the upper jaw and the horizontal arms of the lower jaw were described as slim when slender with a compressed cross-section, and stout when enlarged with a nearly rounded cross-section. Here, we describe body shapes as: pyriform when the body has its largest depth at the posterior area of the head with dorsal and ventral outlines narrowing posteriorly, rectangular when the dorsal and ventral outlines are nearly parallel anterior to the caudal peduncle, oval if dorsal and ventral body outlines are gently convex, and rhomboid when the body is deepest at a vertical clearly posterior to the head and has a caret-shaped (Δ) dorsal outline. Specimens were sexed by investigation of the genital papillae.

Measurements and counts were analysed separately using principal component analyses (PCA). These were performed on the variance-covariance matrices of 21 log-transformed measurements and on the correlation matrices of 21 raw counts. To allow for comparison, all measurements, except for SL, were expressed as percentages of a reference measurement (e.g., SL and HL). Pairwise inter-group comparisons of the proportional measurements and of the raw counts were performed with Mann-Whitney *U* (MWU) tests. For all data, size effects were avoided by performing the MWU tests on subsets of specimens of a similar standard-length class [MWU (SL): $P > 0.5$]. For each comparison between two species, the *P*-values resulting from the sets of measurements and counts were corrected with a sequential Bonferroni correction (Rice 1989). Measurements with fin tips as reference points (VL and PL) and measurements and counts taken on a subset of specimens (LPL, LPW, DAL, DAW, LPTp, LPTm, NL, PrOD, OtD, and snout, gape, and lower jaw side inclinations) were excluded from all data analyses. All data analyses were performed in Past ver. 3.18 (Hammer *et al.* 2001).

Drawings of the habitus of the holotypes were made in Inkscape 1.0 and GIMP ver. 2.10 based on the preserved specimens. A photograph of the specimen was used as a starting point and lens distortions were corrected by using measurements taken from the specimen. Fixation artefacts were corrected and details were added by direct observation of the specimen.

Results

We examined 185 specimens of *Haplochromis* with a piscivorous morphology (Fig. 1). All specimens were assigned *a priori* to 12 groups that were constructed based on a combination of the outer oral tooth number and size, and the dominant male colour patterns in life (Fig. 2). Females and juveniles were assigned to the groups by comparing their overall habitus with that of dominant males. A morphological pattern was observed in the number and size of the outer oral teeth of all specimens (Fig. 2a). Six groups had specimens with few and large outer oral teeth, i.e., *H. sp.* ‘latifrons’ (LAT, $n=8$, 75–158 mm SL), *H. mentatus* (MEN, $n=20$, 87–137 mm SL), *H. sp.* ‘rex’ (REX, $n=16$, 81–155 mm SL), *H. sp.* ‘simba’ (SIM, $n=11$, 87–109 mm SL), *H. sp.* ‘glaucus’ (GL, $n=10$, 91–158 mm SL), and *H. sp.* ‘aquila’ (AQ, $n=8$, 84–123 mm SL). These will be referred to as macrodontic groups (Fig. 2a). The remaining six groups had specimens with many and small outer oral teeth: *H. sp.* ‘kimondo’ (KIM, $n=21$, 82–171 mm SL), *H. sp.* ‘falcatus’ (FAL, $n=22$, 75–137 mm SL), *H. sp.* ‘curvidens’ (CUR, $n=8$, 90–112 mm SL), *H. sp.* ‘pardus’ (PAR, $n=20$, 67–96 mm SL), *H. sp.* ‘quasimodo’ (QUA, $n=21$, 79–165 mm SL), and *H. squamipinnis* (SQP, $n=20$, 75–211 mm SL). These will be referred to as microdontic groups (Fig. 2a). The holotypes of *H. mentatus* and *H. squamipinnis* were included in MEN and SQP, respectively. In the macrodontic groups, dominant males were green-yellow with red anterior parts of flanks in specimens of MEN, beige with orange opercula in REX, yellow with orange anterior parts of flanks in SIM, blue with black snouts in GL, and grey with black snouts in AQ (Fig. 2b). No dominant males of LAT were available, but specimens of this group differed from those of all other groups by a shallower body and shorter anal- and dorsal-fin bases. They further differed from specimens of all other macrodontic groups by the presence of a well-defined mid-lateral band. Of the microdontic groups, dominant males were grey-yellow in specimens of KIM, green with red anterior parts of flanks in FAL, purple-black in PAR, violet-blue in QUA, and blue-green in SQP, and blue-green with blue flanks in non-dominant males of CUR (unknown for dominant males). For more detailed descriptions of the colour patterns, see the species descriptions below.

A PCA was performed on the variance-covariance matrix of 21 log-transformed measurements of 182 specimens (Table S1). The first principal component (PC 1; 96.3% of variance) had large, positive loadings of a similar magnitude for all variables, and was interpreted as a variable describing size (Zelditch *et al.* 2004). Principal component 2 (1.1%) was mainly determined by AFB, BD, and IOW. In a plot of PC 2 against PC 1, four clusters were observed and defined (Fig. 3a): cluster 1 consisted of all specimens of LAT, which had higher values than all other specimens for PC 2; cluster 2 consisted of

those of MEN, REX, SIM, GL, and KIM, which had mainly positive scores for PC 2; cluster 3 consisted of those of AQ, FAL, CUR, and SQP, which had mainly negative scores for PC 2; and cluster 4 contained those of PAR and QUA, which had mostly lower values for PC 2 than all other specimens. Clusters 1 and 2 correspond to the macrodontic groups and clusters 3 and 4 to the microdontic groups with the exceptions of the microdontic group KIM in cluster 2 and the macrodontic group AQ in cluster 3.

For each of the four clusters, PCAs were performed on the log-transformed measurements to investigate further separation between groups. As above, the first PC for each of these analyses is interpreted as a variable describing size (Zelditch *et al.* 2004). Cluster 1 only contained all specimens of LAT and no notable patterns were observed from a PCA of only these specimens (not shown). From a PCA of cluster 2, i.e., all specimens of MEN, REX, SIM, GL, and KIM (Table S2; PC 1: 95.7%), PC 2 (1.4%) was mainly determined by LJW, IOW, and HW and PC 3 (1.1%) by IOW, CPL, and ChD. In a plot of

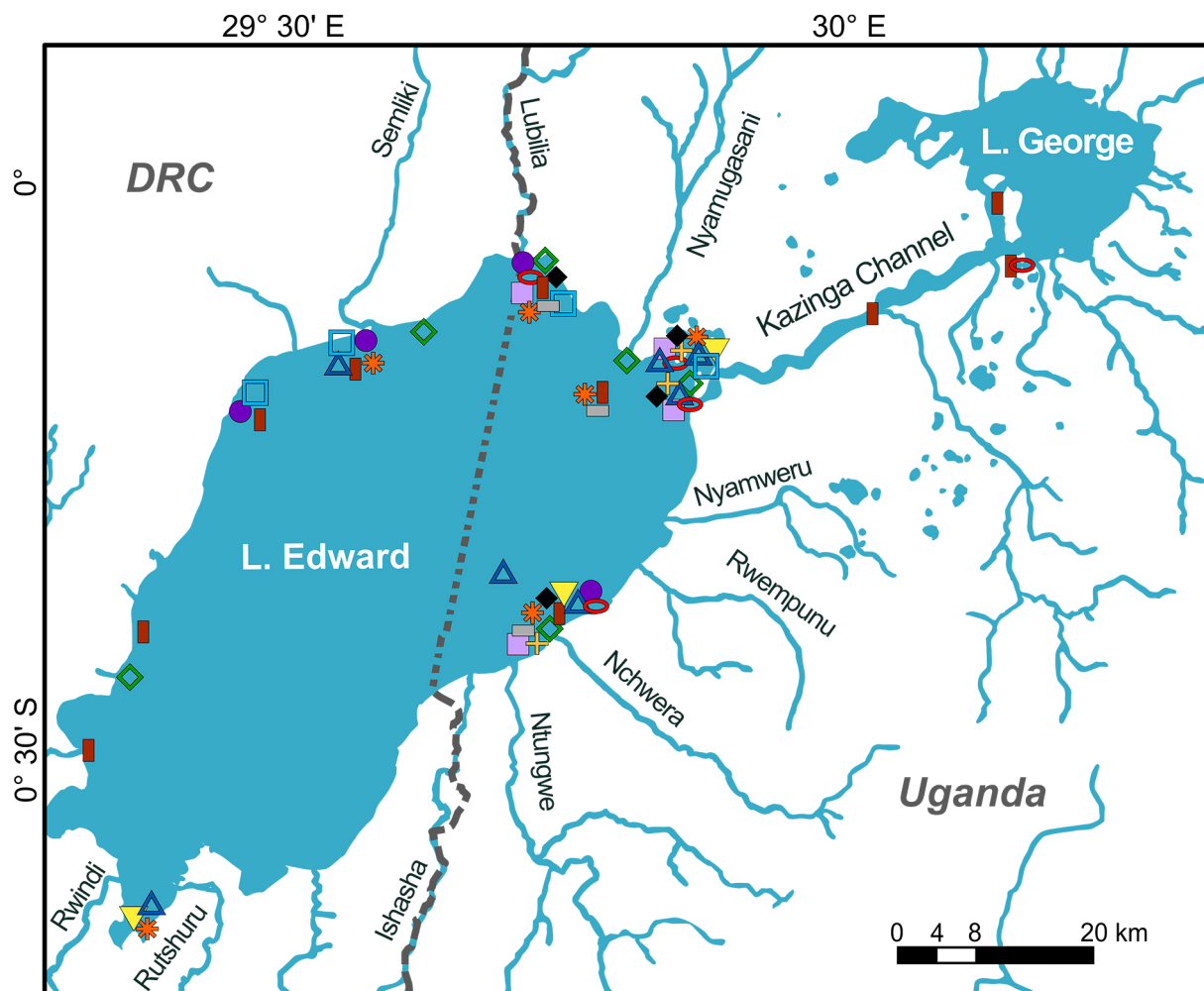


Fig. 1. The Lake Edward system, consisting of Lakes Edward and George that are connected through the Kazinga Channel. The catch localities of all examined specimens are indicated: *Haplochromis* sp. ‘latifrons’ (▣), *H. mentatus* Regan, 1925 (○), *H.* sp. ‘rex’ (*), *H.* sp. ‘simba’ (▽), *H.* sp. ‘glaucus’ (□), *H.* sp. ‘aquila’ (◻), *H.* sp. ‘kimondo’ (●), *H.* sp. ‘falcatus’ (◇), *H.* sp. ‘curvidens’ (+), *H.* sp. ‘pardus’ (◆), *H.* sp. ‘quasimodo’ (△), and *H. squamipinnis* Regan, 1921 (■). The type localities of *H. mentatus* and *H. squamipinnis* are not shown as the exact locations are unknown.

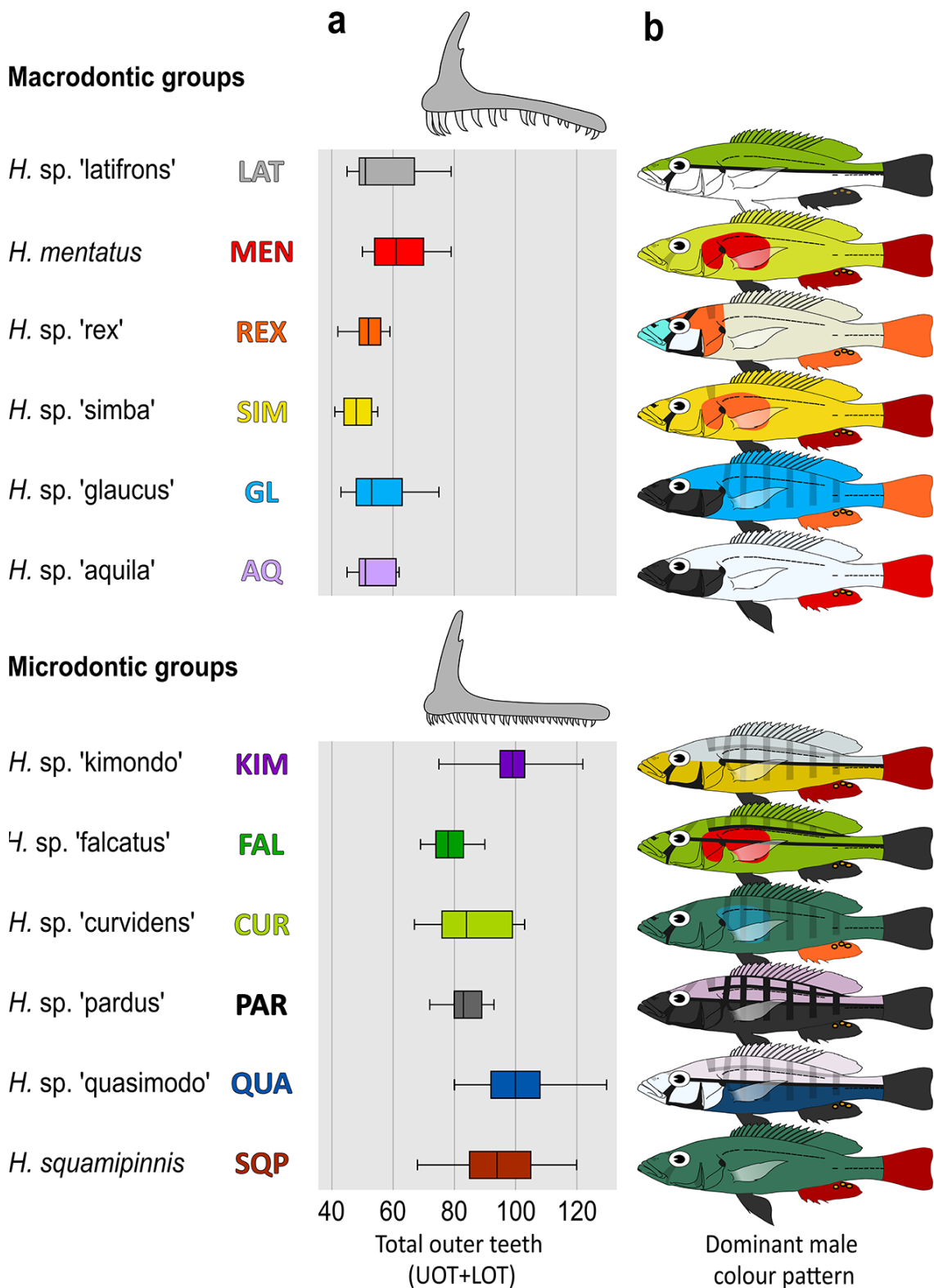


Fig. 2. a. Differences in total number of outer teeth and premaxillary dentition between the macro- and microdontic groups of piscivores from the Lake Edward system. **b.** Schematic presentation of the dominant male colour patterns in life, in the various groups studied. For *H. sp. 'latifrons'* the female and for *H. sp. 'curvidens'* the non-dominant colour patterns are shown, as those of dominant males are unknown.

PC 2 against PC 3 (Fig. 3b), all specimens of KIM and MEN were each completely separated from all other specimens: those of KIM mostly by their lower values for PC 2 and those of MEN by their higher values for PC 3. All specimens of REX, SIM, and GL strongly overlapped on both axes. Both axes were also plotted against PC 1 to test for allometric effects and no additional patterns were observed (not shown). The groups REX, SIM, and GL, which could not be separated in the previous analysis, were investigated in a separate PCA (Table S3; PC 1: 97.4%), for which PC 2 (0.7%) was mainly determined by IOW. On a plot of PC 2 against PC 1 (Fig. 3c), no overlap between the groups was observed. All specimens of REX had negative values for PC 2, those of SIM had values around zero, and those of GL

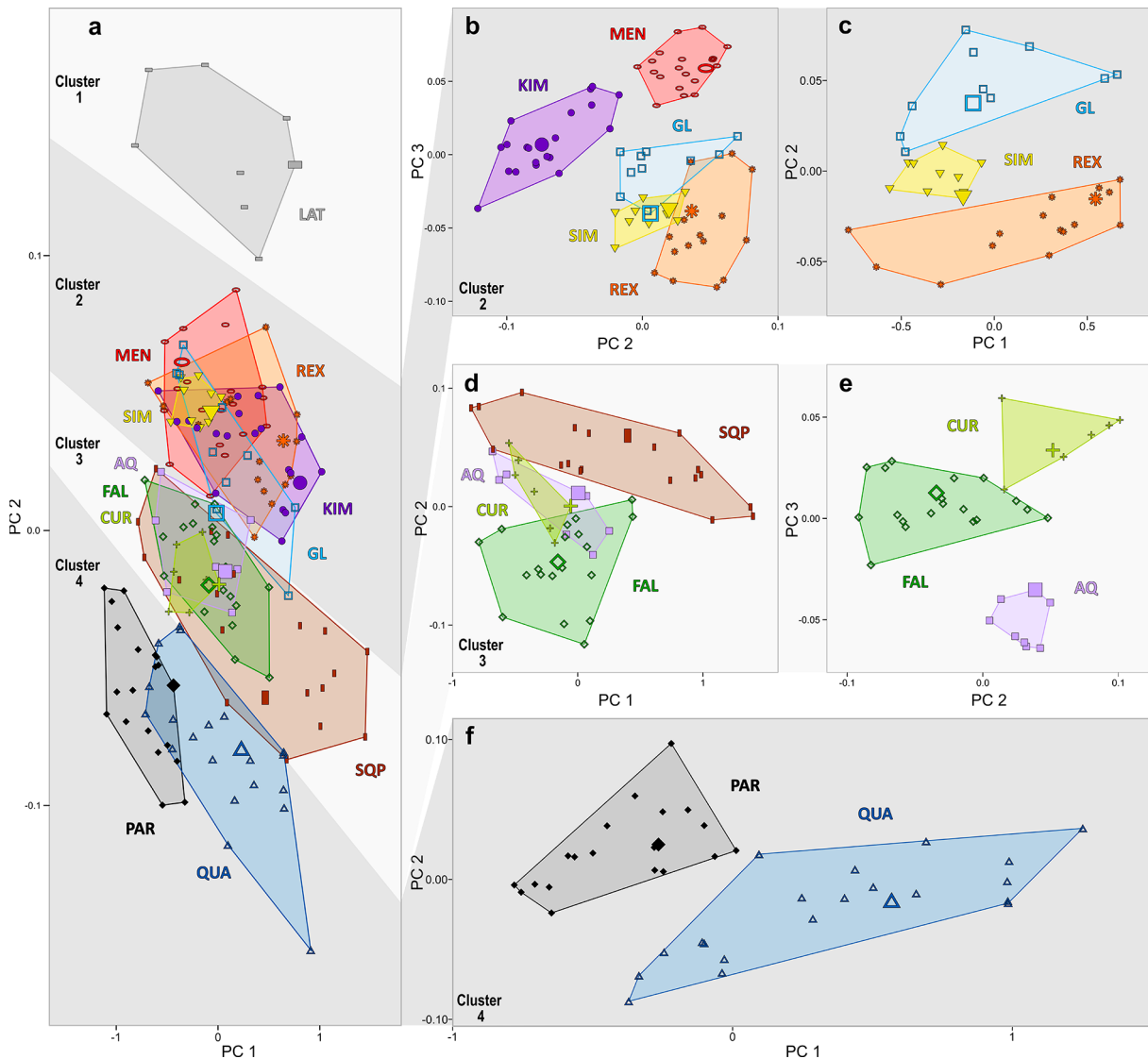


Fig. 3. Plots of principal component analyses of 21 measurements of 12 groups of *Haplochromis* from the Lake Edward system with a piscivorous morphology: *H. sp.* ‘latifrons’ (◻), *H. mentatus* Regan, 1925 (◌), *H. sp.* ‘rex’ (*), *H. sp.* ‘simba’ (▽), *H. sp.* ‘glaucus’ (◻), *H. sp.* ‘aquila’ (◻), *H. sp.* ‘kimondo’ (●), *H. sp.* ‘falcatus’ (◇), *H. sp.* ‘curvidens’ (+), *H. sp.* ‘pardus’ (◆), *H. sp.* ‘quasimodo’ (△), and *H. squamipinnis* Regan, 1921 (■); holotypes are indicated by large symbols. **a.** Based on a PCA of the measurements of all specimens, groups were assigned to four clusters (clusters 1–4), which were analysed further separately (**b-f**).

had positive values. Next, a PCA was performed of all specimens from cluster 3, i.e., those of AQ, FAL, CUR, and SQP (Table S4; PC 1: 97.7%). Principal component 2 (0.8%) was mainly determined by LJW. On a plot of PC 2 against PC 1 (Fig. 3d), specimens of SQP had mostly higher values for PC 2 than those of all other groups when comparing similar-sized specimens (i.e., specimens with similar values for PC1). Specimens of AQ, CUR, and FAL strongly overlapped with each other on PC 2 and were analysed further in a separate PCA (Table S5; PC 1: 94.1%). In this analysis, the most important contributor to PC 2 (2.6%) was CPL and to PC 3 (1.1%) was ChD. On a plot of PC 3 against PC 2 (Fig. 3e), AQ specimens differed from FAL and CUR specimens by their lower values for PC 3 and CUR specimens were separated from FAL specimens by their higher values for PC 2 and PC 3. Both axes were plotted against PC 1 and no notable patterns were observed (not shown). Lastly, a PCA was performed on cluster 4, i.e., all specimens of PAR and QUA (Table S6; PC 1: 98.2%). On a plot of PC 1 against PC 2 (Fig. 3f), which was mainly determined by ChD, CPL, and ED, all specimens of PAR had higher values for PC 2 than those of QUA with a similar size (i.e., specimens with similar values for PC 1).

A PCA was performed on the correlation matrix of the raw counts of all 182 specimens (Table S7). All scale counts, except for LatL1, had high positive loadings for PC 1 (19.4%), while PC 2 (11.7%) was mainly determined by the tooth counts UOT and LOT. Most notably, in a plot of PC 1 against PC 2 (Fig. 4a), most specimens of REX had higher values for PC 1 than those of all other groups. Additional patterns correspond to the distinction between macro- and microdentic groups, which was mainly defined by the tooth counts. All specimens of the macrodentic groups (LAT, MEN, REX, SIM, GL, and AQ) had mostly higher values for PC 1 and mostly lower values for PC 2 than those of the microdentic groups (KIM, FAL, CUR, PAR, QUA, and SQP). Principal component 3 was mainly determined by DFRs, followed by AFRr, V-P, and LatL1. In a plot of PC 1 against PC 3 (Fig. 4b), specimens of SPQ differed partly from those of all other groups by their negative values for both PC 1 and PC 3. Within the other microdentic groups, specimens of FAL were partially separated from those of all other groups (CUR,

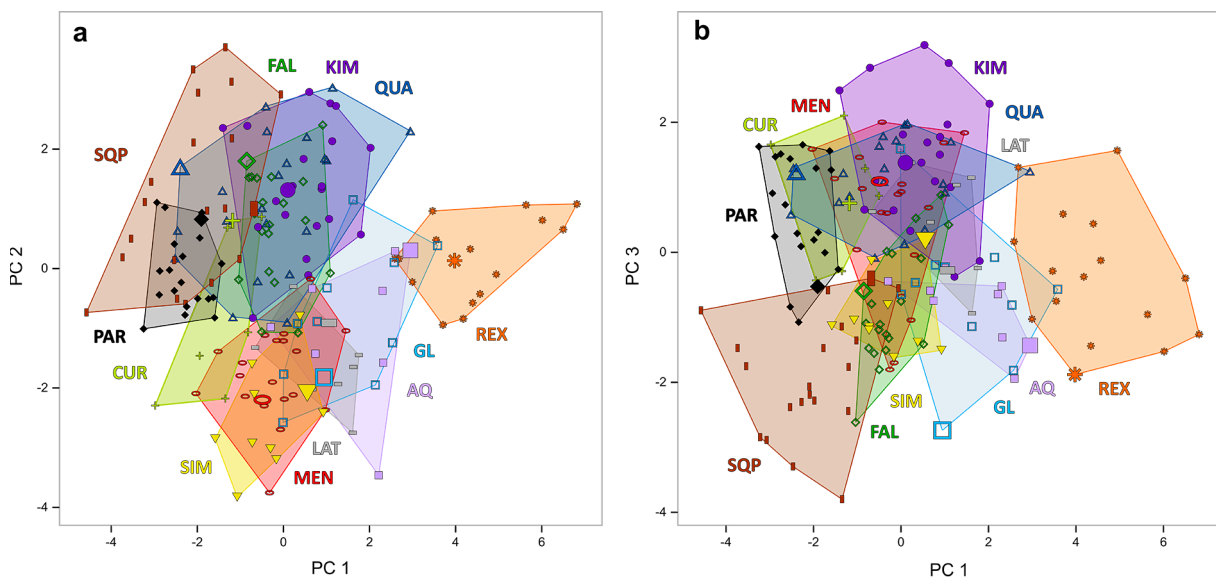


Fig. 4. Plots of a principal component analysis of 21 counts of 12 groups of *Haplochromis* from the Lake Edward system with a piscivorous morphology: *H. sp.* ‘latifrons’ (■), *H. mentatus* Regan, 1925 (○), *H. sp.* ‘rex’ (*), *H. sp.* ‘simba’ (▽), *H. sp.* ‘glaucus’ (□), *H. sp.* ‘aquila’ (■), *H. sp.* ‘kimondo’ (●), *H. sp.* ‘falcatus’ (◇), *H. sp.* ‘curvidens’ (+), *H. sp.* ‘pardus’ (◆), *H. sp.* ‘quasimodo’ (△), and *H. squamipinnis* Regan, 1921 (■); holotypes are indicated by larger symbols.

Table 1. (continued on the next three pages). Measurements and counts of the piscivorous species of *Haplochromis* from the Lake Edward system.

	<i>H. latifrons</i> sp. nov.			<i>H. mentatus</i>			<i>H. rex</i> sp. nov.			<i>H. simba</i> sp. nov.			<i>H. glaucus</i> sp. nov.			<i>H. aquila</i> sp. nov.			
	Mean ± SD	Range	n = 8, *2	Mean ± SD	Range	n = 20, *2	Mean ± SD	Range	n = 16, *2	Mean ± SD	Range	n = 11, *2	Mean ± SD	Range	n = 10, *2	Mean ± SD	Range	n = 8, *2	
SL (mm)	120.3 ± 30.9	75.3–158.2		110.3 ± 16.2	87.2–137.2		128.7 ± 23.8	80.5–154.8		98.8 ± 7.4	87.1–109.0		112.7 ± 22.6	90.7–158.3		104.6 ± 16.4	83.9–122.9		
HL % SL	35.0 ± 0.6	34.2–36.0		35.1 ± 1.0	33.4–37.0		36.6 ± 0.6	35.8–37.8		36.8 ± 0.6	35.7–37.6		36.9 ± 0.7	35.9–37.9		36.3 ± 0.7	35.5–37.6		
BD % SL	28.6 ± 1.2	27.2–30.1		31.2 ± 0.8	29.0–32.3		31.8 ± 1.7	28.4–35.1		31.3 ± 1.1	30.1–33.3		33.5 ± 2.3	29.7–36.0		32.4 ± 1.8	29.0–34.5		
PdD % SL	35.9 ± 0.3	35.4–36.4		35.3 ± 0.9	33.3–36.4		38.0 ± 1.1	36.1–39.2		37.3 ± 0.5	36.6–38.0		36.1 ± 0.5	35.4–37.0		37.2 ± 0.8	36.5–38.9		
PrA % SL	67.7 ± 0.5	67.0–68.2		66.9 ± 1.2	64.2–68.2		68.5 ± 1.0	66.2–69.6		67.3 ± 1.1	66.1–69.4		68.9 ± 1.2	66.5–70.3		67.4 ± 1.4	64.7–69.3		
PP % SL	36.1 ± 0.4	35.7–36.8		36.0 ± 1.2	33.1–38.2		37.6 ± 0.6	36.5–38.8		37.8 ± 0.8	36.2–39.2		38.1 ± 0.9	36.4–39.4		37.2 ± 1.1	35.5–39.3		
PrV % SL	41.8 ± 0.4	41.2–42.2		42.4 ± 1.2	39.4–44.3		43.1 ± 1.0	41.4–44.8		42.7 ± 0.9	41.5–44.0		44.3 ± 1.4	41.9–45.9		42.8 ± 1.4	40.6–45.5		
PL % SL	27.8 ± 0.6	27.1–28.7		27.5 ± 1.7	25.2–30.4		27.6 ± 1.7	23.4–29.8		29.0 ± 1.4	27.1–30.8		28.0 ± 1.0	27.1–29.7		29.8 ± 1.0	28.1–31.1		
VL % SL	23.5 ± 0.9	22.2–25.0		24.6 ± 1.8	22.6–28.8		24.2 ± 2.0	21.8–28.3		27.5 ± 1.8	24.2–30.4		25.9 ± 1.5	23.3–27.7		25.0 ± 2.0	21.6–28.4		
DFB % SL	49.0 ± 0.9	47.2–50.1		52.3 ± 1.2	50.3–54.2		51.5 ± 0.8	49.8–53.1		51.3 ± 1.3	49.4–53.1		51.9 ± 1.5	49.8–55.0		51.7 ± 0.6	50.5–52.6		
AFB % SL	15.7 ± 1.0	14.7–17.3		18.0 ± 0.7	16.7–19.2		18.7 ± 1.1	17.1–21.4		18.0 ± 0.6	17.3–19.0		18.6 ± 0.9	17.3–20.3		18.3 ± 0.4	17.3–18.7		
CPL % SL	17.0 ± 0.7	15.8–18.0		16.6 ± 0.6	15.7–17.5		14.8 ± 0.8	13.5–16.2		15.6 ± 0.5	14.8–16.6		14.8 ± 1.0	13.4–16.1		15.0 ± 0.3	14.6–15.4		
CPD % CPL	65.2 ± 4.3	59.3–72.0		69.6 ± 3.4	64.8–78.6		80.6 ± 3.8	74.4–87.9		73.6 ± 2.8	70.1–78.3		81.0 ± 7.2	69.3–90.7		80.6 ± 3.7	73.6–86.8		
HW % HL	41.8 ± 1.1	40.5–43.2		40.8 ± 1.0	39.4–42.3		39.2 ± 1.5	36.8–41.6		40.8 ± 0.7	39.5–41.5		39.7 ± 0.6	38.9–40.9		42.0 ± 1.3	40.1–43.7		
ED % HL	24.4 ± 1.6	22.3–26.7		27.2 ± 1.2	25.4–29.9		24.6 ± 1.7	22.2–28.3		28.3 ± 0.8	26.7–29.5		26.8 ± 1.7	23.2–28.7		30.6 ± 0.6	30.0–31.5		
IOW % HW	60.0 ± 2.3	57.4–63.3		55.5 ± 2.3	51.3–61.0		48.9 ± 2.1	44.9–52.7		48.1 ± 1.5	45.5–50.4		53.8 ± 1.9	50.9–57.1		48.0 ± 2.6	45.3–53.3		
SNL % HL	35.6 ± 1.1	33.9–37.3		34.2 ± 1.5	30.0–35.9		34.7 ± 1.9	31.1–37.9		32.5 ± 0.8	31.3–34.0		32.8 ± 1.3	31.0–35.1		30.3 ± 1.3	28.0–31.9		
LaD % HL	20.7 ± 1.6	18.8–23.0		19.7 ± 0.9	18.1–20.9		20.8 ± 1.0	18.9–22.5		19.5 ± 0.6	18.7–20.5		19.8 ± 1.3	18.0–22.7		18.3 ± 0.7	17.0–19.1		
ChD % HL	27.7 ± 2.4	24.3–30.9		26.4 ± 1.7	23.8–31.1		31.1 ± 1.6	27.6–33.5		28.3 ± 0.8	27.0–29.6		28.5 ± 1.5	26.2–31.3		28.3 ± 1.3	26.8–30.8		
PPL % HL	25.4 ± 0.6	24.5–26.0		26.0 ± 0.7	25.0–27.3		25.1 ± 0.7	23.8–26.2		24.5 ± 0.9	23.4–26.1		25.8 ± 1.2	23.8–28.6		25.1 ± 0.7	24.1–26.3		
UJL % HL	38.2 ± 2.4	35.3–41.6		37.0 ± 1.9	33.8–41.0		38.1 ± 1.2	36.1–40.0		38.6 ± 1.2	36.3–40.1		38.6 ± 1.5	36.8–42.1		38.2 ± 1.7	36.5–41.1		
LJL % HL	47.8 ± 1.3	45.6–49.4		48.5 ± 2.0	43.9–51.0		47.8 ± 1.3	45.6–50.1		48.4 ± 1.0	47.1–50.0		49.0 ± 2.2	46.0–53.1		47.1 ± 1.6	45.0–49.2		
LJW % LJL	43.5 ± 2.8	39.6–46.4		39.3 ± 1.7	35.2–41.8		44.7 ± 2.4	39.5–47.9		40.8 ± 1.5	38.2–42.8		40.5 ± 2.1	36.2–43.1		41.8 ± 1.8	38.1–43.4		
LPL % HL	30.7 ± 0.3	30.5–30.9*		29.9 ± 0.6	29.4–30.3*		29.2 ± 1.6	28.1–30.3*		30.3 ± 0.0	30.3–30.3*		28.9 ± 0.1	28.8–28.9*		31.0 ± 1.1	30.2–31.7*		
LPW % LPL	89.7 ± 4.4	86.6–92.8*		84.7 ± 1.5	83.6–85.7*		89.3 ± 3.7	86.6–91.9*		85.8 ± 2.8	83.8–87.9*		94.2 ± 1.3	93.3–95.1*		88.3 ± 6.7	83.6–93.1*		
DAL % LPL	54.9 ± 2.4	53.3–56.6*		57.4 ± 1.6	56.3–58.5*		61.1 ± 2.0	59.7–62.5*		59.4 ± 2.0	58.0–60.9*		60.9 ± 4.3	57.8–63.9*		56.8 ± 1.1	56.0–57.6*		
DAW % LPW	64.5 ± 1.3	63.6–65.4*		67.0 ± 3.6	64.5–69.6*		67.0 ± 2.5	65.2–68.8*		67.0 ± 1.7	65.8–68.3*		63.8 ± 0.4	63.5–64.1*		64.1 ± 2.3	62.5–65.7*		

Table 1. (continued). Measurements and counts of the piscivorous species of *Haplochromis* from the Lake Edward system.

	<i>H. latifrons</i> sp. nov. n = 8	<i>H. mentatus</i> n = 20	<i>H. rex</i> sp. nov. n = 16	<i>H. simba</i> sp. nov. n = 11	<i>H. glaucus</i> sp. nov. n = 10	<i>H. aquila</i> sp. nov. n = 8
	Number & frequency	Number & frequency	Number & frequency	Number & frequency	Number & frequency	Number & frequency
UOT	24–42 (median 31)	28–46 (median 36)	24–36 (median 29)	22–31 (median 27)	25–47 (median 30)	25–37 (median 31)
LOT	18–37 (median 24)	20–33 (median 27)	18–27 (median 24)	18–33 (median 21)	13–29 (median 24)	16–26 (median 24)
UTR/LTR	1/1 (1); 2/1 (4); 3/2 (1)	1/1 (2); 1/2 (2); 2/1 (8); 2/2 (8)	2/1 (2); 2/2 (14)	2/1 (9); 2/2 (1)	2/1 (6); 2/2 (4); 3/1 (1)	1/1 (1); 2/1 (1); 2/2 (6)
LPTp/LPTm	15/10 (1); 16/10 (1)	14/11 (1); 21/11 (1)	15/11 (1); 16/11 (1)	16/12 (1); 18/12 (1)	15/10 (1); 16/12 (1)	17/12 (1); 16/12 (1)
DFR	XV/9 (4); XV/10 (2); XVI/9 (2)	XV/10 (8); XVI/9 (4); XVI/10 (8)	XIV/10 (1); XIV/11 (1); XV/9 (1); XV/10 (9); XV/11 (2); XVI/9 (1); XV/10 (1)	XIV/9 (1); XV/9 (4); XV/10 (4); XVI/9 (1); XVI/10 (1)	XIV/9 (2); XV/9 (3); XV/10 (3); XVI/9 (2); XVI/10 (1)	XIV/10 (1); XV/9 (1); XV/10 (5); XVI/9 (1)
AFR	III/7 (3); III/8 (5)	III/8 (8); III/9 (11); III/10 (1)	III/8 (2); III/9 (13); III/10 (1)	III/8 (2); III/9 (8)	III/8 (2); III/9 (7); III/10 (2)	III/8 (1); III/9 (7)
PFR	12 (6); 13 (2)	11 (1); 12 (17); 13 (2)	11 (1); 12 (7); 13 (8)	12 (8); 13 (2)	12 (8); 13 (3)	11 (1); 12 (6); 13 (1)
GR	8/1/2 (1); 8/1/3 (1); 9/1/3 (4); 9/1/4 (1); 11/1/3 (1)	8/1/2 (1); 8/1/3 (4); 9/1/2 (4); 9/1/3 (4); 10/1/2 (4); 10/1/3 (1); 11/1/2 (1); 11/1/3 (1)	8/1/2 (2); 8/1/3 (2); 9/1/2 (1); 9/1/3 (6); 10/1/2 (2); 10/1/3 (1); 11/1/3 (1); 12/1/3 (1)	8/1/3 (4); 9/1/2 (1); 9/1/3 (3); 10/1/2 (1); 11/1/3 (1)	9/1/2 (3); 9/1/3 (4); 10/1/2 (1); 10/1/3 (1); 11/1/3 (2)	8/1/3 (1); 9/1/2 (1); 9/1/3 (3); 10/1/3 (3)
V	14/16 (8)	13/17 (1); 14/16 (5); 14/17 (10); 14/18 (1); 15/16 (2); 15/17 (1)	13/16 (1); 14/15 (3); 14/16 (11); 14/17 (1)	13/17 (3); 14/16 (6); 14/17 (1)	14/15 (3); 14/16 (8)	14/16 (8)
LongL	33 (5); 34 (3)	32 (2); 33 (9); 34 (8); 35 (1)	34 (5); 35 (6); 36 (1); 37 (3); 38 (1)	32 (6); 33 (4)	32 (3); 33 (4); 34 (1); 35 (2); 37 (1)	32 (2); 33 (3); 34 (2); 35 (1)
LatLu	20 (1); 21 (3); 22 (2); 23 (2)	19 (1); 20 (3); 21 (8); 22 (7); 23 (1)	22 (2); 23 (5); 24 (4); 25 (2); 26 (1); 27 (1)	19 (1); 20 (3); 21 (5); 22 (1)	21 (5); 22 (1); 23 (3); 24 (1); 25 (1)	20 (1); 21 (2); 22 (2); 23 (3)
LatLJ	9 (1); 10 (2); 11 (3); 12 (2)	8 (1); 9 (5); 10 (4); 11 (2); 12 (5); 13 (2); 14 (1)	8 (1); 9 (2); 10 (1); 11 (1); 12 (6); 13 (4); 14 (1)	8 (3); 9 (1); 10 (6)	8 (2); 11 (3); 12 (4); 13 (2)	10 (1); 11 (1); 12 (1); 13 (3); 14 (2)
D-UllL	6 (5); 7 (3)	5 (2); 6 (15); 7 (3)	6 (2); 7 (11); 8 (3)	5 (6); 6 (4)	5 (1); 6 (5); 7 (5)	5 (1); 6 (5); 7 (2)
ULL-A	11 (3); 12 (4); 13 (1); 17 (4); 18 (3); 19 (1);	10 (3); 11 (7); 12 (6); 13 (4); 16 (8); 17 (5); 18 (5); 19 (2);	12 (1); 13 (4); 14 (3); 15 (6); 16 (2); 18 (5); 19 (5); 20 (6);	9 (1); 10 (3); 11 (6); 16 (4); 17 (1); 18 (2); 19 (3);	10 (3); 11 (1); 12 (3); 13 (3); 15 (1);	11 (1); 12 (1); 13 (2); 14 (2); 15 (2);
CPS	17 (4); 18 (3); 19 (1);	16 (8); 17 (5); 18 (5); 19 (2);	18 (5); 19 (5); 20 (6);	16 (4); 17 (1); 18 (2); 19 (3);	16 (1); 17 (1); 18 (4); 19 (2); 20 (3);	17 (3); 18 (2); 19 (2); 20 (1);
P-V	6 (2); 7 (6);	5 (2); 6 (15); 7 (1); 8 (2);	7 (8); 8 (3); 9 (4); 10 (1);	5 (3); 6 (6); 7 (1);	6 (3); 7 (5); 8 (3);	7 (6); 8 (2);
ChSi	4 (7); 5 (1)	3 (10); 4 (10)	4 (1); 5 (9); 6 (5); 7 (1)	4 (3); 5 (7)	3 (2); 4 (8); 5 (1)	3 (2); 4 (4); 5 (2)
ChSp	9 (2); 10 (2); 11 (2); 12 (2)	8 (4); 9 (6); 10 (7); 11 (1); 12 (2)	10 (4); 11 (5); 12 (6); 13 (1)	9 (3); 10 (1); 11 (3); 12 (3)	9 (2); 10 (5); 11 (2); 12 (2)	9 (1); 10 (4); 11 (1); 12 (2)

Table 1. (continued). Measurements and counts of the piscivorous species of *Haplochromis* from the Lake Edward system.

	<i>H. kimondo</i> sp. nov.			<i>H. falcatus</i> sp. nov.			<i>H. curvidens</i> sp. nov.			<i>H. pardus</i> sp. nov.			<i>H. quasimodo</i> sp. nov.			<i>H. squamipinnis</i>		
	Mean ± SD	Range	n = 21, *2	Mean ± SD	Range	n = 20, *2	Mean ± SD	Range	n = 7, *2	Mean ± SD	Range	n = 20, *2	Mean ± SD	Range	n = 21, *2	Mean ± SD	Range	n = 20, *2
SL (mm)	126.5 ± 25.1	81.6–171.3	103.2 ± 16	75.0–137.1	98.7 ± 7.5	90.2–112.0	80.1 ± 9	67.4–96.1	113.6 ± 25.8	78.9–164.9	136.7 ± 43.4	75.9–211.4						
HL % SL	36.5 ± 0.9	34.8–38.5	38.2 ± 0.9	36.6–39.6	36.1 ± 1.4	34.1–37.9	35.2 ± 0.8	34.0–36.7	35.5 ± 0.9	33.9–37.2	36.0 ± 0.6	35.1–36.9						
BD % SL	33.0 ± 1.6	29.9–35.3	33.2 ± 1.2	30.4–35.2	30.8 ± 1.0	29.0–32.0	31.8 ± 1.6	29.2–35.3	37.4 ± 2.3	33.5–41.7	35.7 ± 2.1	32.4–39.3						
PtD % SL	38.0 ± 1.0	36.0–40.1	39.5 ± 1.0	36.9–41.1	36.3 ± 1.3	34.5–37.9	36.0 ± 1.0	34.1–37.8	37.7 ± 1.0	35.5–39.1	36.7 ± 0.7	35.0–38.3						
PtA % SL	66.9 ± 0.7	65.8–68.2	67.1 ± 1.3	64.7–69.0	66.6 ± 1.0	65.3–67.9	65.3 ± 0.9	64.1–66.9	66.0 ± 1.5	63.0–68.7	66.5 ± 1.0	64.4–68.6						
PtP % SL	36.7 ± 0.7	35.3–38.2	38.6 ± 0.7	37.1–39.9	36.7 ± 1.1	35.0–38.0	35.7 ± 1.0	34.2–37.8	35.8 ± 0.9	33.9–37.2	37.0 ± 0.6	35.9–38.3						
PtV % SL	40.8 ± 0.7	39.2–42.1	43.5 ± 1.0	41.4–45.4	41.0 ± 0.9	40.1–42.5	40.9 ± 0.8	39.6–42.3	41.4 ± 1.4	38.6–45.4	42.8 ± 1.1	41.4–45.8						
PL % SL	26.3 ± 1.6	23.1–29.4	27.2 ± 1.5	24.6–30.2	29.1 ± 1.3	27.7–30.6	28.5 ± 2.1	25.1–32.2	32.8 ± 2.4	28.3–37.5	30.5 ± 1.9	26.5–33.1						
VL % SL	23.2 ± 1.7	21.0–27.5	23.5 ± 1.0	21.6–25.7	25.3 ± 1.6	23.0–27.4	26.1 ± 3.6	21.2–35.7	29.4 ± 2.1	26.2–33.7	28.8 ± 2.7	25.2–35.4						
DFB % SL	53.1 ± 1.2	50.7–55.3	51.4 ± 1.4	48.8–53.4	52.4 ± 0.9	51.4–54.1	52.4 ± 1.2	50.3–55.3	54.1 ± 1.5	50.8–57.8	52.2 ± 1.5	49.7–55.1						
AFB % SL	18.0 ± 0.7	17.0–19.2	19.3 ± 0.5	18.4–20.3	18.3 ± 0.2	17.9–18.6	20.5 ± 0.8	19.2–22.2	19.9 ± 0.9	18.1–21.7	19.9 ± 1.0	18.6–21.9						
CPL % SL	15.1 ± 0.6	14.0–16.2	14.6 ± 0.8	13.7–16.5	15.7 ± 0.7	14.9–16.6	14.7 ± 0.8	13.8–16.6	15.5 ± 0.9	14.2–17.4	15.0 ± 0.4	13.9–16.1						
CPD % CPL	79.0 ± 4.6	70.7–87.5	86.7 ± 5.3	77.7–97.3	76.7 ± 3.8	72.0–82.0	81.8 ± 4.8	72.8–90.0	81.4 ± 5.0	71.3–91.5	85.0 ± 4.7	77.3–96.0						
HW % HL	45.1 ± 1.3	42.9–48.0	42.9 ± 1.2	39.9–44.4	43.4 ± 0.7	42.4–44.2	42.6 ± 1.0	40.1–44.1	45.3 ± 1.5	42.0–48.1	42.5 ± 2.3	38.4–47.0						
ED % HL	27.5 ± 1.9	24.6–30.8	28.9 ± 1.5	25.2–31.5	30.4 ± 0.7	29.4–31.1	31.9 ± 1.3	29.8–34.1	29.2 ± 1.6	26.2–31.8	26.6 ± 2.0	23.1–29.7						
IOW % HW	52.8 ± 2.6	49.2–58.5	47.7 ± 2.5	41.9–53.3	49.1 ± 2.0	46.4–52.5	44.6 ± 2.6	39.3–48.4	43.9 ± 2.3	40.5–48.7	51.9 ± 2.0	48.6–55.6						
SNL % HL	34.5 ± 1.8	31.3–37.7	32.4 ± 0.9	30.3–33.4	30.1 ± 1.1	28.9–32.1	30.3 ± 1.5	27.6–33.2	31.0 ± 1.2	28.2–33.1	33.5 ± 2.1	29.9–37.1						
LaD % HL	19.7 ± 1.4	16.9–22.0	18.0 ± 0.6	16.1–18.8	16.7 ± 0.6	16.0–17.8	17.3 ± 0.7	16.0–18.3	18.6 ± 1.0	16.6–20.6	19.6 ± 1.2	17.3–23.0						
ChD % HL	30.9 ± 2.4	27.1–35.2	26.0 ± 1.0	23.3–28.0	23.2 ± 0.8	22.4–24.9	22.5 ± 1.1	20.8–24.4	27.5 ± 2.2	23.7–32.9	29.0 ± 2.9	24.9–36.0						
PPL % HL	26.7 ± 1.0	25.0–28.5	26.9 ± 0.7	25.2–28.1	25.1 ± 0.9	23.7–26.3	27.0 ± 1.1	24.5–28.7	26.8 ± 1.0	25.4–29.4	27.9 ± 1.2	25.2–30.5						
UJL % HL	39.3 ± 2.5	35.8–43.8	38.5 ± 1.3	36.4–41.8	36.4 ± 0.7	35.3–37.3	34.6 ± 1.2	32.7–36.8	37.9 ± 1.8	34.6–41.0	40.7 ± 2.8	35.8–47.1						
LJL % HL	47.7 ± 2.4	44.7–52.0	49.5 ± 1.3	47.6–52.1	47.3 ± 1.3	45.8–49.7	44.7 ± 1.2	42.4–46.7	47.1 ± 1.6	44.2–49.6	52.7 ± 2.8	47.8–58.6						
LJW % LJL	49.3 ± 2.5	44.7–53.3	42.5 ± 1.7	40.2–45.6	40.8 ± 1.5	38.5–43.2	41.3 ± 2.0	37.3–44.6	45.9 ± 2.5	41.0–50.6	37.2 ± 3.7	32.6–44.7						
LPL % HL	28.9 ± 0.1	28.8–29.0*	29.4 ± 0.0	29.4–29.4*	29.5 ± 1.1	28.7–30.3*	29.4 ± 1.0	28.7–30.1*	30.7 ± 3.0	28.6–32.8*	31.7 ± 2.1*	30.2–33.1*						
LPW % LPL	99.8 ± 2.1	98.3–101.3*	96.3 ± 0.4	96.0–96.6*	86.6 ± 4.9	83.2–90.1*	93.6 ± 0.0	93.6–93.7*	95.9 ± 7.7	90.4–101.3*	90.5 ± 2.4*	88.9–92.2*						
DAL % LPL	57.3 ± 1.8	56.0–58.6*	55.7 ± 3.9	52.9–58.4*	56.2 ± 3.1	54.0–58.3*	57.2 ± 2.0	55.8–58.5*	60.8 ± 0.5	60.4–61.2*	57.5 ± 2.3*	55.8–59.1*						
DAW % LPW	65.4 ± 0.3	65.2–65.6*	64.6 ± 3.0	62.5–66.7*	68.7 ± 2.1	67.2–70.2*	68.8 ± 1.1	68.0–69.6*	68.8 ± 0.8	68.2–69.4*	67.8 ± 2.9*	65.7–69.8*						

Table 1. (continued). Measurements and counts of the piscivorous species of *Haplochromis* from the Lake Edward system.

	<i>H. kimondo</i> sp. nov. n = 21	<i>H. falcatus</i> sp. nov. n = 20	<i>H. curvidens</i> sp. nov. n = 7	<i>H. pardus</i> sp. nov. n = 20	<i>H. quasimodo</i> sp. nov. n = 21	<i>H. squamipinnis</i> n = 20
	Number & frequency	Number & frequency	Number & frequency	Number & frequency	Number & frequency	Number & frequency
UOT	43–70 (median 56)	39–51 (median 45)	45–60 (median 49)	39–56 (median 48)	46–71 (median 58)	39–79 (median 58)
LOT	32–55 (median 44)	26–40 (median 34)	20–46 (median 38)	29–41 (median 36)	34–59 (median 41)	29–44 (median 37)
UTR/LTR	1/2 (2); 2/1 (2); 2/2 (13); 2/3 (2); 3/2 (2)	1/1 (1); 1/2 (1); 2/1 (6); 2/2 (12)	1/1 (1); 2/1 (4); 2/2 (2)	2/2 (19); 3/2 (1)	1/1 (2); 2/1 (7); 2/2 (12)	2/1 (2); 2/2 (11); 3/1 (1); 3/2 (6)
LPTp/LPTm	18/10 19/10	16/10 21/10	20/10 22/11	22/11 22/12	20/13 21/11	17/11 18/11
DFR	XIV/10 (1); XV/9 (4); XV/10 (10); XV/11 (1); XVI/9 (4); XVI/10 (1)	XIV/9 (1); XIV/10 (1); XV/9 (7); XV/10 (10); XVI/10 (1)	XV/9 (2); XV/10 (2); XVI/8 (1); XVI/9 (2)	XV/10 (4); XVI/8 (2); XVI/9 (11); XVI/10 (3)	XV/9 (1); XV/10 (1); XV/11 (1); XVI/9 (1); XVI/10 (5); XVI/11 (2)	XV/9 (13); XV/10 (6); XVI/8 (1)
AFR	III/8 (7); III/9 (13); III/10 (1)	III/8 (2); III/9 (15); III/10 (3)	III/8 (2); III/9 (5)	III/8 (1); III/9 (14); III/10 (5)	III/8 (1); III/9 (18); III/10 (2)	III/9 (17); III/10 (2); III/11 (1)
PFR	11 (1); 12 (9); 13 (11)	12 (7); 13 (13)	12 (3); 13 (4)	12 (17); 13 (3)	12 (9); 13 (12)	11 (1); 12 (14); 13 (5)
GR	8/1/2 (5); 8/1/3 (2); 9/1/2 (6); 9/1/3 (3); 10/1/2 (2); 10/1/3 (2)	7/1/2 (1); 8/1/2 (2); 8/1/3 (5); 9/1/2 (1); 9/1/3 (11)	7/1/3 (1); 8/1/2 (1); 9/1/2 (1); 9/1/3 (1); 10/1/3 (2)	7/1/2 (1); 8/1/2 (5); 8/1/3 (5); 9/1/2 (3); 9/1/3 (4); 10/1/2 (1); 10/1/3 (1)	8/1/2 (2); 8/1/3 (2); 9/1/2 (4); 9/1/3 (8); 10/1/2 (3); 10/1/3 (1); 10/1/4 (1)	7/1/3 (1); 8/1/2 (2); 8/1/3 (4); 9/1/3 (8); 10/1/2 (1); 10/1/3 (4)
V	13/17 (1); 14/16 (18); 14/17 (2)	13/15 (1); 13/16 (16); 13/17 (2); 14/15 (1)	13/16 (1); 13/17 (1); 14/15 (1); 14/16 (3); 14/17 (1)	13/16 (3); 13/17 (8); 14/16 (9)	13/16 (4); 13/17 (3); 14/16 (12); 14/17 (2)	13/16 (16); 13/17 (2); 14/16 (2)
LongL	31 (2); 32 (4); 33 (8); 34 (6); 36 (1)	29 (1); 31 (4); 32 (9); 33 (4); 34 (2)	31 (1); 32 (3); 33 (2); 34 (1)	31 (2); 32 (10); 33 (7); 34 (1)	31 (1); 32 (6); 33 (8); 34 (4); 35 (1); 36 (1)	30 (2); 31 (6); 32 (8); 33 (2); 34 (2)
LatLu	19 (1); 20 (2); 21 (9); 22 (6); 23 (2); 24 (1)	20 (8); 21 (8); 22 (3); 23 (1)	20 (1); 21 (2); 22 (3); 23 (1)	20 (3); 21 (4); 22 (12); 23 (1)	18 (1); 19 (1); 20 (2); 21 (3); 22 (10); 23 (2); 24 (1); 27 (1)	17 (2); 19 (3); 20 (7); 21 (6); 22 (2)
LatLI	8 (2); 9 (6); 10 (6); 11 (5); 12 (2)	9 (1); 10 (4); 11 (6); 12 (4); 13 (2); 14 (3)	8 (2); 9 (2); 10 (1); 11 (2)	10 (3); 11 (7); 12 (5); 13 (2); 14 (3)	9 (2); 10 (5); 11 (3); 12 (6); 13 (5)	9 (1); 11 (3); 12 (9); 13 (5); 14 (1); 19 (1)
D-UULL	6 (4); 7 (15); 8 (2)	6 (11); 7 (8); 8 (1)	5 (3); 6 (1); 7 (3)	5 (4); 6 (14); 7 (2);	6 (11); 7 (9); 8 (1)	5 (9); 6 (8); 7 (3)
ULL-A	11 (4); 12 (12); 13 (4); 14 (1);	11 (5); 12 (6); 13 (7); 14 (2);	10 (2); 11 (5);	10 (11); 11 (9);	10 (6); 11 (5); 12 (3); 13 (6); 14 (1);	10 (1); 11 (4); 12 (9); 13 (5); 14 (1);
CP	17 (7); 18 (8); 19 (6);	17 (6); 18 (9); 19 (5);	16 (4); 17 (3);	16 (19); 17 (1);	16 (2); 17 (6); 18 (6); 19 (5); 20 (2);	16 (1); 17 (3); 18 (9); 19 (5); 20 (2);
V-P	6 (1); 7 (13); 8 (6); 10 (1);	6 (9); 7 (10); 8 (1);	5 (1); 6 (6);	5 (3); 6 (13); 7 (4);	6 (7); 7 (8); 8 (6);	4 (5); 5 (12); 6 (3);
ChSi	3 (4); 4 (15); 5 (2)	3 (6); 4 (9); 5 (5)	3 (4); 4 (3)	2 (1); 3 (18); 4 (1)	3 (3); 4 (12); 5 (6)	3 (10); 4 (6); 5 (4)
ChSp	9 (2); 10 (4); 11 (10); 12 (5)	8 (1); 9 (1); 10 (7); 11 (9); 12 (2)	9 (1); 10 (2); 11 (3); 12 (1)	9 (10); 10 (10)	8 (1); 9 (3); 10 (8); 11 (7); 12 (1); 13 (1)	8 (2); 9 (11); 10 (4); 11 (3)

PAR, KIM, and QUA) by mostly lower values for PC 3. All CUR and PAR specimens were partially separated from KIM and QUA specimens by their lower values for PC 1. Within the macrodontic groups, all specimens of LAT and MEN had mostly higher values for PC 3 than those of REX, SIM, GL, and AQ. Specimens of SIM had mostly lower values for PC 1 than those of AQ and GL, and those of REX had higher values for PC 1 than all other groups as mentioned above. Given that tooth counts often show allometric effects, all PCs were also plotted against SL, but no additional patterns were observed (not shown).

The MWU tests revealed significant ($P < 0.05$) differences between all groups tested (Table S8). The comparisons of REX-SIM revealed significant differences only in counts, while those of GL-SIM and GL-AQ revealed significant differences only in measurements. All other inter-group comparisons revealed significant differences in both measurements and counts. Comparisons of CUR-PAR could not be performed due to the limited size-range overlap. Besides differences in dominant male colour pattern and in oral outer tooth size (by which the groups were defined, see Fig. 2), all groups also differed in other qualitative traits, most notably in body shape, premaxillary pedicel prominence, snout outline in dorsal view, oral jaw stoutness, and oral outer tooth curvature (see Differential diagnoses in species descriptions below). Therefore, we confirm that all twelve a priori defined groups represent distinct species, of which ten constitute species so far unknown to science. Below, we present redescriptions of *H. squamipinnis* and *H. mentatus* and formal descriptions of *H. latifrons* sp. nov., *H. rex* sp. nov., *H. simba* sp. nov., *H. glaucus* sp. nov., *H. aquila* sp. nov., *H. kimondo* sp. nov., *H. falcatus* sp. nov., *H. curvidens* sp. nov., *H. pardus* sp. nov., and *H. quasimodo* sp. nov. For all species, the proportions of the measurements and the raw counts are summarised in Table 1.

Taxonomic account

Phylum Chordata Haeckel, 1874
Class Actinopterygii Klein, 1885
Order Cichliformes Betancur-R *et al.*, 2013
Family Cichlidae Bonaparte, 1840
Subfamily Pseudocrenilabrinae Fowler, 1934
Tribe Haplochromini Poll, 1986

Genus *Haplochromis* Hilgendorf, 1888

Haplochromis Hilgendorf, 1888: 76 (as a subgenus of *Chromis* Cuvier, 1814).

Haplochromis latifrons sp. nov.

[urn:lsid:zoobank.org:act:F6BB9E11-AF52-476E-87CE-5C2602859D1B](https://zoobank.org/urn:lsid:zoobank.org:act:F6BB9E11-AF52-476E-87CE-5C2602859D1B)

Figs 1–2, 5–7; Table 1

Differential diagnosis

Species with a piscivorous morphology; body very shallow [BD 27.2–30.1 (mean 28.6) % SL]; interorbital area flat and broad [IOW 57.4–63.3 (60.0) % HW]; outer oral teeth few and large [UOT 24–42 (median 31)]; females green dorsally, white ventrally, and with a well-defined mid-lateral band; dominant male colour pattern unknown.

Amongst piscivorous species from the Lake Edward system, *H. latifrons* sp. nov. differs from all, except *H. mentatus* and *H. kimondo* sp. nov., by the combination of a broader interorbital area [IOW 57.4–63.3 (60.0) vs 39.3–57.1 (43.9–53.8) % HW], a shorter anal fin base [AFB 14.7–17.3 (15.7) vs 17.1–22.2 (18.0–20.5) % SL], and a smaller number of branched anal-fin rays [AFRr 7–8 vs 9–11, rarely 8].

It differs from *H. mentatus* by the combination of a shorter dorsal-fin base [DFB 47.2–50.1 (49.0) vs 50.3–54.2 (52.3) % SL], a strongly vs weakly prominent premaxillary pedicel, a gentler sloping lower jaw side (25–30° vs 30–45°), juveniles and females green dorsally and white ventrally vs uniformly yellow-green, and presence vs absence of a well-defined mid-lateral band.

It differs from *H. kimondo* sp. nov. by the combination of large vs small outer oral teeth, a smaller number of outer upper jaw teeth [UOT 24–42 (31) vs 43–70 (56)], and a shorter anal fin base [AFB 14.7–17.3 (15.7) vs 17.0–19.2 (18.0) % SL].

Etymology

Specific name from Latin '*latus*' for 'wide' and '*frons*' for 'forehead'; referring to very broad interorbital area for a piscivorous species.

Material examined

Holotype

UGANDA • ♀, 158.2 mm SL; Lake Edward; 0°24'16.0" S, 29°46'24.8" E; 24 Jan. 2018; HIPE3 exped. leg.; bought at Rwenshama landing site; RMCA 2018.008.P.0330.

Paratypes

UGANDA – **Lake Edward** • 3 ♀♀, 122.8–134.9 mm SL; 0°12'00.0" S, 29°47'38.4" E; deep catch, open water ± 20 m deep; 23 Oct. 2016; HIPE1 exped. leg.; RMCA 2016.035.P.0199 to 0201 • 1 ♀, 105.4 mm SL; Rwenshama, rocky shore; 0°24'05.7" S, 29°46'35.1" E; 25 Mar. 2017; HIPE2 exped. leg.; RMCA 2017.006.P.0340 • 1 ♂, 82.2 mm SL; Kayanja offshore; 0°05'34.8" S, 29°45'28.8" E; 31 Mar. 2017; HIPE2 exped. leg.; RMCA 2017.006.P.0341 • 1 ♂, 75.3 mm SL; Kayanja offshore; 0°05'31.2" S, 29°45'30.3" E; 20 Jan. 2018; HIPE3 exped. leg.; RMCA 2018.008.P.0328 • 1 ♀, 155.7 mm SL; 0°24'16.0" S, 29°46'24.8" E; 24 Jan. 2018; HIPE3 exped. leg.; bought at Rwenshama landing site; RMCA 2018.008.P.0329.

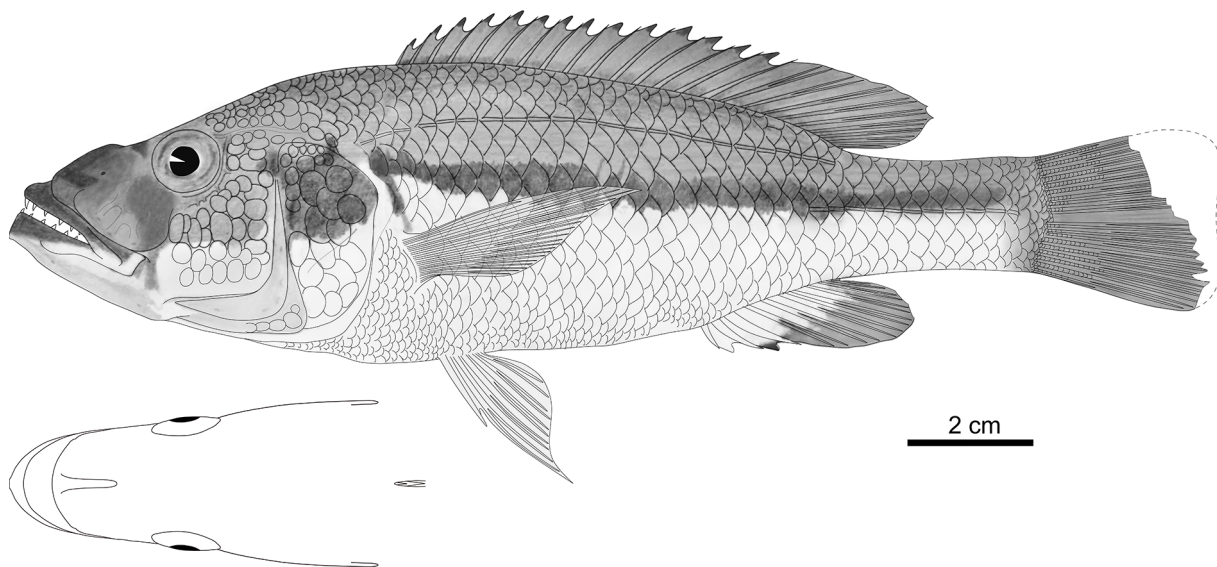


Fig. 5. *Haplochromis latifrons* sp. nov., holotype, ♀, 158.2 mm SL (RMCA 2018.008.P.0330). Drawn by N. Vranken.

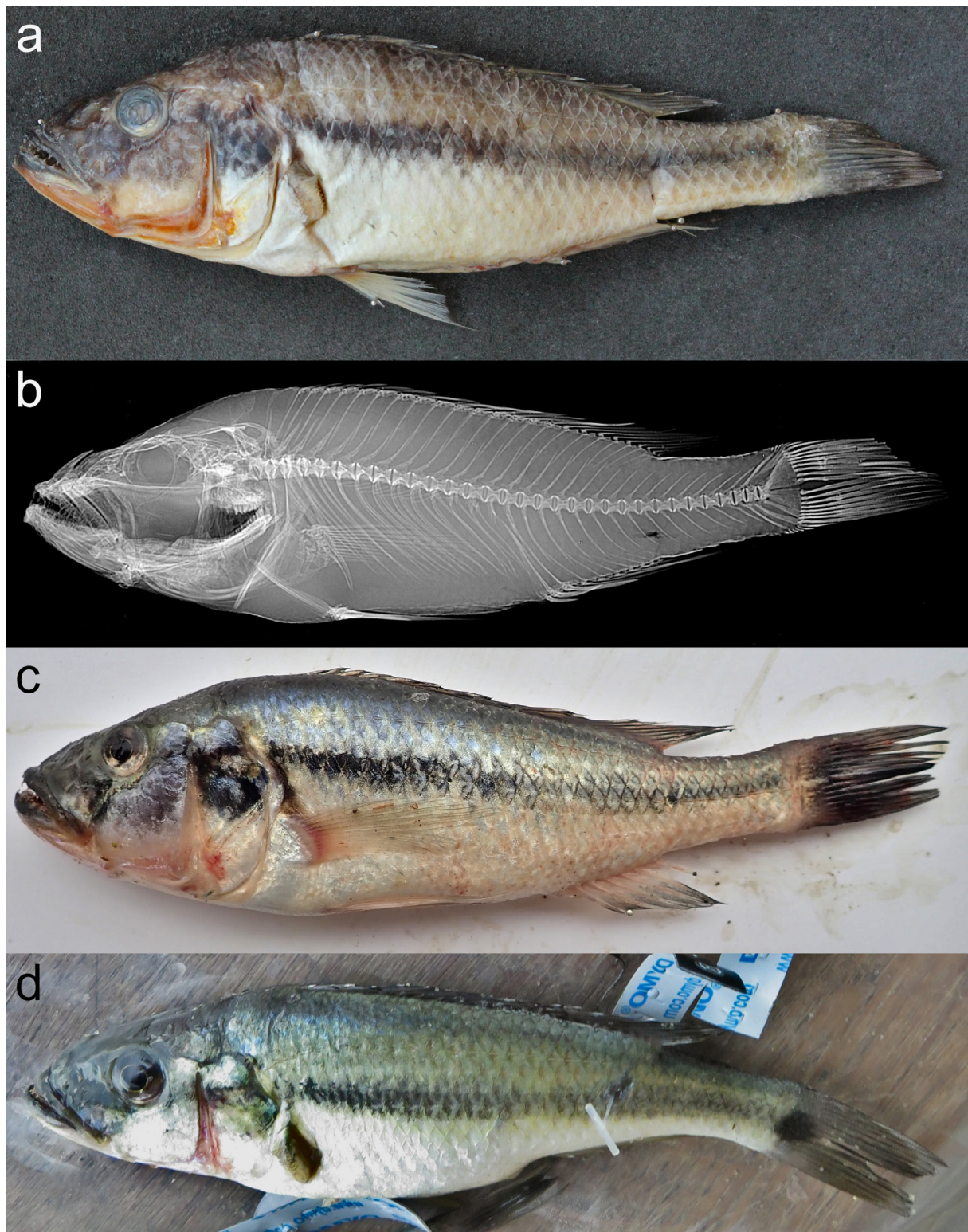


Fig. 6. *Haplochromis latifrons* sp. nov. **a.** Photograph of preserved holotype (RMCA 2018.008.P.0330; 158.2 mm SL). **b.** X-ray image of holotype. **c–d.** Photographs of freshly caught specimens. **c.** Holotype. **d.** Another female (RMCA 2017.006.P.0340; 105.4 mm SL) to illustrate the live colour patterns. The contrast was slightly enhanced.

Description

Based on 8 specimens (75.3–158.2 mm SL); body very shallow (Table 1) and oval to pyriform; caudal peduncle long (Fig. 5). Head narrow, dorsally flat, and with straight dorsal outline; interorbital area flat and average in width in comparison to generalised *H. elegans* (but very broad for a piscivorous species); eye very small and high on head; cheek and lacrimal deep. Snout very long, acute, and slopes gently at 30–40°; premaxillary pedicel long and strongly prominent. Jaws isognathous, long, stout, very narrow, and rounded in dorsal view; gape large and slopes gently at 15–25°; maxilla (almost) extends to vertical through anterior margin of orbit. Lower jaw relatively deep and with a weakly convex ventral outline in lateral view, mental prominence absent or weakly developed, and lower jaw side nearly flat with an inclination of 25–30° to horizontal in anterior view. Upper jaw expanded anteriorly. Lips and oral mucosa large. Neurocranium shallow, ethmo-vomerine block decurved, preorbital region very shallow (19–21% NL), orbital region shallow (27–32% NL), and supraoccipital crest very shallow and pyramidal or wedge-shaped (Fig. 6b).

Outer oral teeth few, unicuspid, and large. Necks stout, conical, and straight; crowns recurved and acutely pointed. Dental arcades rounded. Outer teeth widely and very irregularly set with neck-distances of 1–5 neck-widths. In upper jaw, 2–3 posteriormost teeth enlarged. Inner teeth relatively large, recurved, unicuspid in large specimens (> 75 mm SL), tricuspid in small specimens (< 75 mm SL). Tooth bands

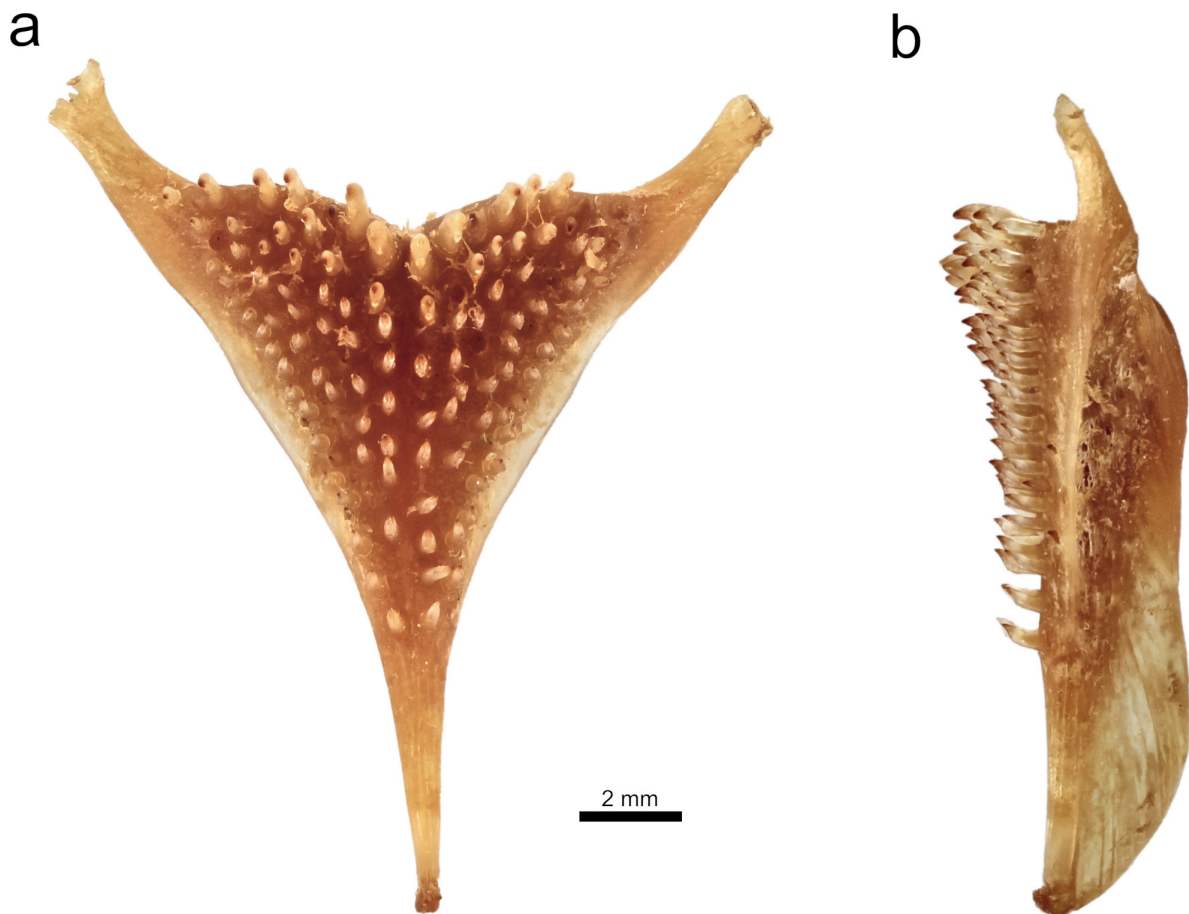


Fig. 7. *Haplochromis latifrons* sp. nov. (RMCA 2018.008.P.0329; 155.7 mm SL). **a.** Dorsal view of the lower pharyngeal jaw. **b.** Lateral view of the lower pharyngeal jaw.

very slender crescent-shaped with 1–3 rows of inner teeth and narrow posteriorly until only outer row remains past $\frac{2}{3}$ length of tooth band in upper jaw, past $\frac{1}{2}$ length of tooth band in lower jaw. Inner teeth widely and irregularly set on $\frac{1}{2}$ –1 outer neck-width from outer row; implantation erect in first row and recumbent in subsequent rows; size decreases slightly buccally and posteriorly.

Lower pharyngeal bone long, narrow, slim, and shallow over entire length (Fig. 7). Pharyngeal teeth relatively large and slender; major cusps acutely pointed; cusp gaps concave; minor cusps and cusp protuberances very small. Teeth in two median longitudinal rows equal in size and form to lateral teeth, about 10 in each row. Posterior transverse row with 15–16 teeth, implanted recumbently with lateral inclination; major cusps recurved, bluntly pointed, and laterally compressed; minor cusps small.

Chest scales small; transition to larger flank scales gradual. Minute scales on proximal half of caudal fin.

Caudal fin emarginate; dorsal and anal fins reach to vertical through 2–4 scales anterior to caudal-fin base. Pectoral and pelvic fins reach to just anterior to genital opening in females, unknown in males; first branched pelvic-fin ray slightly elongated in all specimens.

Ceratobranchial gill rakers in outer row of first gill arch short, stout, and simple; posteriormost rakers simple to trifold or anvil-shaped. Epibranchial gill rakers slender and simple.

Colouration in life

Dominant males: colour pattern unknown.

Females and juveniles: dorsal parts of body and operculum olive-green; ventral parts of body and operculum white; abrupt transition at height of lower lateral line (Fig. 6c–d). Flank with a well-defined black mid-lateral band from posterior margin of eye to caudal-fin base. Dorsum with a blue sheen; cheek and lower jaw white; lacrimal, snout, and lips dusky olive-green; eye with dark grey outer ring and golden inner ring. Nostril and interorbital stripes faint; lacrimal blotch large anteroventrally of eye. Pectoral fin yellowish; pelvic fin hyaline with a greenish sheen; dorsal and caudal fins uniformly dusky, dorsal fin with black lappets (i.e., distal extensions of membrane between spines); anal fin with a hyaline-white base, a dusky-yellow distal part, and 1–2 small spots resembling egg-spots.

Preserved colouration

Females and juveniles: dorsal part of body brown; ventral part of body, cheek, and lower jaw white; lacrimal, snout and lips dusky (Fig. 6a). Flank with a mid-lateral band from posterior margin of eye to caudal-fin base. Nostril and interorbital stripes faint, lacrimal blotch present. Pectoral fin hyaline; pelvic fin white; dorsal and caudal fins uniformly dusky, dorsal fin with black lappets; anal fin with a white base and dusky distally.

Distribution and ecology

Only known from Lake Edward, found in offshore areas. Based on its morphology, most probably a piscivorous species.

Haplochromis mentatus Regan, 1925

Figs 1–2, 8–10; Table 1

Haplochromis mentatus Regan, 1925: 188, pl. 10.

Haplochromis mentatus – Greenwood 1973: 204.

Harpagochromis mentatus – Greenwood 1980: index.

Differential diagnosis

Species with a piscivorous morphology; body shallow [BD 29.0–32.3 (mean 31.2) % SL]; snout very acute in dorsal and lateral views; outer oral teeth few and large [UOT 28–46 (median 36)]; vertebrae many (Va+Vc 30–32); dominant males yellow-green with a red anterior part of flank.

Amongst piscivorous species from the Lake Edward system, *H. mentatus* differs from *H. latifrons* sp. nov. by the combination of a longer dorsal fin base [DFB 50.3–54.2 (52.3) vs 47.2–50.1 (49.0) % SL], a weakly vs strongly prominent premaxillary pedicel, a steeper sloping lower jaw side (30–45° vs 25–30°), and absence vs presence of a well-defined mid-lateral band.

It differs from *H. rex* sp. nov. and *H. aquila* sp. nov. by the combination of a longer caudal peduncle [CPL 15.7–17.5 (16.6) vs 13.5–16.2 (14.8–15.0) % SL], a gentler sloping snout (30–35° vs 35–50°), and dominant males yellow-green with a red anterior part of flank vs cream-coloured with an orange operculum, or light grey with a black head, respectively; further from *H. rex* sp. nov. by a larger number of infraorbital cheek scales [ChSi 3–4 vs 5–6 (rarely 4 or 7)]; further from *H. aquila* sp. nov. by smaller eyes [ED 25.4–29.9 (27.2) vs 30.0–31.5 (30.6) % HL].

It differs from *H. simba* sp. nov. by the combination of a broader interorbital area [IOW 51.3–61.0 (55.5) vs 45.5–50.4 (48.1) % HW], a larger number of outer upper jaw teeth [UOT 28–46 (36) vs 22–31 (27)], absent to weakly prominent vs strongly prominent premaxillary pedicel and mentum, and dominant males yellow-green with a red anterior part of flank vs yellow with an orange anterior part of flank.

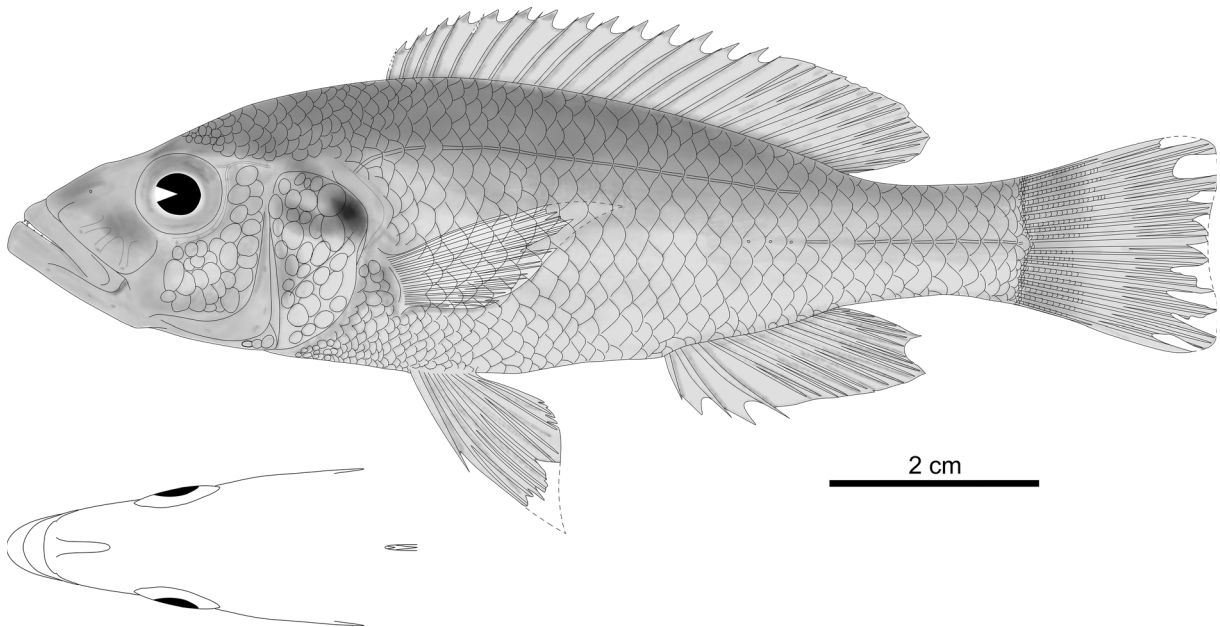


Fig. 8. *Haplochromis mentatus* Regan, 1925, holotype, ♀, 93.1 mm SL (MCZ 31523) reconstructed with a straightened vertebral column. Drawn by N. Vranken.

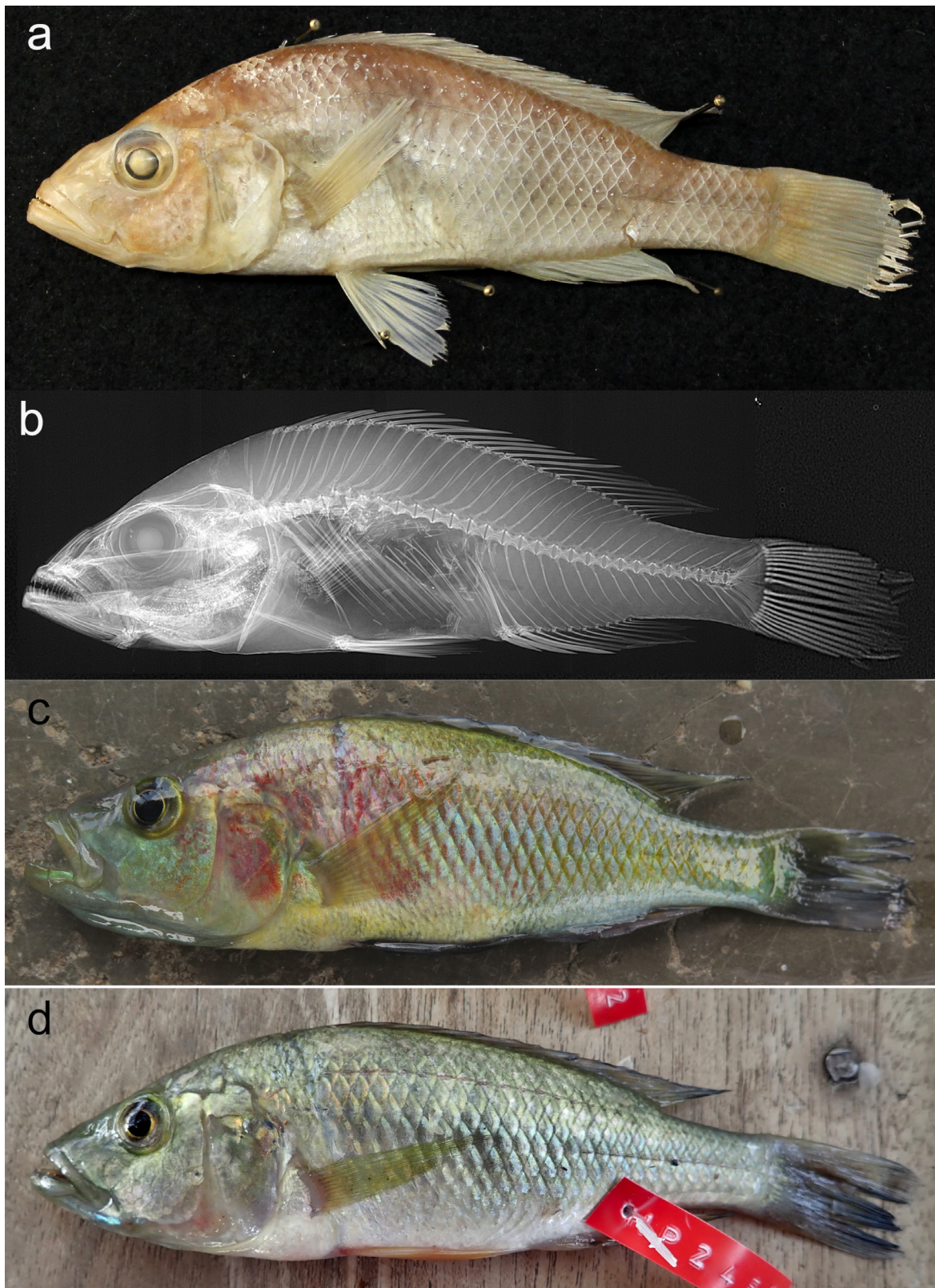


Fig. 9. *Haplochromis mentatus* Regan, 1925. **a.** Photograph of preserved holotype (MCZ 31523; 93.1 mm SL). **b.** X-ray image of holotype. **c–d.** Photographs of freshly caught specimens. **c.** Dominant male (RMCA 2017.006.P.0424; 107.9 mm SL). **d.** Female (RMCA 2018.008.P(HP2453); 116.2 mm SL) to illustrate the live colour patterns. The contrast was slightly enhanced.

It differs from *H. glaucus* sp. nov. by the combination of a longer caudal peduncle [CPL 15.7–17.5 (16.6) vs 13.4–16.1 (14.8) % SL], a narrower lower pharyngeal bone [LPW 83.6–85.7 vs 93.3–95.1% LPL], a slightly shorter pre-pectoral distance [PrP 33.1–38.2 (36.0) vs 36.4–39.4 (38.1) % SL], and dominant males yellow-green with a red anterior part of flank vs uniformly blue.

It differs from *H. kimondo* sp. nov. and *H. quasimodo* sp. nov. by the combination of a narrower head [HW 39.4–42.3 (40.8) vs 42.0–48.1 (45.1–45.3) % HL] and dominant males yellow-green with a red anterior part of flank vs grey dorsally and yellow or blue-black ventrally; further from *H. kimondo* sp. nov. by a very acute vs blunt snout, and a gentler sloping snout (30–35° vs 40–50°); further from *H. quasimodo* sp. nov. by a shallower body [BD 27.2–30.1 (28.6) vs 33.5–41.7 (37.4) % SL].

It differs from *H. falcatus* sp. nov. by the combination of a shorter predorsal distance [PrD 33.3–36.4 (35.3) vs 36.9–41.1 (39.5) % SL], a shorter head [HL 33.4–37.0 (35.1) vs 36.6–39.6 (38.2) % SL], straight to weakly recurved vs strongly recurved outer oral teeth, a steeper lower jaw side (30–45° vs 15–25°), absence vs presence of well-defined mid-lateral and dorsal-lateral bands.

It differs from *H. curvidens* sp. nov. and *H. pardus* sp. nov. by the combination of a deeper lacrimal [LaD 18.1–20.9 (19.7) vs 16.0–18.3 (16.7–17.3) % HL] and smaller eyes [ED 25.4–29.9 (27.2) vs

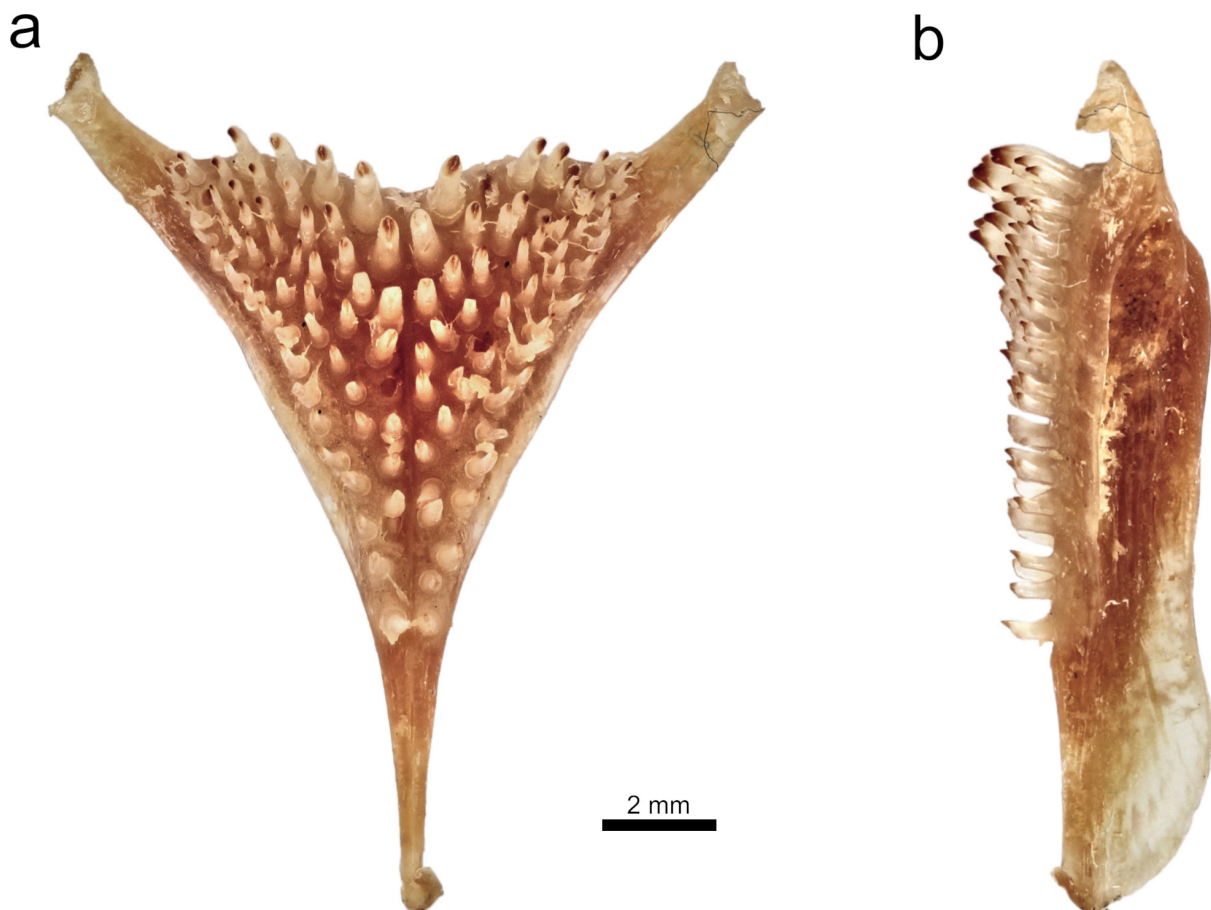


Fig. 10. *Haplochromis mentatus* Regan, 1925 (RMCA 2018.008.P.0389; 137.1 mm SL). **a.** Dorsal view of the lower pharyngeal jaw. **b.** Lateral view of the lower pharyngeal jaw.

29.4–34.1 (30.4–31.9) % HL]; further from *H. pardus* sp. nov. by dominant males yellow-green with a red anterior part of flank vs speckled to uniformly black.

It differs from *H. squamipinnis* by the combination of large vs small outer oral teeth and a smaller number of outer upper jaw teeth [UOT 28–46 (36) vs 46–71 (58)], a shallower body [BD 29.0–32.3 (31.2) vs 32.4–39.3 (35.7) % SL], absence vs presence of minute scales on proximal part of dorsal fin, and dominant males yellow-green with a red anterior part of flank vs uniformly slate blue.

Etymology

Specific name not explained in original description, probably derived from the Latin ‘*mentum*’ for ‘chin’; probably referring to the protruding lower jaw (i.e., projecting lower jaw sensu Regan 1925).

Material examined

Holotype

UGANDA • ♀, 93.1 mm SL; Lake Edward; 1924; J.C. Phillips leg.; MCZ 31523.

Other material

UGANDA – **Lake Edward** • 1 ♂, 94.4 mm SL; ‘Coral Reef’, hard substrate at mouth of Nyamugasani River; 0°10′08.4″ S, 29°49′37.2″ E; 21 Oct. 2016; HIPE1 exped. leg.; RMCA 2016.035.P.0255 • 1 ♂, 2 ♀♀, 111.3–128.1 mm SL; Rwenshama, rocky shore; 0°24′05.7″ S, 29°46′35.1″ E; 25 Mar. 2017; HIPE2 exped. leg.; RMCA 2017.006.P.0408 to 0410 • 3 ♂♂, 111.5–118.5 mm SL; Kayanja offshore; 0°05′34.8″ S, 29°45′28.8″ E; 30 Mar. 2017; HIPE2 exped. leg.; RMCA 2017.006.P.0411 to 0413 • 1 ♂, 117.7 mm SL; same collection data as for preceding; RMCA 2017.006.P.0414 • 1 ♀, 1 ♂, 87.2–133.2 mm SL; islands near Katwe; 0°10′04.9″ S, 29°52′27.4″ E; 18 Jan. 2018; HIPE3 exped. leg.; RMCA 2018.008.P.0380 to 0381 • 1 ♀, 1 ♂, 87.8–95.5 mm SL; same collection data as for preceding; RMCA 2018.008.P.0383 to 0384 • 2 ♀♀, 108.3–137.2 mm SL; 0°24′16.0″ S, 29°46′24.8″ E; 24 Jan. 2018; HIPE3 exped. leg.; bought at Rwenshama landing site; RMCA 2018.008.P.0387 to 0388 • 1 ♂, 137.1 mm SL; 0°24′16.0″ S, 29°46′24.8″ E; 1 Feb. 2018; HIPE3 exped. leg.; bought at Rwenshama landing site; RMCA 2018.008.P.0389. – **Lake George** • 1 ♂, 107.9 mm SL; ‘Bivalve Site’, north of Kankurunga Island; 0°00′39.6″ N, 30°08′13.2″ E; 29 Mar. 2017; HIPE2 exped. leg.; RMCA 2017.006.P.0424 • 1 ♀, 92.1 mm SL; Kashaka bay, north of inlet; 0°04′52.2″ S, 30°10′47.3″ E; 2 Feb. 2018; HIPE3 exped. leg.; RMCA 2018.008.P.0394 • 2 ♀♀, 94.0, 120.0 mm SL; same collection data as for preceding; RMCA 2018.008.P.0395 to 0396.

Description

Based on 20 specimens (87.2–137.2 mm SL); body shallow (Table 1) and oval; caudal peduncle long (Fig. 8). Head very narrow and with a straight dorsal outline and a slightly convex nape; cheek average in depth; lacrimal deep; eye small; interorbital area narrow in comparison to generalised *H. elegans* (but relatively broad for a piscivorous species). Snout long, very acute in dorsal and lateral views, and slopes very gently at 30–35°; premaxillary pedicel long and weakly prominent. Jaws long, very narrow, acute in dorsal view, relatively slim, and isognathous; gape large and slopes gently at 20–30°; posterior tip of maxilla reaches a vertical just past anterior margin of orbit. Lower jaw slim and with a straight to weakly concave ventral outline in lateral view, mental prominence absent or weakly developed, and lower jaw side steep with an inclination of 30–45° to horizontal in anterior view. Upper jaw expanded anteriorly and weakly ventrally. Lips and oral mucosa large. Neurocranium shallow, ethmo-vomerine block decurved, preorbital region very shallow (18–22% NL), orbital region shallow (28–31% NL), and supraoccipital crest shallow and wedge-shaped (Fig. 9b).

Outer oral teeth few, unicuspid, and large. Necks stout, conical, and straight; crowns slightly recurved and acutely pointed. Dental arcades acute. Outer teeth widely and irregularly set with neck-distances of

$\frac{1}{2}$ –2 neck-widths. In upper jaw, 1–3 posteriormost teeth slightly enlarged. Inner teeth small, strongly recurved, unicuspid, and acutely pointed. Tooth bands very slender crescent-shaped with 1–2 rows of inner teeth, and narrow posteriorly until only outer row remains past $\frac{2}{3}$ length of tooth band in upper jaw, past $\frac{1}{2}$ length of tooth band in lower jaw. Inner teeth closely and regularly set on 1–2 outer neck-widths from outer row; implantation recumbent; size uniform.

Lower pharyngeal bone long, narrow, slim, and shallow over whole length (Fig. 10). Pharyngeal teeth relatively large and slender; major cusps acutely pointed; cusp gaps concave; minor cusps and cusp protuberances mostly absent. Teeth in two median longitudinal rows equal in size and form to lateral teeth, 11 in each row. Posterior transverse row with 14–21 teeth, implanted recumbently with a lateral inclination; major cusps nearly straight, bluntly pointed, and laterally compressed; minor cusps mostly absent.

Chest scales small; transition to larger flank scales gradual. In some specimens, basal parts of membranes between anal-fin spines covered by few (1–3) minute, ellipsoid scales (nearly invisible to naked eye); remaining part of anal and dorsal fins scale-less. Minute scales on proximal half of caudal fin.

Caudal fin emarginate; dorsal and anal fins reach to between vertical through caudal-fin base and two scales anterior to this vertical. Pectoral and pelvic fins reach to between genital opening and first anal-fin spine; pelvic fin reaches to third anal-fin spine in males; first branched pelvic-fin ray slightly elongated in all specimens.

Ceratobranchial gill rakers in outer row of first gill arch short, stout, and simple; posteriormost rakers mostly anvil-shaped or weakly bifid. Epibranchial rakers slender and simple.

Colouration in life

Dominant males: body, cheek, and lower jaw yellow-green with blue sheen; flank, dorsal part of head, and operculum bright red; belly and chest speckled black (Fig. 9c). Snout and lips dusky; branchiostegal membrane black; eye with (dark) grey outer ring and yellow inner ring. Flank with very faint mid-lateral, dorsal-lateral, and 5–7 vertical stripes; nostril stripe faint. Dorsal and anal fins dusky and with black lappets; anal fin with a crimson distal part and 2 small orange egg spots with dusky rings. Caudal fin dusky with a crimson distal part. Pectoral fin dusky yellow and pelvic fin black.

Females and juveniles: dorsal parts of body and operculum green-yellow; gradual transition to white ventral parts of body and operculum, cheek, and lower jaw; flank with a blue sheen (Fig. 9d). Lacrimals, snout, and lips dusky green; lacrimals with a blue sheen; eye with (dark) grey outer ring and yellow inner ring. Nostril stripe faint. Dorsal fin dusky and with black lappets; anal fin white-yellow and with 1–2 small spots resembling egg-spots; caudal fin dusky. Pectoral fin yellowish; pelvic fin white-yellow.

Preserved colouration

In dominant males, body uniformly brown, pectoral fin dusky, pelvic fin black, and anal fin dusky and with 1–2 small egg-spots (Fig. 9a). In females, dorsal part of body yellowish, gradual transition to white ventral part of body, cheek light yellow, pectoral fin hyaline, pelvic fin yellowish, and anal fin with a white base and a dusky distal part. In all specimens, snout dusky and nostril, interorbital, and lacrimal stripes faint. Dorsal fin dusky and with black lappets; caudal fin dusky.

Distribution and ecology

Endemic to Lake Edward system, found in offshore areas, mostly in shallow waters. Based on its morphology, most probably a piscivorous species.

Systematic comment

Both Trewavas (1933) and Greenwood (1973) noted that the holotype of *H. mentatus* strongly resembled *H. squamipinnis*. Greenwood recognised that this specimen deviated from *H. squamipinnis* in that it lacked minute scales on the basal parts of the dorsal- and anal-fin membranes, but he was uncertain about the relevance of this difference. We found this trait to be present in all *H. squamipinnis* specimens. We discovered that abdominal vertebrae 6–9 of the holotype of *H. mentatus* are broken and the vertebral column kinked (Fig. 9b). This resulted in the holotype of *H. mentatus* having an aberrant rhomboid-shaped instead of an oval body as in other specimens of its species. Because of this deformation, the specimen indeed resembles *H. squamipinnis* in overall habitus.

Haplochromis rex sp. nov.

[urn:lsid:zoobank.org:act:EF8B7189-BCA4-4A72-8387-498689D76CEB](https://zoobank.org/act:EF8B7189-BCA4-4A72-8387-498689D76CEB)

Figs 1–2, 11–13; Table 1

Differential diagnosis

Species with a piscivorous morphology; head narrow [HW 36.8–41.6 (mean 39.2) % HL]; cheek deep [ChD 27.6–33.5 (31.1) % HL]; eye small [ED 22.2–28.3 (24.6) % HL]; outer oral teeth few and large [UOT 24–36 (median 29)]; dominant males cream-coloured with an orange operculum and a light blue snout.

Amongst piscivorous species from the Lake Edward system, *H. rex* sp. nov. differs from *H. latifrons* sp. nov. and *H. mentatus* by the combination of a shorter caudal peduncle [CPL 13.5–16.2 (14.8) vs 15.7–18.0 (16.6–17.0) % SL] and a narrower interorbital area [IOW 44.9–52.7 (48.9) vs 51.3–63.3 (55.5–60.0) % HW]; further from *H. latifrons* sp. nov. by absence vs presence of a well-defined mid-lateral band; further from *H. mentatus* by dominant males cream-coloured with an orange operculum vs yellow-green with a red anterior part of flank.

It differs from *H. simba* sp. nov. by the combination of a larger number of longitudinal line scales (LongL 34–38 vs 32–33), a larger number of scales between first anal-fin spine and upper lateral line (ULL-A 12–16 vs 9–11), absent or weakly developed vs strongly developed mental prominence, and dominant males cream-coloured with an orange operculum and a light blue snout vs yellow with an orange anterior part of flank and a yellow snout.

It differs from *H. glaucus* sp. nov. by the combination of a narrower interorbital area [IOW 44.9–52.7 (48.9) vs 50.9–57.1 (53.8) % HW], a steeper snout (40–50° vs 30–40°), rounded vs acute oral jaws in dorsal view, and dominant males cream-coloured with an orange operculum and a light blue snout vs uniformly light blue with a dusky snout.

It differs from *H. aquila* sp. nov. by the combination of a deeper lacrimal [LaD 18.9–22.5 (20.8) vs 17.0–19.1 (18.3) % HL], smaller eye [ED 22.2–28.3 (24.6) vs 30.0–31.5 (30.6) % HL], and dominant males cream-coloured with an orange operculum vs light grey with a black head.

It differs from *H. kimondo* sp. nov., *H. falcatus* sp. nov., *H. curvidens* sp. nov., *H. pardus* sp. nov., *H. quasimodo* sp. nov., and *H. squamipinnis* by the combination of stout vs slim oral jaws, large vs small outer oral teeth, and a smaller number of outer upper jaw teeth [UOT 24–36 (29) vs 39–79 (45–58)].

It further differs from *H. kimondo* sp. nov., *H. curvidens* sp. nov., and *H. quasimodo* sp. nov. by a narrower head [HW 36.8–41.6 (39.2) vs 42.0–48.1 (43.4–45.3) % HL]; further from *H. kimondo* sp. nov. and *H. quasimodo* sp. nov. by dominant males cream-coloured with an orange operculum vs grey dorsally and yellow or blue-black ventrally.

It further differs from *H. falcatus* sp. nov., *H. pardus* sp. nov., and *H. squamipinnis* by a larger number of longitudinal line scales (LongL 34–38 vs 29–33, rarely 34) and dominant males cream-coloured with an orange operculum vs uniformly olive-green with an orange-red anterior part of flank, speckled to uniformly black, or uniformly slate blue, respectively.

Etymology

Specific name from the Latin ‘*rex*’ for ‘king’ (one that holds a preeminent position); referring to very small eyes, deep cheeks, and strong jaws set with large and acute teeth indicating this piscivore has most specialised morphology among all piscivores from the Lake Edward system to hunt on large prey (Barel *et al.* 1977).

Material examined

Holotype

UGANDA • ♂, 148.5 mm SL; Lake Edward; 0°24'16.0" S, 29°46'24.8" E; 24 Jan. 2018; HIPE3 exped. leg.; bought at Rwenshama landing site; RMCA 2018.008.P.0345.

Paratypes

DEMOCRATIC REPUBLIC OF THE CONGO • 1 ♂, 131.5 mm SL; “Lac Edouard: Vitshumbi (contre le pier)” [Lake Edward: Vitshumbi (against the pier)]; 0°40'50.6" S, 29°23'22.6" E (inferred); 26 Mar. 1953; KEA exped. leg.; IRSNB 13474 • 1 ♂, 154.2 mm SL; “Lac Edouard: 2–3 km ± 500 m au large à l’Ouest de Kiavinionge” [Lake Edward: 2–3 km ± 500 m offshore west of Kiavinionge]; 0°11'39" S, 29°32'31" E (inferred); 1 Jun. 1953; KEA exped. leg.; IRSNB 13480 • 1 ♀, 154.8 mm SL; “Lac Edouard: 2–3 km à l’Ouest de Kiavinionge” [Lake Edward: 2–3 km west of Kiavinionge]; 0°11'39" S, 29°32'31" E (inferred); 1 Jun. 1953; KEA exped. leg.; IRSNB 13485.

UGANDA – Lake Edward • 1 ♂, 114.4 mm SL; 0°12'00.0" S, 29°47'38.4" E; 23 Oct. 2016; HIPE1 exped. leg.; deep catch, open water ± 20 m deep; RMCA 2016.035.P.0220 • 1 ♂, 154.5 mm SL;

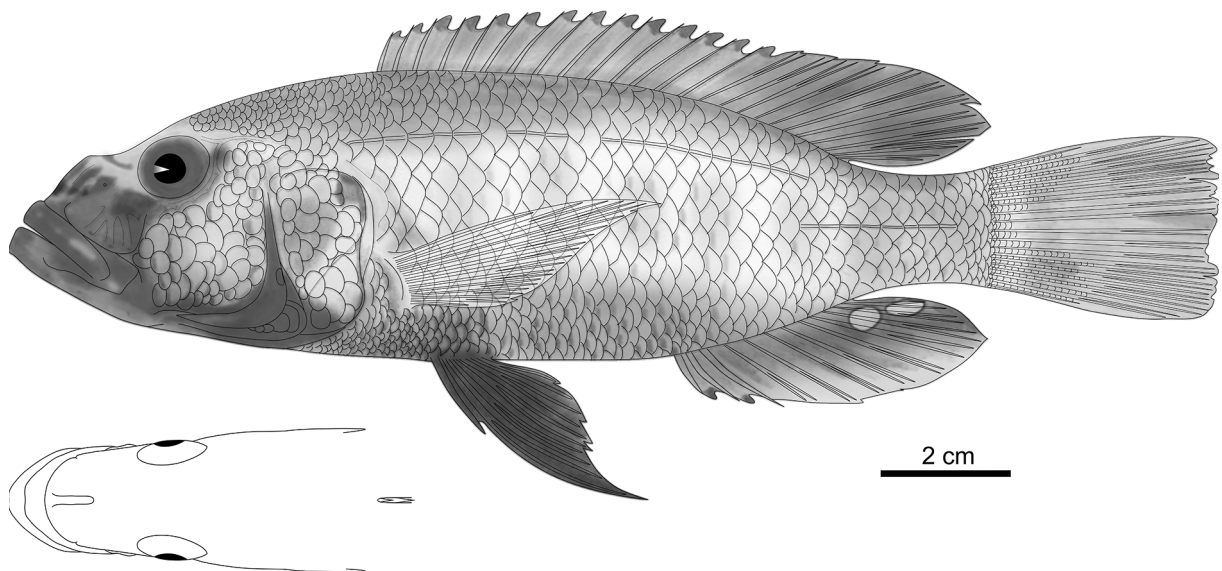


Fig. 11. *Haplochromis rex* sp. nov., holotype, ♂, 148.5 mm SL (RMCA 2018.008.P.0345). Drawn by N. Vranken.

0°08'51.9" S, 29°52'59.6" E; 24 Oct. 2016; HIPE1 exped. leg.; bought at Katwe landing site; RMCA 2016.035.P.0221 • 1 ♂, 114.7 mm SL; Rwenshama, rocky shore; 0°24'05.7" S, 29°46'35.1" E; 26 Mar. 2017; HIPE2 exped. leg.; RMCA 2017.006.P.0352 • 1 ♂, 2 ♀♀, 101.0–140.0 mm SL; Kayanja offshore; 0°05'34.8" S, 29°45'28.8" E; 31 Mar. 2017; HIPE2 exped. leg.; RMCA 2017.006.P.0353 to 0355 • 1 ♀, 80.5 mm SL; Kayanja offshore; 0°05'31.2" S, 29°45'30.3" E; 20 Jan. 2018; HIPE3 exped. leg.; RMCA 2018.008.P.0342 • 1 ♂, 1 ♀, 134.6, 147.7 mm SL; 0°24'16.0" S, 29°46'24.8" E; 24 Jan. 2018; HIPE3 exped. leg.; bought at Rwenshama landing site; RMCA 2018.008.P.0343 to 0344 • 1 ♀, 84.2 mm SL; Rwenshama, offshore; 0°24'14.4" S, 29°45'57.0" E; 24 Jan. 2018; HIPE3 exped. leg.; RMCA 2018.008.P.0346 • 1 ♂, 128.3 mm SL; Kagoro fishing ground; 0°12'50.1" S, 29°49'19.7" E; 4 Feb. 2018; HIPE3 exped. leg.; open water; RMCA 2018.008.P.0347 • 1 ♀, 134.2 mm SL; Kayanja offshore; 0°05'34.8" S, 29°45'28.8" E; 21 Mar. 2019; HIPE4 exped. leg.; RMCA 2019.002.P.0014.

Description

Based on 16 specimens (80.5–154.8 mm SL); body shallow (Table 1) and oval to rectangular (Fig. 11). Head long, very narrow, and with a (weakly) convex dorsal outline; cheek deep; lacrimal very deep; eye very small and very high on head; interorbital area very narrow. Snout long, rounded in dorsal view, blunt, and slopes at 40–50°; premaxillary pedicel long and strongly prominent. Jaws isognathous to weakly prognathous, long, very narrow, stout, and rounded in dorsal view; jaws expand slightly laterally, hereby often broader than snout. Gape large and slopes gently at 15–25°; maxilla extends to vertical through anterior margin of orbit. Lower jaw relatively deep and with a straight ventral outline in lateral view, mental prominence absent or weakly developed, and lower jaw side with an inclination of 30–35° to horizontal in anterior view. Upper jaw strongly expanded anteriorly. Lips and oral mucosa large. Neurocranium shallow, ethmo-vomerine block decurved, preorbital region very shallow (18–20% NL), orbital region shallow (26–29% NL), and supraoccipital crest shallow and wedge-shaped (Fig. 12b).

Outer oral teeth few, unicuspid, and large. Necks very stout, conical, and straight; crowns weakly recurved, rarely straight, and acutely pointed. Dental arcades rounded. Outer teeth widely and regularly set with neck-distances of 1–2 neck-widths. No enlarged teeth posterior in upper jaw. Inner teeth straight to recurved, unicuspid, and relatively small in small specimens (< 125 mm SL), and large in large specimens (> 125 mm SL). Tooth bands very slender crescent-shaped with 1–3 rows of inner teeth, and narrow posteriorly until only outer row remains past $\frac{2}{3}$ length of tooth band in upper jaw, past $\frac{1}{2}$ length of tooth band in lower jaw. Inner teeth widely and regularly set on 1–2 outer neck-widths from outer row; implantation erect in first row and recumbent in subsequent rows; size decreases slightly buccally and posteriorly.

Lower pharyngeal bone average in length, narrow, slim, and shallow over whole length (Fig. 13). Pharyngeal teeth relatively large and slender; major cusps acutely pointed; cusp gaps concave; minor cusps and cusp protuberances mostly absent. Teeth in two median longitudinal rows equal in size and form to lateral teeth, 11 in each row. posterior transverse row with 15–16 teeth, implanted recumbently with a lateral inclination; major cusps weakly recurved, bluntly pointed, and laterally compressed; minor cusps mostly absent.

All scales relatively small, many scale rows between anal fin and upper lateral line (12–16), infraorbital scales on cheek (4–7), and scales around caudal peduncle (18–20); many scales in longitudinal line (34–38); chest scales small; transition to larger flank scales gradual. Minute scales on proximal half of caudal fin.

Caudal fin emarginate; dorsal and anal fins reach to between verticals through two scales anterior to and one scale posterior to caudal-fin base. Pectoral fin reaches to between anal opening and three scales

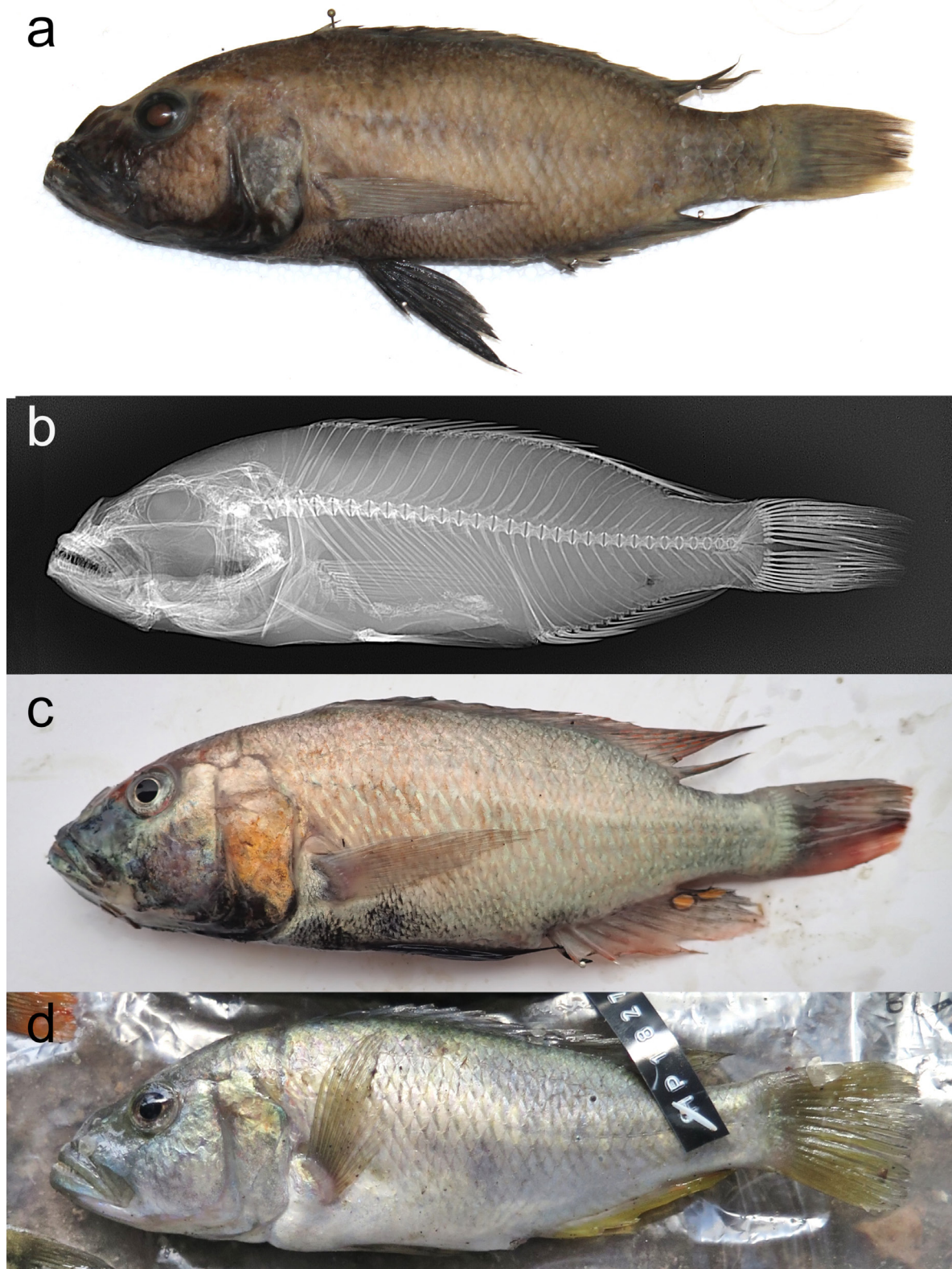


Fig. 12. *Haplochromis rex* sp. nov. **a.** Photograph of preserved holotype (RMCA 2018.008.P.0345; 148.5 mm SL). **b.** X-ray image of holotype **c–d.** Photographs of freshly caught specimens. **c.** Holotype, a dominant male. **d.** A female (RMCA 2017.006.P.0355; 135.7 mm SL) to illustrate the live colour patterns. The contrast was slightly enhanced.

anterior to this point; pelvic fin reaches to anal opening in females, to first anal-fin spine in males; first branched pelvic-fin ray not elongated.

Ceratobranchial gill rakers in outer row of first gill arch short, stout, and simple; posteriormost rakers anvil-shaped to weakly trifold. Epibranchial gill rakers relatively slender and simple.

Colouration in life

Dominant males: body cream-coloured with faint orange sheen; dorsum greyish; belly and chest black; caudal peduncle with blue sheen (Fig. 12c). Operculum, dorsal part of head, and interorbital area orange; snout, lower jaw, and lips light blue; cheek white and speckled black; eye with (dark) grey outer ring and silver inner ring. Nostril, interorbital, supraorbital, and lacrimal stripes faint; mental blotch present. Pectoral and dorsal fin hyaline; dorsal fin with a dusky base, a dusky and maculated posterior part, and orange lappets, except for black anteriormost lappets. Pelvic fin black; anal and caudal fins orange-red and with dusky bases; anal fin with dusky posterior part and 1–3 small orange egg-spots with dusky rings; caudal fin dorsally maculated orange.

Females and juveniles: body cream-coloured with yellow sheen; dorsum and dorsal part of head greyish; belly, chest, operculum, cheek, and lower jaw white; snout dusky and faint light blue; eye with (dark) grey outer ring and silver inner ring (Fig. 12d). Nostril, interorbital, supraorbital, and lacrimal stripes slender and well-defined; mental blotch present. Pectoral, pelvic, anal, and caudal fins yellowish; anal

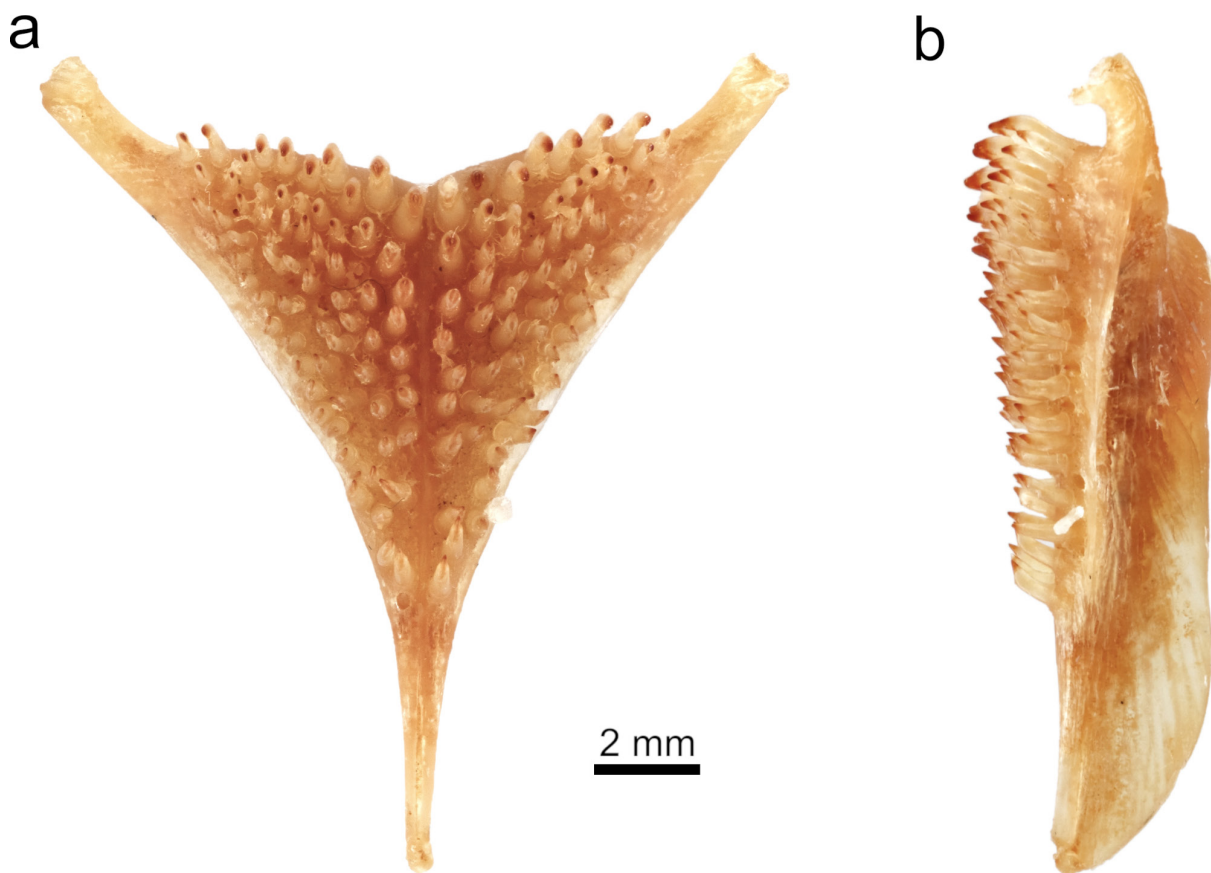


Fig. 13. *Haplochromis rex* sp. nov. (IRSNB 13480; 154.2 mm SL). **a.** Dorsal view of the lower pharyngeal jaw. **b.** Lateral view of the lower pharyngeal jaw.

fin with 2 spots resembling egg-spots; caudal fin with dusky base and dorsal part; dorsal fin dusky and with black lappets.

Preserved colouration

Body, belly, operculum, and cheek yellowish; dorsum brown; chest yellowish in females, black in males (Fig. 12a). Flank rarely with 7–8 very faint narrow vertical stripes. Snout dusky; in males, lower jaw black. In females, all head stripes faint and lacrimal stripe reduced to blotch below eye; in males, head stripes as described here. Nostril and interorbital stripes narrow, well-defined, and horizontally inclined in lateral view, while positioned anterior of nostrils and orbits, respectively, in dorsal view; lacrimal stripe distinct, broad (may cover whole lacrimal), and vaguely delineated; vertical preopercular stripe well-defined; supraorbital stripe present; nape band and mental blotch faint. Pectoral and anal fins yellowish; anal fin with dusky base and posterior margin and 2 small egg-spots in males; pelvic fin yellowish with a black first ray in females, black in males. Dorsal and caudal fins dusky and with yellowish posterior parts; dorsal fin with black lappets and maculated posterior parts.

Distribution and ecology

Only known from Lake Edward, found over sandy substrates. Based on its morphology, most probably a piscivorous species.

Haplochromis simba sp. nov.

[urn:lsid:zoobank.org:act:266E8987-E220-4EC4-AD72-0A46BE085EC8](https://doi.org/10.26661/zoobank.org/act:266E8987-E220-4EC4-AD72-0A46BE085EC8)

Figs 1–2, 14–16; Table 1

Differential diagnosis

Species with a piscivorous morphology; premaxillary pedicel and mental prominences strongly developed; outer oral teeth few and large [UOT 22–31 (median 27)]; dominant males yellow with an orange anterior part of flank.

Amongst piscivorous species from the Lake Edward system, *H. simba* sp. nov. differs from *H. latifrons* sp. nov., *H. mentatus*, and *H. glaucus* sp. nov. by the combination of a narrower interorbital area [IOW 45.5–50.4 (mean 48.1) vs 50.9–63.3 (53.8–60.0) % HW] and a strongly developed vs absent or weakly developed mental prominence. It further differs from *H. latifrons* sp. nov. by a longer anal fin base [AFB 17.3–19.0 (18.0) vs 14.7–17.3 (15.7) % SL] and absence vs presence of a well-defined mid-lateral band; further from *H. mentatus* by a smaller number of outer upper jaw teeth [UOT 22–31 (27) vs 28–46 (36)] and dominant males yellow with an orange anterior part of flank vs green-yellow with a red anterior part of flank; further from *H. glaucus* sp. nov. by a narrower lower pharyngeal element [LPW 83.8–87.9 vs 93.3–95.1% LPL] and dominant males yellow with an orange anterior part of flank vs uniformly light-blue.

It differs from *H. rex* sp. nov. and *H. aquila* sp. nov. by the combination of a smaller number of scales between first anal-fin spine and upper lateral line (ULL-A 9–11 vs 12–16, rarely 11) and a strongly developed vs absent or weakly developed mental prominence. It further differs from *H. rex* sp. nov. by a larger number of longitudinal line scales (LongL 32–33 vs 34–38) and dominant males uniformly yellow with an orange anterior part of flank vs cream-coloured with an orange operculum and a light blue snout; further from *H. aquila* sp. nov. by a smaller eye [ED 26.7–29.5 (28.3) vs 30.0–31.5 (30.6) % HL] and dominant males yellow with an orange anterior part of flank and a yellow head vs uniformly light grey with a black head.

It differs from *H. kimondo* sp. nov., *H. falcatus* sp. nov., *H. curvidens* sp. nov., *H. pardus* sp. nov., *H. quasimodo* sp. nov., and *H. squamipinnis* by the combination of large vs small outer oral teeth and a smaller number of outer upper jaw teeth [UOT 22–31 (27) vs 39–79 (45–58)].

It further differs from *H. falcatus* sp. nov., *H. curvidens* sp. nov., and *H. pardus* sp. nov. by a deeper lacrimal [LaD 18.7–20.5 (19.5) vs 16.0–18.8 (16.7–18.0) % HL]; further from *H. kimondo* sp. nov. and *H. quasimodo* sp. nov. by a narrower head [HW 39.5–41.5 (40.8) vs 42.0–48.1 (45.1–45.3) % HL]; further from *H. squamipinnis* by absence vs presence of minute scales on proximal part of dorsal fin.

Etymology

Specific name from Swahili ‘simba’ for ‘lion’; referring to yellow body, orange cheeks that resemble manes, and predatory morphology.

Material examined

Holotype

UGANDA • ♂, 105.8 mm SL; Lake Edward; 0°24'16.0" S, 29°46'24.8" E; 9 Nov. 2016; HIPE1 exped. leg.; bought at Rwenshama landing site; RMCA 2016.035.P.0225.

Paratypes

DEMOCRATIC REPUBLIC OF THE CONGO • 1 ♂, 98.4 mm SL; “Lac Edouard: Vitshumbi (au Nord)” [Lake Edward: north of Vitshumbi]; 0°40'50.6" S, 29°23'22.6" E (inferred); 2 Jul. 1953; KEA exped. leg.; IRSNB 13488.

UGANDA – **Lake Edward** • 2 ♂♂, 1 ♀, 97.9–105.5 mm SL; 0°24'16.0" S, 29°46'24.8" E; 9 Nov. 2016; HIPE1 exped. leg.; bought at Rwenshama landing site; RMCA 2016.035.P.0222 to 0224 • 1 ♀, 87.1 mm SL; Rwenshama, rocky shore; 0°24'05.7" S, 29°46'35.1" E; 25 Mar. 2017; HIPE2 exped. leg.; RMCA 2017.006.P.0356 • 3 ♂♂, 90.0–100.3 mm SL; same collection data as for preceding; RMCA 2017.006.P.0357 to 0359 • 1 ♀, 109.0 mm SL; 0°24'16.0" S, 29°46'24.8" E; 24 Jan. 2018; HIPE3 exped. leg.; bought at Rwenshama landing site; RMCA 2018.008.P.0348.

Description

Based on 10 specimens (87.1–109.0 mm SL); body shallow (Table 1) and oval to slightly pyriform; caudal peduncle shallow (Fig. 14). Head long, narrow, and with a straight to weakly convex dorsal outline and a weak concavity above eye; eye small and high on head; interorbital area narrow; cheek and lacrimal deep. Snout long, rounded in dorsal outline, acute in lateral view, and slopes gently at 30–45°; premaxillary pedicel average in length and strongly prominent. Jaws isognathous to prognathous, long, slim, very narrow, and rounded in dorsal view; gape large and slopes gently at 20–25°; maxilla extends to between verticals through anterior point of orbit and just past this point. Lower jaw relatively shallow and with a straight ventral outline in lateral view, mental prominence strongly developed, and lower jaw side steep with an inclination of 35–40° to horizontal in anterior view. Upper jaw expanded anteriorly and ventrally. Lips and oral mucosa thin. Neurocranium shallow, ethmo-vomerine block decurved, preorbital region very shallow (18–20% NL), orbital region shallow (26–28% NL), and supraoccipital crest shallow and wedge-shaped (Fig. 15b).

Outer oral teeth few, unicuspid, and very large. Necks stout, conical, and straight; crowns straight to weakly recurved, and acutely pointed. Dental arcades rounded. Outer teeth widely and irregularly set with neck-distances of 1–4 neck-widths. In upper jaw, 1–2 posteriormost teeth enlarged. Inner teeth small, recurved, unicuspid, and acutely pointed. Tooth bands very slender crescent-shaped with 1–2 rows of inner teeth, and narrow posteriorly until only outer row remains past $\frac{2}{3}$ length of tooth band. Inner teeth widely and irregularly set on 1–2 outer tooth neck-widths from outer row; implantation

erect in first row and recumbent in subsequent rows; in upper jaw, size decreases slightly buccally and posteriorly.

Lower pharyngeal bone long, very narrow, slim, and shallow over whole length (Fig. 16). Pharyngeal teeth relatively large and slender; major cusps acutely pointed; cusp gaps concave; minor cusps and cusp protuberances very small. Teeth in two median longitudinal rows equal in size and form to lateral teeth, 12 in each row. Posterior transverse row with 16–18 teeth, implanted recumbently with a lateral inclination; major cusps weakly recurved, bluntly pointed, and laterally compressed; minor cusps mostly absent.

Chest scales small; transition to larger flank scales gradual. Minute scales on proximal half of caudal fin.

Caudal fin emarginate; dorsal and anal fins reach to between verticals through two scales anterior to and one scale posterior to caudal-fin base. Pectoral fin reaches to between anal opening and second anal-fin spine; pelvic fin reaches to between first and second anal-fin spines; first branched pelvic-fin ray elongated.

Ceratobranchial gill rakers in outer row of first gill arch short, stout, and simple; posteriormost rakers anvil-shaped to weakly bifid. Epibranchial gill rakers slender and simple.

Colouration in life

Dominant males: body yellow; operculum, cheek, and anterior part of flank orange; belly and chest white (Fig. 15c). Snout dusky; lower jaw and lips pink; eye with (dark) grey outer ring and silver to golden inner ring. Nostril and lacrimal stripes faint; mental blotch present. pectoral fin yellow; pelvic fin black; dorsal fin hyaline to dusky and with black lappets and a dusky posterior part; anal fin faint crimson and with 2–3 very large orange egg-spots with hyaline rings; caudal fin dusky and with a faint crimson ventral part and a maculated dorsal part. Non-dominant males: anterior part of flank,

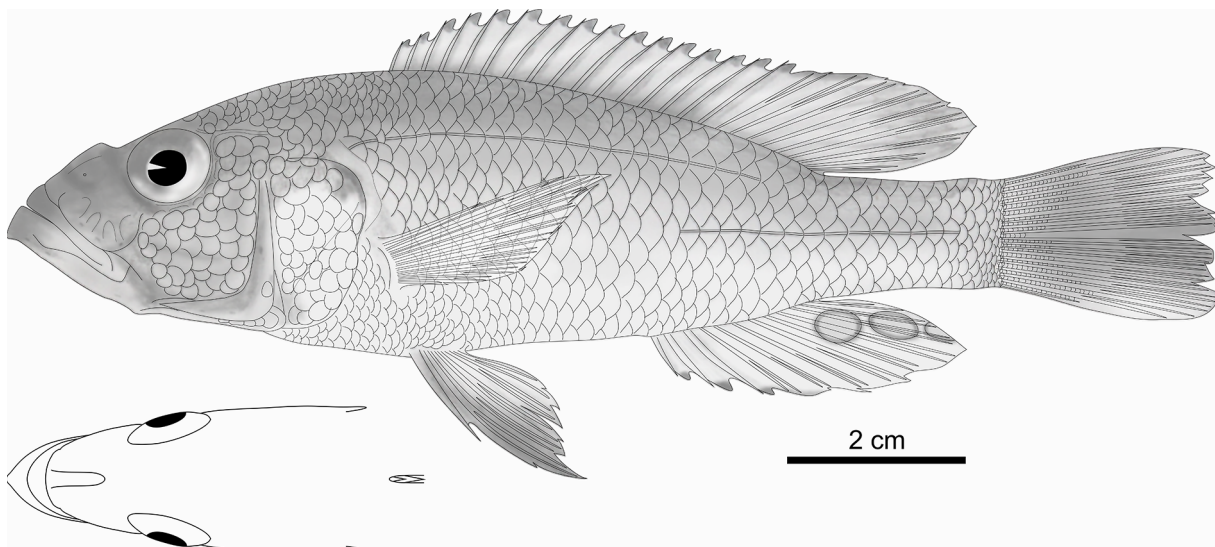


Fig. 14. *Haplochromis simba* sp. nov., holotype, ♂, 105.8 mm SL (RMCA 2016.035.P.0225). Drawn by N. Vranken.

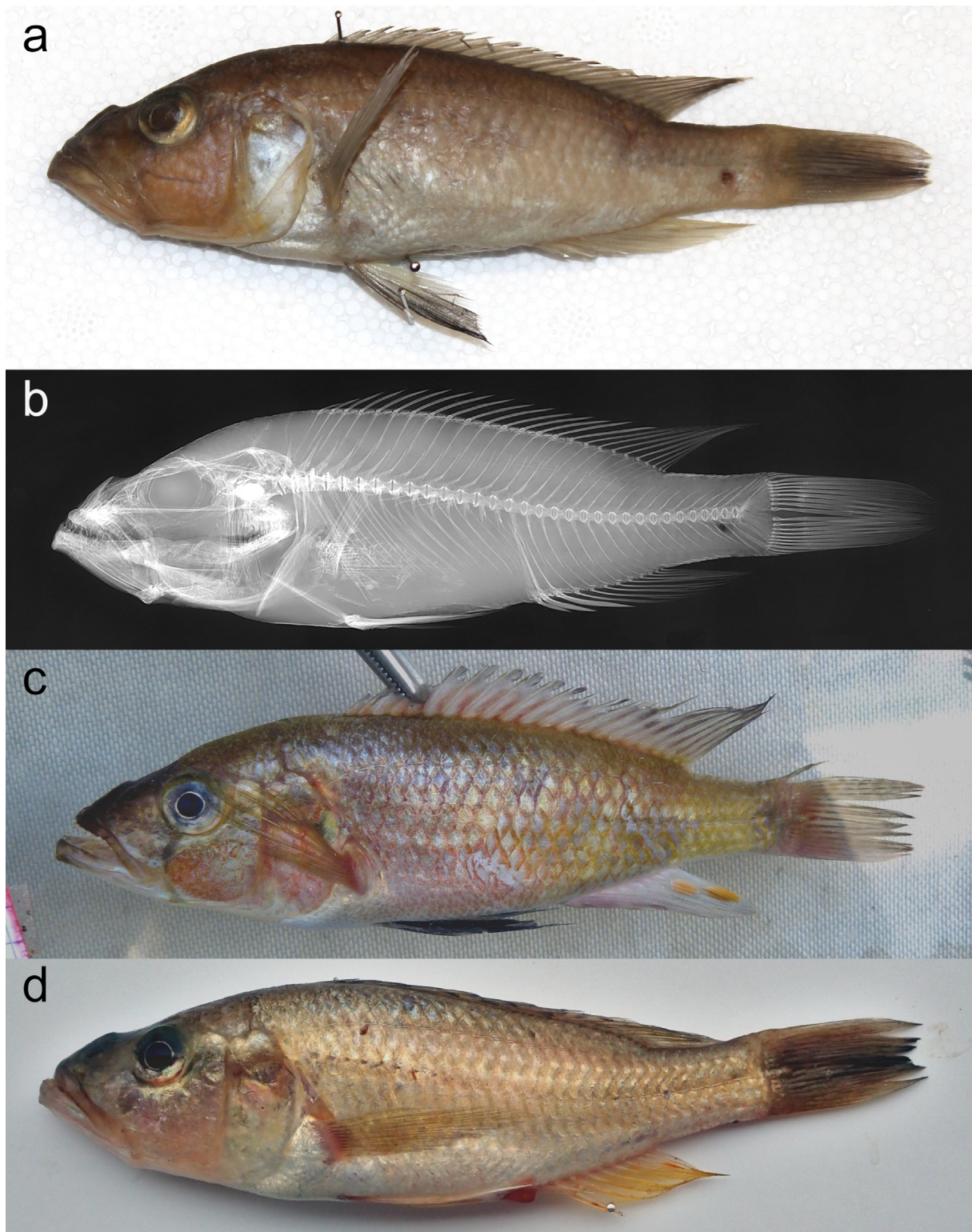


Fig. 15. *Haplochromis simba* sp. nov. **a.** Photograph of preserved holotype (RMCA 2016.035.P.0225; 105.8 mm SL). **b.** X-ray image of holotype. **c–d.** Photographs of freshly caught specimens. **c.** Dominant male (RMCA 2016.035.P.0224; 97.9 mm SL). **d.** Female (RMCA 2018.008.P.0348; 109.0 mm SL) to illustrate the live colour patterns. The contrast was slightly enhanced.

operculum, and cheek with pink sheen; anal fin with crimson anterior part and hyaline posterior part; caudal fin uniformly dusky.

Females and juveniles: body, operculum, and cheek yellow; belly and chest white; lacrimal and lower jaw pink; snout dusky; eye with (dark) grey outer ring and silver to golden inner ring (Fig. 15d). Nostril and interorbital stripes faint; mental blotch present. Pectoral, anal, and caudal fins yellow; anal fin with a white base; caudal fin with a dusky base; dorsal fin hyaline and with black lappets and a dusky distal part.

Preserved colouration

Body whitish; dorsum and cheek brown; belly, chest, and operculum white; snout dusky (Fig. 15a). Nostril stripe well-defined; lacrimal stripe and mental blotch present; interorbital stripe and nape band faint. Pectoral fin dusky; pelvic fin yellowish in females, black in males; dorsal fin dusky and with black lappets and sooty posterior part; anal fin yellowish and with 1–2 large egg-spots; caudal fin dusky and with a maculated dorsal part.

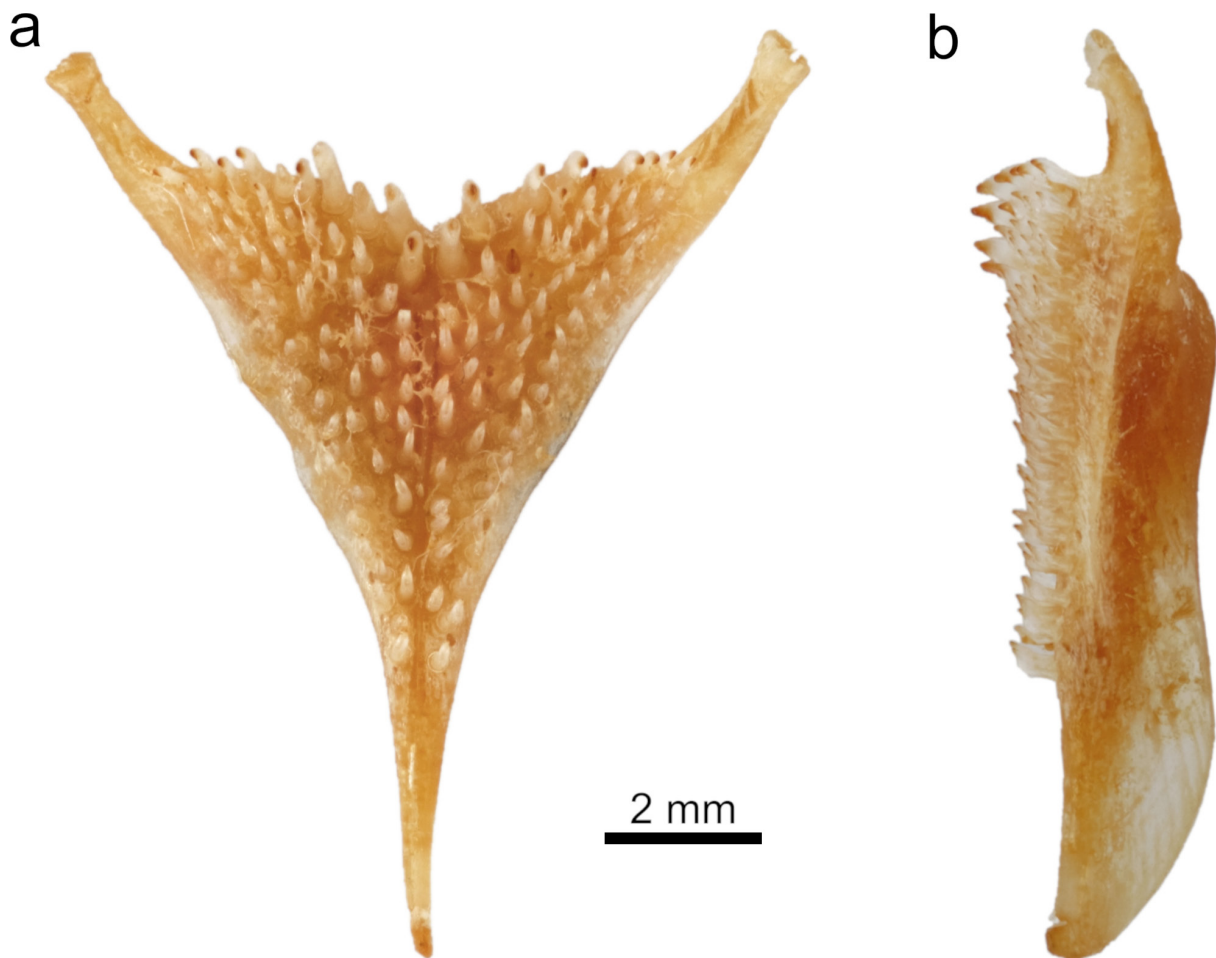


Fig. 16. *Haplochromis simba* sp. nov. (RMCA 2016.035.P.0223; 105.5 mm SL). **a.** Dorsal view of the lower pharyngeal jaw. **b.** Lateral view of the lower pharyngeal jaw.

Distribution and ecology

Only known from Lake Edward, found in inshore areas over hard substrates. Based on its morphology, most probably a piscivorous species.

Haplochromis glaucus sp. nov.

[urn:lsid:zoobank.org:act:E5948349-E3F9-49A1-81CD-1C7D332E2F00](https://doi.org/10.21203/rs.3.rs-1988881/v1)

Figs 1–2, 17–19; Table 1

Differential diagnosis

Species with a piscivorous morphology; snout acute in lateral view; outer oral teeth few and large [UOT 25–47 (median 30)]; males grey with light blue flank and a dusky to black head; female colour pattern similar to males.

Amongst piscivorous species from the Lake Edward system, *H. glaucus* sp. nov. differs from *H. latifrons* sp. nov. and *H. mentatus* by a shorter caudal peduncle [CPL 13.4–16.1 (mean 14.8) vs 15.7–18.0 (16.6–17.0) % SL]; further from *H. latifrons* sp. nov. by a longer anal fin base [AFB 17.3–20.3 (18.6) vs 14.7–17.3 (15.7) % SL] and absence vs presence of a well-defined mid-lateral band; further from *H. mentatus* by a broader lower pharyngeal bone [LPW 93.3–95.1 vs 83.6–85.7% LPL], a slightly longer pre-pectoral distance [PrP 36.4–39.4 (38.1) vs 33.1–38.2 (36.0) % SL], and dominant males uniformly light blue vs yellow-green with a red anterior part of flank.

It differs from *H. rex* sp. nov. and *H. simba* sp. nov. by a broader interorbital area [IOW 50.9–57.1 (53.8) vs 44.9–52.7 (48.1–48.9) % HW]; further from *H. rex* sp. nov. by a gentler sloping snout (30–40° vs 40–50°), acute vs rounded oral jaws in dorsal view, and dominant males light blue with a blackish operculum and a dusky snout vs cream-coloured with an orange operculum and a light blue snout; further from *H. simba* sp. nov. by a broader lower pharyngeal bone [LPW 93.3–95.1 vs 83.8–87.9% LPL], absent or weakly developed vs strongly developed mental prominence, and dominant males uniformly light-blue vs yellow with an orange anterior part of flank.

It differs from *H. aquila* sp. nov. by the combination of a smaller eye [ED 23.2–28.7 (26.8) vs 30.0–31.5 (30.6) % HL], a narrower head [HW 38.9–40.9 (39.7) vs 40.1–43.7 (42.0) % HL], and dominant males light blue with crimson anal and caudal fins vs light grey with bright red anal and caudal fins.

It differs from *H. kimondo* sp. nov., *H. curvidens* sp. nov., and *H. quasimodo* sp. nov. by the combination of a narrower head [HW 38.9–40.9 (39.7) vs 42.0–48.1 (43.4–45.3) % HL], large vs small outer oral teeth, and a smaller number of outer upper jaw teeth [UOT 25–47 (30) vs 43–71 (49–58)]; further from *H. kimondo* sp. nov. and *H. quasimodo* sp. nov. by dominant males light blue vs grey dorsally and yellow or blue-black ventrally.

It differs from *H. falcatus* sp. nov. by the combination of a shorter pre-dorsal distance [PrD 35.4–37.0 (36.1) vs 36.9–41.1 (39.5) % SL], a steeper lower jaw side (35–45° vs 15–25°), weakly recurved vs strongly recurved outer oral teeth, and dominant males uniformly light blue vs olive-green with an orange-red anterior part of flank.

It differs from *H. pardus* sp. nov. by the combination of deeper lacrimal [LaD 18.0–22.7 (19.8) vs 16.0–18.3 (17.3) % HL], a broader interorbital area [IOW 50.9–57.1 (53.8) vs 39.3–48.4 (44.6) % HW], and dominant males light blue vs speckled to uniformly black.

It further differs from *H. squamipinnis* by the combination of a gentler gape inclination (20–30° vs 30–45°), absence vs presence of minute scales on proximal parts of dorsal and anal fins, and dominant males light blue vs slate blue.

Etymology

Specific name from the Latin ‘*glaucus*’ for ‘greyish blue’; referring to grey and light-blue colour pattern of all adult specimens.

Material examined

Holotype

UGANDA • ♂, 106.2 mm SL; Lake Edward, Kayanja offshore; 0°05′34.8″ S, 29°45′28.8″ E; 21 Mar. 2019; HIPE4 exped. leg.; RMCA 2019.002.P.0016.

Paratypes

DEMOCRATIC REPUBLIC OF THE CONGO • 1 ♂, 158.3 mm SL; “Lac Edouard: au large de la riv. Kigera” [Lake Edward: offshore Kigera river]; 0°29′42″ S, 29°38′14″ E (inferred); 25 May 1953; KEA exped. leg.; IRSNB 13477 • 1 ♂, 150.9 mm SL; “Lac Edouard: 2–3 km ± 500 m au large à l’Ouest de Kiavinionge” [Lake Edward: 2–3 km ± 500 m offshore west of Kiavinionge]; 0°11′39″ S, 29°32′31″ E (inferred); 1 Jun. 1953; KEA exped. leg.; IRSNB 13480.

UGANDA – **Lake Edward** • 1 ♀, 1 ♂, 90.7–93.6 mm SL; Kagoro fishing ground; 0°12′50.1″ S, 29°49′19.7″E; 4 Feb. 2018; HIPE3 exped. leg.; open water; RMCA 2018.008.P.0365 to 0366 • 1 ♀, 92.6 mm SL; same collection data as for preceding; RMCA 2018.008.P.0367 • 1 ♀, 1 ♂, 102.1–104.7 mm SL; Kayanja offshore; 0°05′34.8″ S, 29°45′28.8″ E; 21 Mar. 2019; HIPE4 exped. leg.; RMCA

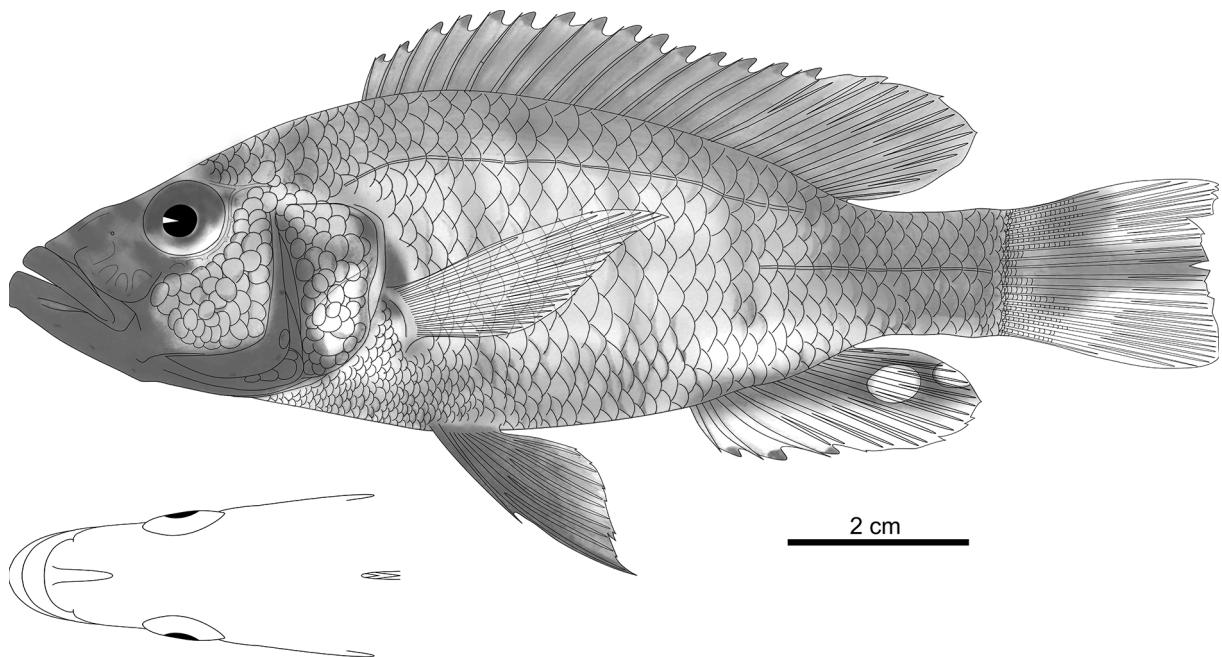


Fig. 17. *Haplochromis glaucus* sp. nov., holotype, ♂, 106.2 mm SL (RMCA 2019.002.P.0016). Drawn by N. Vranken.

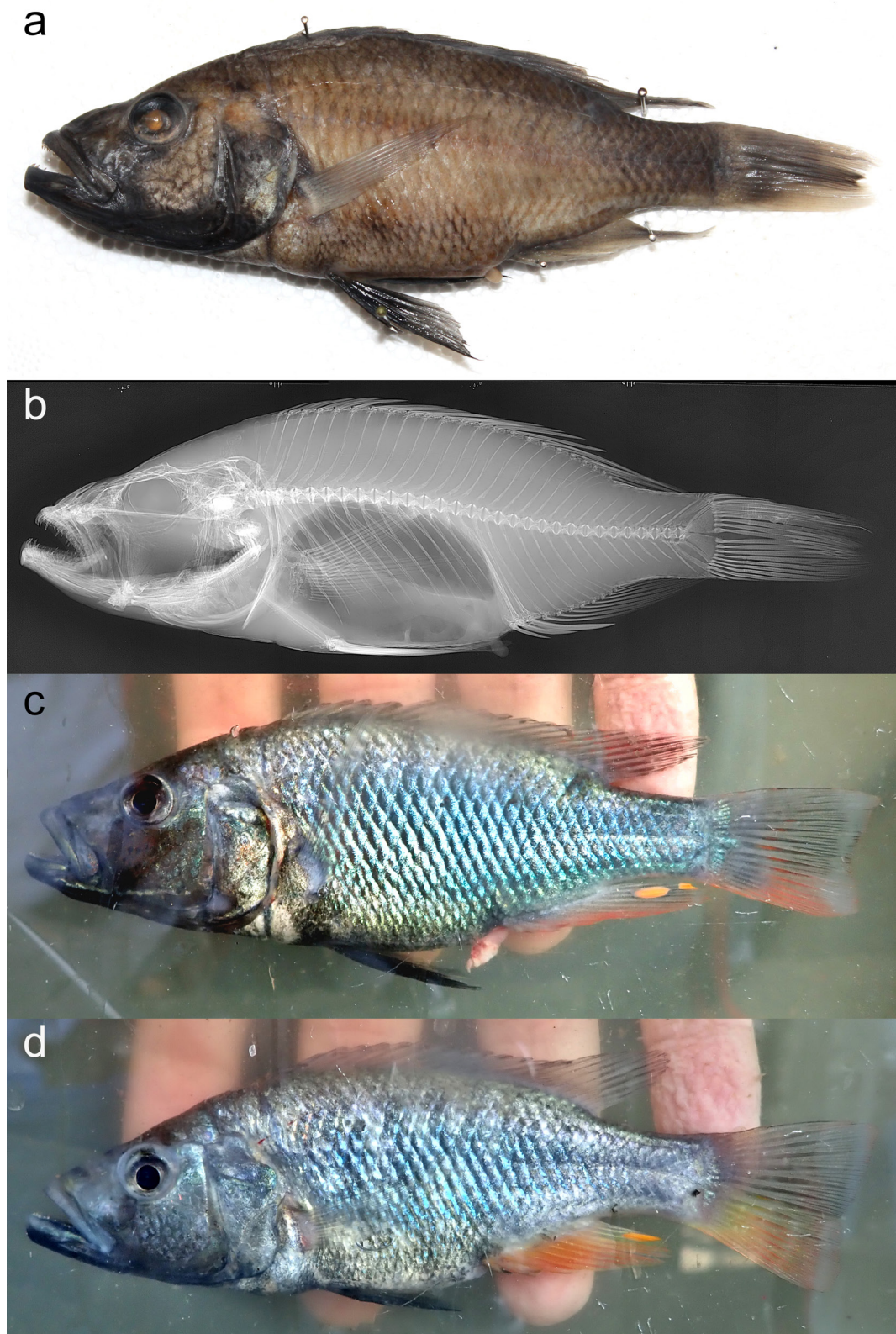


Fig. 18. *Haplochromis glaucus* sp. nov. **a.** Photograph of preserved holotype (RMCA 2019.002.P.0016; 106.2 mm SL). **b.** X-ray image of holotype **c–d.** Photographs of freshly caught specimens. **c.** Dominant male, the holotype. **d.** Female (RMCA 2019.002.P.0017; 102.1 mm SL) to illustrate the live colour patterns. The contrast was slightly enhanced.

2019.002.P.0017 to 0018 • 1 ♂, 2 ♀♀, 107.7–122.3 mm SL; same collection data as for preceding; RMCA 2019.002.P.0019 to 0021.

Description

Based on 11 specimens (90.7–158.3 mm SL); body shallow (Table 1) and oval (Fig. 17). Head long, very narrow, and with a straight dorsal outline; eye small; interorbital area narrow; lacrimal and cheek deep. Snout long, rounded in dorsal view, very narrow, acute, and slopes gently at 30–40°; premaxillary pedicel long and weakly prominent. Jaws long, relatively stout, narrow, isognathous, and acute in dorsal view; gape large and slopes gently at 20–30°; maxilla extends (almost) to vertical through anterior margin of orbit. Lower jaw relatively stout and with a straight to slightly convex ventral outline in lateral view, mental prominence absent or weakly developed, and lower jaw side steep with an inclination of 35–45° to horizontal in anterior view. Upper jaw expanded anteriorly and weakly ventrally. Lips and oral mucosa large. Neurocranium shallow, ethmo-vomerine block decurved, preorbital region shallow (20–23% NL), orbital region shallow (28–31% NL), and supraoccipital crest shallow and wedge-shaped (Fig. 18b).

Outer oral teeth few, unicuspid, and very large. Necks conical, stout, and straight; crowns recurved and acutely pointed. Dental arcades rounded. Outer teeth widely and irregularly set with neck-distances of 1–4 neck-widths. In upper jaw, 1–3 posteriormost teeth slightly enlarged. Inner teeth small, strongly

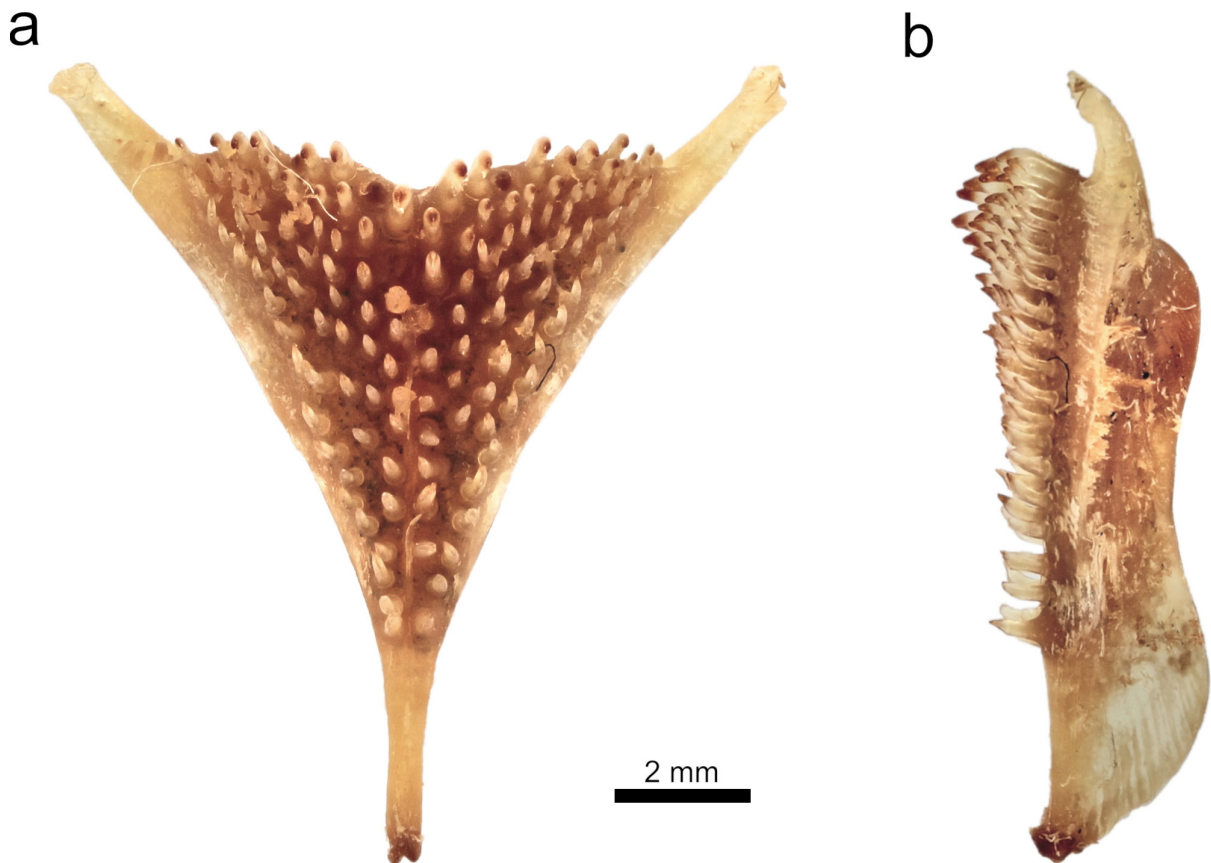


Fig. 19. *Haplochromis glaucus* sp. nov. (RMCA 2019.002.P.0020; 110.9 mm SL). **a.** Dorsal view of the lower pharyngeal jaw. **b.** Lateral view of the lower pharyngeal jaw.

recurved, unicuspid, and acutely pointed. Tooth bands very slender crescent-shaped with 1–3 rows of inner teeth, and narrow posteriorly until only outer row remains past $\frac{3}{4}$ length of tooth band. Inner teeth closely and regularly set on 1–2 outer neck-widths from outer row; implantation recumbent; size decreases slightly buccally and posteriorly.

Lower pharyngeal bone average in length, triangular, slim, and shallow over whole length (Fig. 19). Pharyngeal teeth relatively large and slender; major cusps acutely pointed; cusp gaps straight; minor cusps and cusp protuberances mostly absent. Teeth in two median longitudinal rows equal in size and form to lateral teeth, 10–12 in each row. Posterior transverse row with 15–16 teeth, implanted recumbently with a lateral inclination; major cusps recurved, bluntly pointed, and laterally compressed; minor cusps small.

Chest scales small; transition to larger flank scales gradual. Minute scales on proximal half of caudal fin.

Caudal fin emarginate; dorsal and anal fins reach to between verticals through one scale anterior to and two scales posterior to caudal-fin base. Pectoral and pelvic fins reach to between anal opening and first anal-fin spine; first branched pelvic-fin ray not elongated.

Ceratobranchial gill rakers in outer row of first gill arch short, stout, and simple; posteriormost rakers anvil-shaped to rarely weakly trifid. Epibranchial gill rakers slender and simple.

Colouration in life

Dominant males: flank and caudal peduncle light-blue; dorsum grey with a yellow sheen; belly, chest, and operculum blackish with a yellow sheen; flank with 5–7 faint vertical stripes (Fig. 18c). Preoperculum black; cheek black with blue sheen; lacrimal and snout dusky; lower jaw blackish; branchiostegal membrane black; eye with dark grey outer ring and silver inner ring. Nostril, interorbital, supraorbital, and lacrimal stripes well-defined; nape band, vertical preopercular stripe, and mental blotch present; operculum with black posterior border. Pectoral and dorsal fins hyaline; dorsal fin with black lappets, dusky base, and dusky and maculated crimson posterior part. Anal and caudal fins crimson; anal fin with dusky posterior part and 1–2 large orange egg-spots with dusky rings; caudal fin with dusky base, hyaline posterior part, and crimson maculae.

Females: strikingly similar to dominant males. Body, dorsum, and caudal peduncle grey with a yellow sheen; flanks light blue and with 5–7 faint vertical stripes; belly and chest blackish with a yellow sheen (Fig. 18d). Operculum, preoperculum, cheek, lacrimal, and snout grey; operculum with blue sheen; cheek with black sheen; lower jaw blackish; branchiostegal membrane black; eye with dark grey outer ring and silver inner ring. Nostril, interorbital, supraorbital, and lacrimal stripes well-defined; nape band, vertical preopercular stripe, and mental blotch faint; operculum with faint black posterior border. Pectoral and dorsal fins hyaline; dorsal fin with black lappets, dusky base, and dusky posterior part. Anal and caudal fins yellow with a red sheen; anal fin with hyaline posterior part and 1–2 spots resembling egg-spots; caudal fin with dusky base, hyaline posterior part, and dusky maculae. Juveniles: dorsum greyish, belly, chest, operculum, and cheek white; transition gradual. Nostril, interorbital, supraorbital, and lacrimal stripes, nape band, and mental blotch faint. Pectoral, pelvic, dorsal, and anal fins hyaline; dorsal fin with black lappets and dusky base and posterior part; anal fin with a yellow sheen and 1–2 spots resembling egg-spots. Caudal fin dusky and with black maculae and a yellow ventral part.

Preserved colouration

Dorsum brown; belly and chest speckled black; flank dark yellowish and with 6–8 faint vertical stripes. Cheek yellow and speckled black; snout dusky; lower jaw and pre- and subopercula black (Fig. 18a). Nostril, interorbital, and vertical preopercular stripes well-defined; lacrimal stripe broad and well-

defined; supraorbital stripe and nape band faint. Pectoral and anal fins hyaline; anal fin with black lappets, a dusky posterior margin, and 1–2 large egg-spots; pelvic fin black; dorsal fin dusky and with black lappets and a maculated posterior part; caudal fin dorsally dusky, ventrally hyaline, and with a dusky base.

Distribution and ecology

Only known from Lake Edward, found over sandy substrates. Based on its morphology, most probably a piscivorous species.

Haplochromis aquila sp. nov.

[urn:lsid:zoobank.org:act:18BC8C85-5A02-48F0-8D90-7B069122A09D](https://zoobank.org/act:18BC8C85-5A02-48F0-8D90-7B069122A09D)

Figs 1–2, 20–22; Table 1

Differential diagnosis

Species with a piscivorous morphology; eye large [ED 30.0–31.5 (mean 30.6) % HL]; outer oral teeth few and large [UOT 25–37 (median 31)]; dominant males light grey with a black head and a bright red anal fin.

Amongst piscivorous species from the Lake Edward system, *H. aquila* sp. nov. differs from *H. latifrons* sp. nov., *H. mentatus*, *H. rex* sp. nov., *H. simba* sp. nov., and *H. glaucus* sp. nov. by a larger eye [ED 30.0–31.5 (30.6) vs 22.2–29.9 (24.4–28.3) % HL].

It further differs from *H. latifrons* sp. nov. and *H. mentatus* by a shorter caudal peduncle [CPL 14.6–15.4 (15.0) vs 15.7–18.0 (16.6–17.0) % SL]; further from *H. latifrons* sp. nov. by the absence vs presence of a well-defined mid-lateral band; further from *H. mentatus* by dominant males uniformly light grey vs yellow-green with a red anterior part of flank.

It further differs from *H. rex* sp. nov. by a shallower lacrimal [LaD 17.0–19.1 (18.3) vs 18.9–22.5 (20.8) % HL] and dominant males light grey with black operculum and snout vs cream-coloured with an orange operculum and a light blue snout.

It further differs from *H. simba* sp. nov. by a larger number of scales between first anal-fin spine and upper lateral line (ULL-A 12–15, rarely 11 vs 9–11), an absent vs strongly developed mental prominence, and dominant males light grey with a black head vs uniformly yellow with an orange anterior part of flank.

It further differs from *H. glaucus* sp. nov. by a broader head [HW 40.1–43.7 (42.0) vs 38.9–40.9 (39.7) % HL] and dominant males light grey with bright red anal and caudal fins vs light blue with crimson anal and caudal fins.

It differs from *H. kimondo* sp. nov., *H. falcatus* sp. nov., *H. curvidens* sp. nov., *H. pardus* sp. nov., *H. quasimodo* sp. nov., and *H. squamipinnis* by the combination of large vs small outer oral teeth and smaller number of outer upper jaw teeth [UOT 25–37 (31) vs 39–79 (45–58)].

It further differs from *H. kimondo* sp. nov., *H. falcatus* sp. nov. and *H. quasimodo* sp. nov. by absence vs mostly presence of a well-defined mid-lateral band and dominant males light grey with a black head vs grey dorsally and yellow ventrally, olive-green with an orange-red anterior part of flank, or light grey dorsally and blue-black ventrally; further from *H. kimondo* sp. nov. by a narrower head [HW 40.1–43.7 (42.0) vs 42.9–48.0 (45.1) % HL].

It further differs from *H. curvidens* sp. nov. and *H. pardus* sp. nov. by a deeper cheek [ChD 26.8–30.8 (28.3) vs 20.8–24.9 (22.5–23.2) % HL]; further from *H. pardus* sp. nov. by dominant males light grey vs speckled to uniformly black.

It further differs from *H. squamipinnis* by larger eyes [ED 30.0–31.5 (30.6) vs 23.1–29.7 (26.6) % HL] and dominant males light grey vs slate blue.

Etymology

Specific name from the Latin ‘*aquila*’ for ‘eagle’; referring to predatory morphology and large eyes.

Material examined

Holotype

UGANDA • ♂, 113.6 mm SL; Lake Edward, Kayanja offshore; 0°05'31.2" S, 29°45'30.3" E; 20 Jan. 2018; HIPE3 exped. leg.; RMCA 2018.008.P.0355.

Paratypes

UGANDA – **Lake Edward** • 1 ♀, 2 ♂♂, 83.9–117.7 mm SL; islands near Katwe; 0°10'04.9" S, 29°52'27.4" E; 18 Jan. 2018; HIPE3 exped. leg.; RMCA 2018.008.P.0349 to 0351 • 1 ♀, 1 ♂, 108.7, 117.6 mm SL; islands near Katwe; 0°10'04.9" S, 29°52'27.4" E; 19 Jan. 2018; HIPE3 exped. leg.; RMCA 2018.008.P.0352 to 0353 • 1 ♂, 85.6 mm SL; mouth of Kazinga Channel; 0°12'34.8" S, 29°53'01.5" E; 19 Jan. 2018; HIPE3 exped. leg.; RMCA 2018.008.P.0354 • 1 ♂, 122.9 mm SL; 0°24'16.0" S, 29°46'24.8" E; 24 Jan. 2018; HIPE3 exped. leg.; bought at Rwenshama landing site; RMCA 2018.008.P.0356.

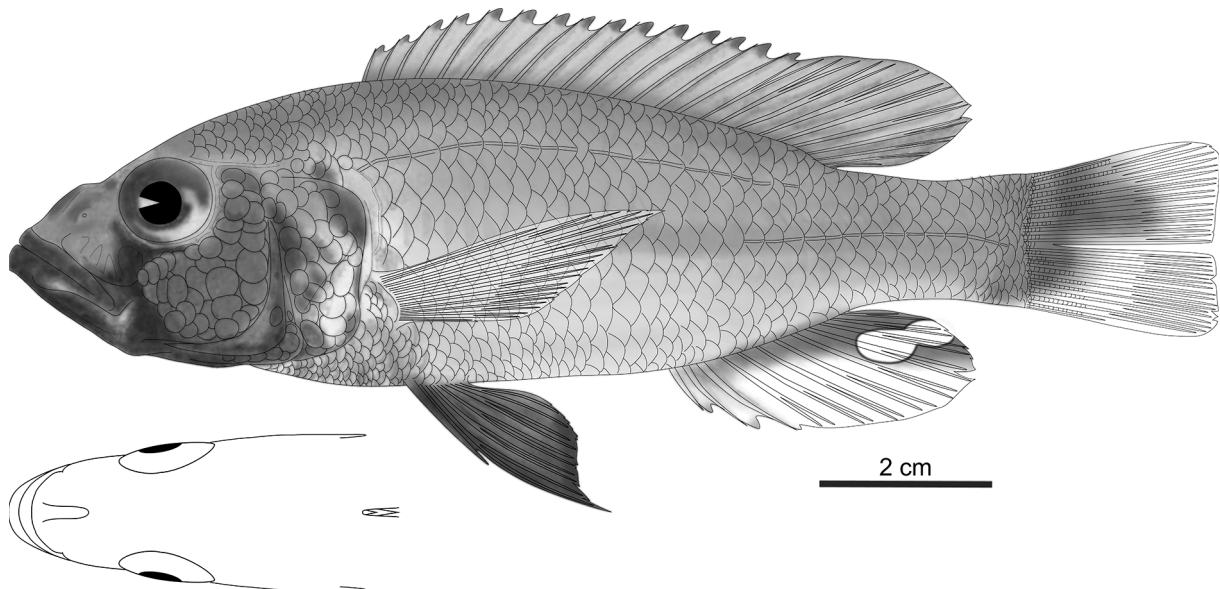


Fig. 20. *Haplochromis aquila* sp. nov., holotype, ♂, 113.6 mm SL (RMCA 2018.008.P.0355). Drawn by N. Vranken.

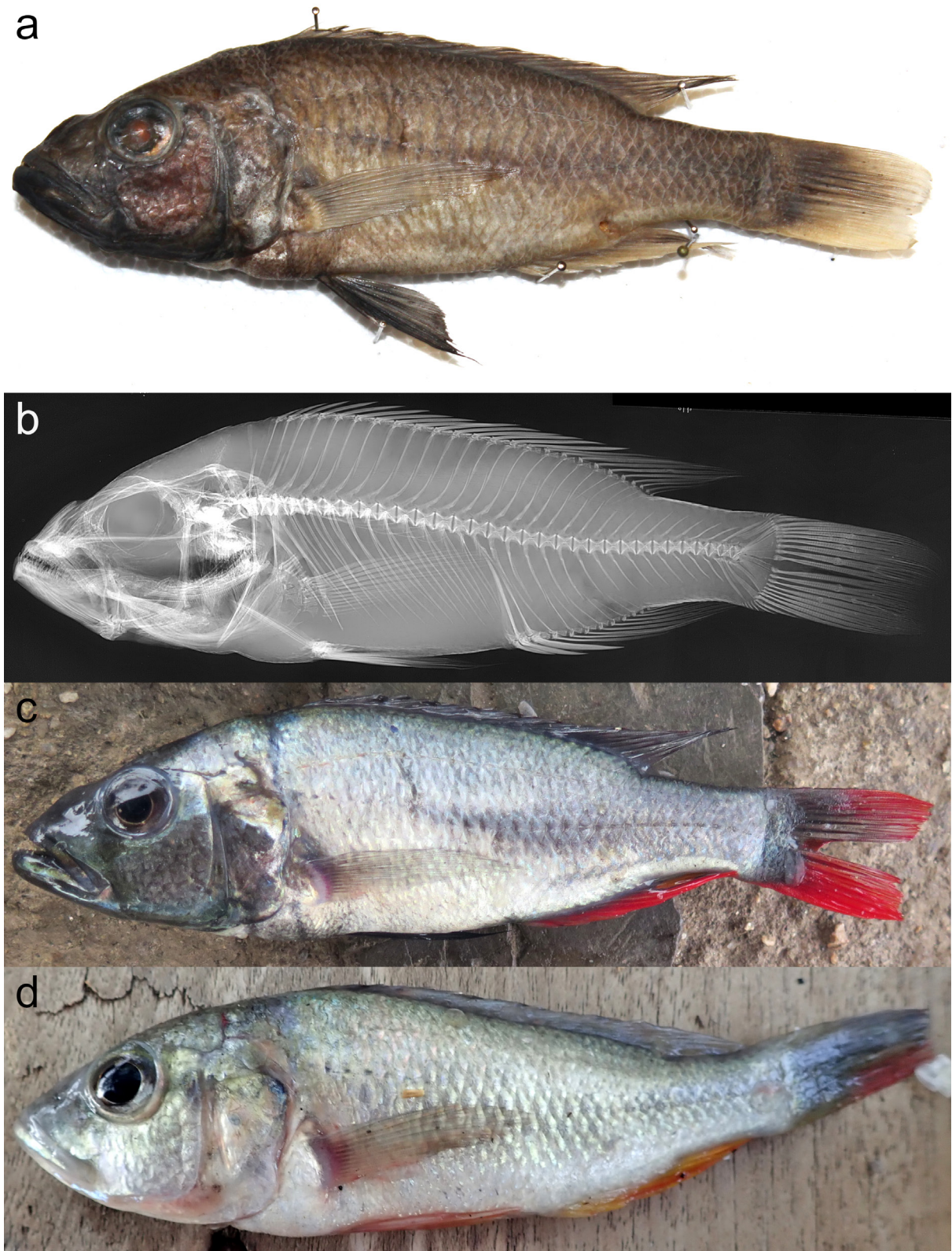


Fig. 21. *Haplochromis aquila* sp. nov. **a.** Photograph of preserved holotype (RMCA 2018.008.P.0355; 113.6 mm SL). **b.** X-ray image of holotype. **c–d.** Photographs of freshly caught specimens. **c.** Dominant male, the holotype. **d.** Female (RMCA 2018.008.P.0352; 108.7 mm SL) to illustrate the live colour patterns. The contrast was slightly enhanced.

Description

Based on 8 specimens (83.9–122.9 mm SL); body shallow (Table 1) and oval (Fig. 20). Head long, narrow, and with a straight to gently convex dorsal outline; interorbital area narrow; eye average in size in comparison to generalised *H. elegans* (but large for a piscivorous species); cheek deep; lacrimal average in depth. Snout average in length, rounded in dorsal view, narrow, relatively blunt, and slopes gently at 35–45°; premaxillary pedicel long and (strongly) prominent. Jaws isognathous to weakly prognathous, long, narrow, and rounded in dorsal view; gape large and slopes at 25–35°; maxilla extends to vertical through anterior margin of pupil. Lower jaw relatively stout and with straight ventral outline in lateral view, mental prominence absent or weakly developed, and lower jaw side nearly flat with an inclination of 25–35° to horizontal in anterior view. Upper jaw expanded anteriorly. Lips and oral mucosa relatively large. Neurocranium average in depth, ethmo-vomerine block decurved, preorbital region shallow (18–24% NL), orbital region average in depth (30–33% NL), and supraoccipital crest shallow and wedge-shaped (Fig. 21b).

Outer oral teeth few, unicuspid, and very large. Necks stout, conical, and straight; crowns straight to weakly recurved and acutely pointed. Dental arcades with anterior half expanded laterally. Outer teeth widely and irregularly set with neck-distances of 1–4 neck-widths. No enlarged teeth posterior in upper jaw. Inner teeth small, recurved, a mixture of unicuspid and weakly tricuspid, weakly tricuspid rare in large specimens (> 100 mm SL), and acutely pointed in all specimens. Tooth bands very slender crescent-shaped with 1–2 rows of inner teeth, and narrow posteriorly until only outer row remains past $\frac{3}{4}$ length of tooth band in upper jaw, past $\frac{2}{3}$ length of tooth band in lower jaw. Inner teeth closely and regularly set on 1 outer neck-width from outer row; implantation recumbent; size uniform throughout tooth band.

Lower pharyngeal bone long, very narrow, slim, and shallow over whole length (Fig. 22). Pharyngeal teeth relatively large and slender; major cusps acutely pointed; cusp gaps concave; minor cusps and cusp protuberances very small. Teeth in two median longitudinal rows equal in size and form to lateral teeth, 12 in each row. Posterior transverse row with 16–17 teeth, implanted erectly with a lateral inclination; major cusps nearly straight, bluntly pointed, and laterally compressed; minor cusps mostly absent.

Chest scales small; transition to larger flank scales gradual. Minute scales on proximal half of caudal fin.

Caudal fin emarginate; dorsal and anal fins reach to between verticals through caudal-fin base and two scales anterior to this vertical. Pectoral fin reaches to between genital opening and second anal-fin spine; pelvic fin reaches to genital opening in females, to between first and second anal-fin spines in males; first pelvic fin slightly elongated in all specimens.

Ceratobranchial gill rakers in outer row of first gill arch short, stout, and simple; posteriormost rakers anvil-shaped or bifid. Epibranchial gill rakers slender and simple.

Colouration in life

Dominant males: body metallic grey; dorsum greyish; belly speckled black; chest, cheek, snout, lower jaw, and lips black; eye with (dark) grey outer ring and golden inner ring (Fig. 21c). Nostril, interorbital, and lacrimal stripes very faint. Pectoral fin hyaline, pelvic fin black; dorsal fin sooty and with black lappets; anal and caudal fins bright red and with dusky bases; anal fin with dusky posterior part and 1–2 large orange egg-spots with dusky rings.

Females and juveniles: body and dorsal part of head silver with yellowish sheen; belly, chest, operculum, cheek, lower jaw, and lips white; snout dusky; eye with (dark) grey outer ring and silver inner ring (Fig. 21d). Nostril and interorbital stripes faint. Pectoral fin hyaline, pelvic fin white; dorsal and caudal

fins dusky; dorsal fin with black lappets; caudal fin with a yellowish base and a faint red distal part; anal fin yellow with a red sheen.

Preserved colouration

Body brown; dorsum dark-brown; ventral part of body and operculum yellowish; chest and lower jaw black in males; cheek yellowish in females, dark-brown in males; snout dusky (Fig. 21a). Nostril and interorbital stripes faint; lacrimal stripe narrow and well-defined; mental blotch present; vertical preopercular stripe well-defined in males. Pectoral fin hyaline; pelvic fin yellowish with blackish first rays in females, black in males; dorsal fin dusky and with black lappets and maculated posterior part; anal fin yellowish with a dusky overlay and, in males, with black lappets and 1–2 large egg spots; caudal fin with a dusky base, a hyaline distal part, and, in males, whole ventral half hyaline.

Distribution and ecology

Only known from Lake Edward, found in inshore areas over muddy substrates. Based on its morphology, most probably a piscivorous species.

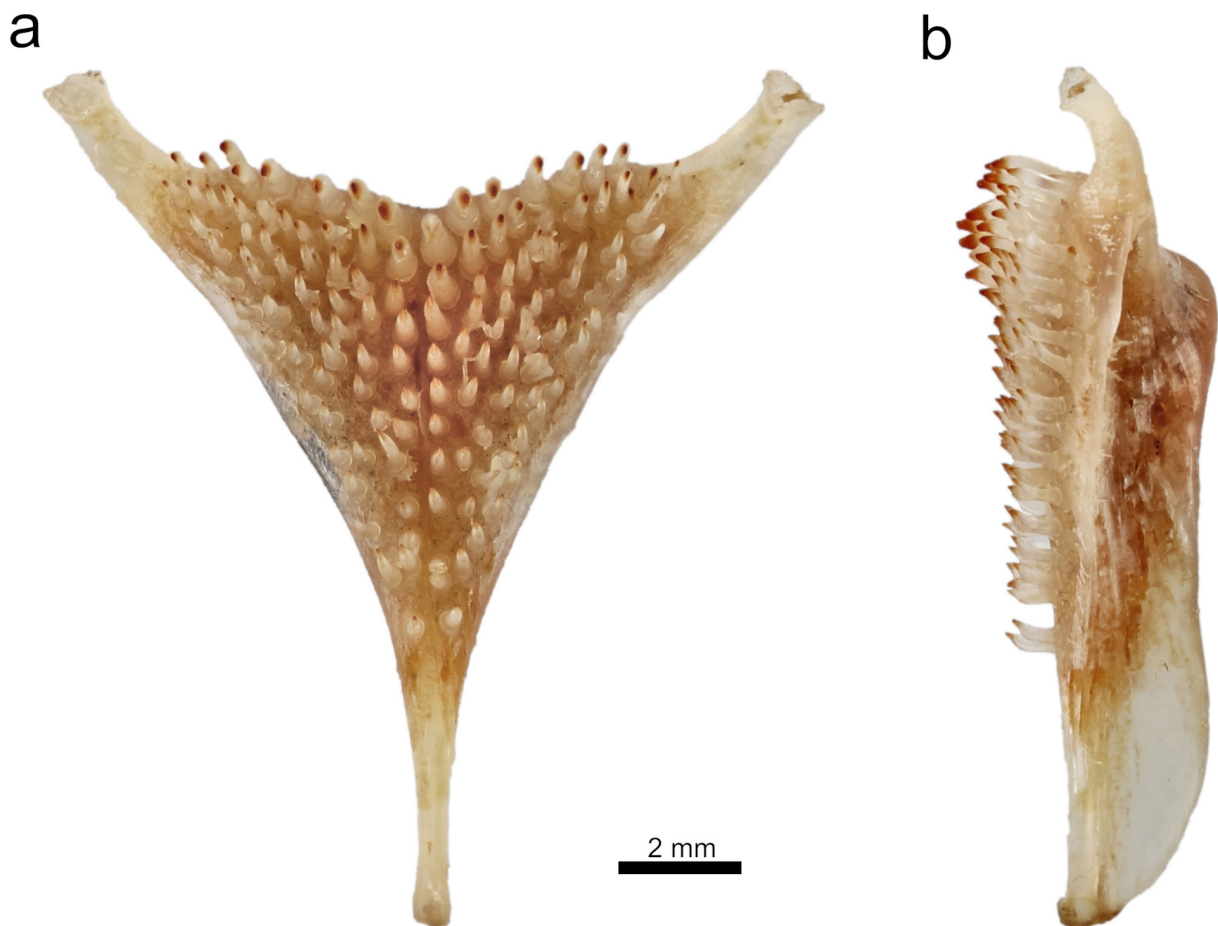


Fig. 22. *Haplochromis aquila* sp. nov. (RMCA 2018.008.P.0356; 122.9 mm SL). **a.** Dorsal view of the lower pharyngeal jaw. **b.** Lateral view of the lower pharyngeal jaw.

Haplochromis kimondo sp. nov.

urn:lsid:zoobank.org:act:24F01142-A596-458D-9887-D5BC8E68A275

Figs 1–2, 23–25; Table 1

Differential diagnosis

Species with a piscivorous morphology; head blunt and with convex dorsal outline; cheek deep [ChD 27.1–35.2 (mean 30.9) % HL]; outer oral teeth many and small [UOT 43–70 (median 56)]; dominant males grey dorsally and yellow ventrally.

Amongst piscivorous species from the Lake Edward system, *H. kimondo* sp. nov. differs from *H. latifrons* sp. nov., *H. mentatus*, *H. rex* sp. nov., *H. simba* sp. nov., *H. glaucus* sp. nov., and *H. aquila* sp. nov. by the combination of a broader head [HW 42.9–48.0 (45.1) vs 36.8–43.7 (39.2–42.0) % HL], small vs large outer oral teeth, and a larger number of outer upper jaw teeth [UOT 43–70 (56) vs 22–47 (27–36)].

It differs from *H. falcatus* sp. nov., *H. curvidens* sp. nov., *H. pardus* sp. nov., *H. quasimodo* sp. nov., and *H. squamipinnis* by the combination of body pyriform vs oval to rhomboid, and snout blunt vs (very) acute in dorsal view.

It further differs from *H. falcatus* sp. nov. and *H. curvidens* sp. nov. by the combination of deeper cheeks [ChD 27.1–35.2 (30.9) vs 22.4–28.0 (23.2–26.0) % HL], broader jaws [LJW 44.7–53.3 (49.3) vs 38.5–45.5 (40.8–42.5) % LJL], and a slightly broader head [HW 42.9–48.0 (45.1) vs 39.9–44.4 (42.6–43.4) % HL]; further from *H. falcatus* sp. nov. by dominant males grey dorsally and yellow ventrally vs olive-green with an orange-red anterior part of flank; further from *H. curvidens* sp. nov. by presence vs absence of a well-defined mid-lateral band in all specimens.

It further differs from *H. pardus* sp. nov., *H. quasimodo* sp. nov., and *H. squamipinnis* by a steeper sloping snout (40–50° vs 30–40°) and dominant males grey dorsally and yellow ventrally vs speckled to uniformly black, light grey dorsally and blue-black ventrally, or slate blue, respectively; further from *H. pardus* sp. nov. and *H. quasimodo* sp. nov. by a broader interorbital area [IOW 49.2–58.5 (52.8) vs 39.3–48.7 (43.9–44.6) % HW]; further from *H. squamipinnis* by absence vs presence of minute scales on proximal part of dorsal and anal fins.

Etymology

Specific name from the Swahili ‘kimondo’ for ‘meteor’; referring to blunt head, pyriform body with mid-lateral band, and yellow colouration of ventral part of body.

Material examined

Holotype

UGANDA • ♂, 152.4 mm SL; Lake Edward, Kayanja offshore; 0°05'34.8" S, 29°45'28.8" E; 21 Mar. 2019; HIPE4 exped. leg.; RMCA 2019.002.P.0015.

Paratypes

DEMOCRATIC REPUBLIC OF THE CONGO • 1 ♀, 158.2 mm SL; “Lac Edouard: au large de la riv. Kigera” [Lake Edward: offshore of the Kigera River]; 0°29'42" S, 29°38'14" E (inferred); 25 May 1953; KEA exped. leg.; IRSBN 13477 • 1 ♂, 1 ♀, 149.9, 171.3 mm SL; “Lac Edouard: 2–3 km à l’Ouest de Kiavinionge” [Lake Edward: 2–3 km west of Kiavinionge]; 0°11'39" S, 29°32'31" E (inferred); 1 Jun. 1953; KEA exped. leg.; IRSBN 13482.

UGANDA – **Lake Edward** • 1 ♀, 146.4 mm SL; Rwenshama; 0°24'05.7" S, 29°46'35.1" E; 8 Nov. 2016; HIPE1 exped. leg.; rocky shore; RMCA 2016.035.P.0226 • 3 ♀♀, 103.8–124.4 mm SL; Rwenshama,;

0°24'05.7" S, 29°46'35.1" E; 26 Mar. 2017; HIPE2 exped. leg.; rocky shore; RMCA 2017.006.P.0360 to 0362 • 1 ♀, 1 ♂, 106.4–131.1 mm SL; Kayanja offshore; 0°05'34.8" S, 29°45'28.8" E; 31 Mar. 2017; HIPE2 exped. leg.; RMCA 2017.006.P.0363 to 0364 • 2 ♂♂, 1 ♀, 81.6–118.4 mm SL; same collection data as for preceding; RMCA 2017.006.P.0365 to 0367 • 1 ♂, 2 ♀♀, 89.6–115.9 mm SL; Kayanja offshore; 0°05'31.2" S, 29°45'30.3" E; 20 Jan. 2018; HIPE3 exped. leg.; RMCA 2018.008.P.0358 to 0360 • 2 ♂♂, 2 ♀♀, 128.1–146.8 mm SL; 0°24'16.0" S, 29°46'24.8" E; 24 Jan. 2018; HIPE3 exped. leg.; bought at Rwenshama landing site; RMCA 2018.008.P.0361 to 0364 • 1 ♀, 142.9 mm SL; Rwenshama; 0°24'05.7" S, 29°46'35.1" E; 24 Jan. 2018; HIPE3 exped. leg.; rocky shore; RMCA 2018.008.P.0357.

Description

Based on 21 specimens (81.6–171.3 mm SL); body shallow (Table 1) and pyriform (Fig. 23). Head long, stout, average in width in comparison to generalised *H. elegans* (but broad for a piscivorous species), and with a convex dorsal outline; eye small; interorbital area average in width; cheek and lacrimal deep. Snout long, blunt, and slopes at 40–50°; premaxillary pedicel long and slightly prominent. Jaws isognathous to slightly prognathous, long, relatively stout, rounded in dorsal view, and narrow; gape large and slopes at 25–30°; maxilla extends to vertical through pupil. Lower jaw with a straight ventral outline in lateral view, mental prominence absent or weakly developed, and lower jaw side nearly flat with an inclination of 15–30° to horizontal in anterior view. Upper jaw weakly expanded anteriorly. Lips and oral mucosa large. Neurocranium average in depth, ethmo-vomerine block decurved, preorbital region average in depth (23–25% NL), orbital region average in depth (31–33% NL), and supraoccipital crest shallow and wedge-shaped (Fig. 24b).

Outer oral teeth numerous and very small. Necks stout, conical, and straight; crowns recurved and unicuspid in large specimens (> 85 mm SL), bicuspid in small specimens (< 85 mm SL); major cusps acutely pointed; minor cusps small. Dental arcades rounded. Outer teeth closely and regularly set with

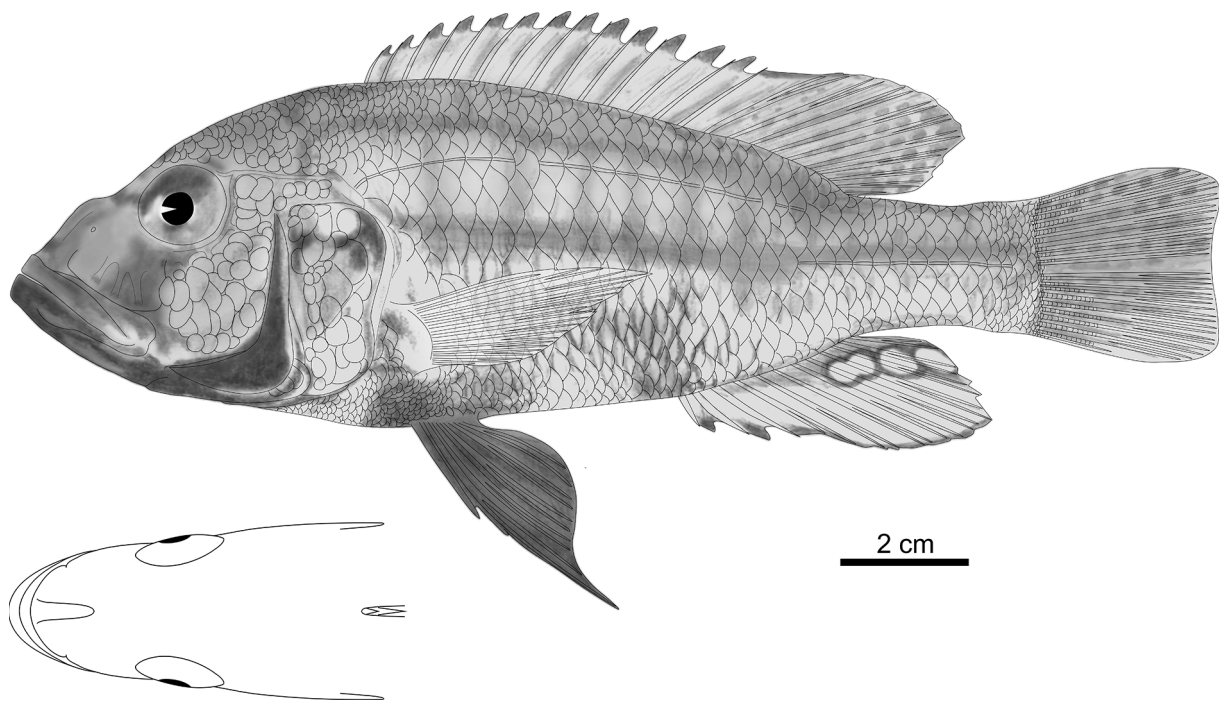


Fig. 23. *Haplochromis kimondo* sp. nov., holotype, ♂, 152.4 mm SL (RMCA 2019.002.P.0015). Drawn by N. Vranken.

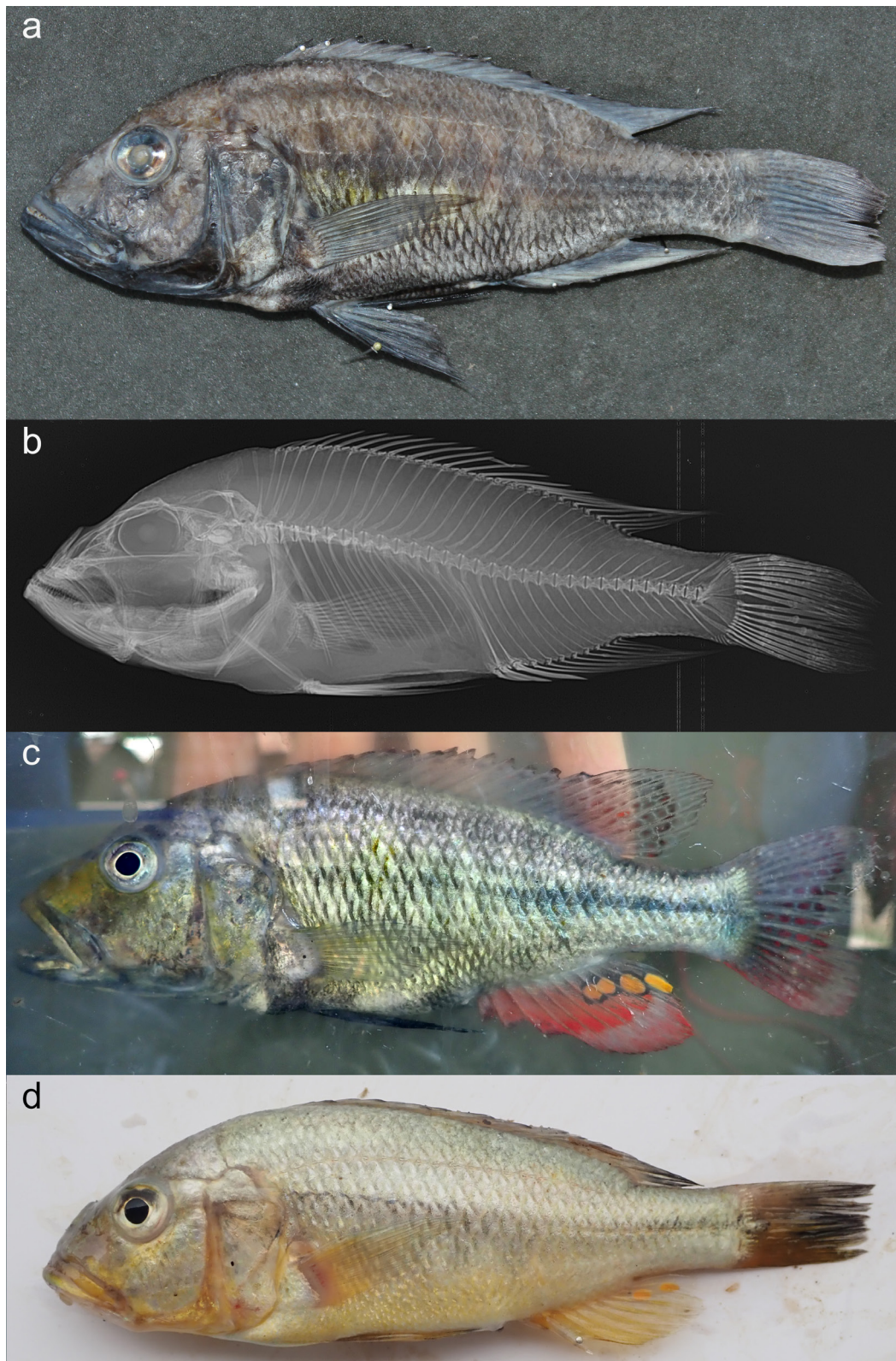


Fig. 24. *Haplochromis kimondo* sp. nov. **a.** Photograph of preserved holotype (RMCA 2019.002.P.0015; 152.4 mm SL). **b.** X-ray image of holotype. **c–d.** Photographs of freshly caught specimens. **c.** Holotype, a dominant male. **d.** Female (RMCA 2018.008.P.0364; 128.1 mm SL) to illustrate the live colour patterns. The contrast was slightly enhanced.

neck-distances of $\frac{1}{2}$ –1 neck-width. In upper jaw, 2–3 posteriormost teeth enlarged. Inner teeth small, weakly recurved, unicuspid in large specimens (> 100 mm SL), weakly tricuspid in small specimens (< 100 mm SL), and acutely pointed in all specimens. Tooth bands very slender crescent-shaped with 1–3 rows of inner teeth, and narrow posteriorly until only outer row remains past $\frac{2}{3}$ length of tooth band in lower jaw, past $\frac{3}{4}$ length of tooth band in upper jaw. Inner teeth closely and regularly set on $\frac{1}{2}$ –1 outer neck-width from outer row; implantation erect; size uniform throughout tooth band.

Lower pharyngeal bone average in length, triangular, slim, and shallow with a slightly deeper keel (Fig. 25). Pharyngeal teeth relatively large and relatively stout; major cusps acutely pointed; cusp gaps concave; minor cusps and cusp protuberances very small. Teeth in two median longitudinal rows equal in size and form to lateral teeth, 10 in each row. Posterior transverse row with 18–19 teeth, implanted erectly with a lateral inclination; major cusps recurved, bluntly pointed, and laterally compressed; minor cusps mostly absent.

Chest scales small; transition to larger flank scales gradual. Minute scales on proximal half of caudal fin.

Caudal fin emarginate to subtruncate; dorsal and anal fins reach to between verticals through one scale anterior to and one scale posterior to caudal-fin base. Pectoral fin reaches to genital opening; pelvic fin reaches to between genital opening and first anal-fin spine in females, to between first and second anal-fin spines in males; first branched pelvic-fin ray slightly elongated in all specimens.

Ceratobranchial gill rakers in outer row of first gill arch short, stout, and simple; posteriormost rakers mostly anvil-shaped. Epibranchial gill rakers relatively slender and simple.

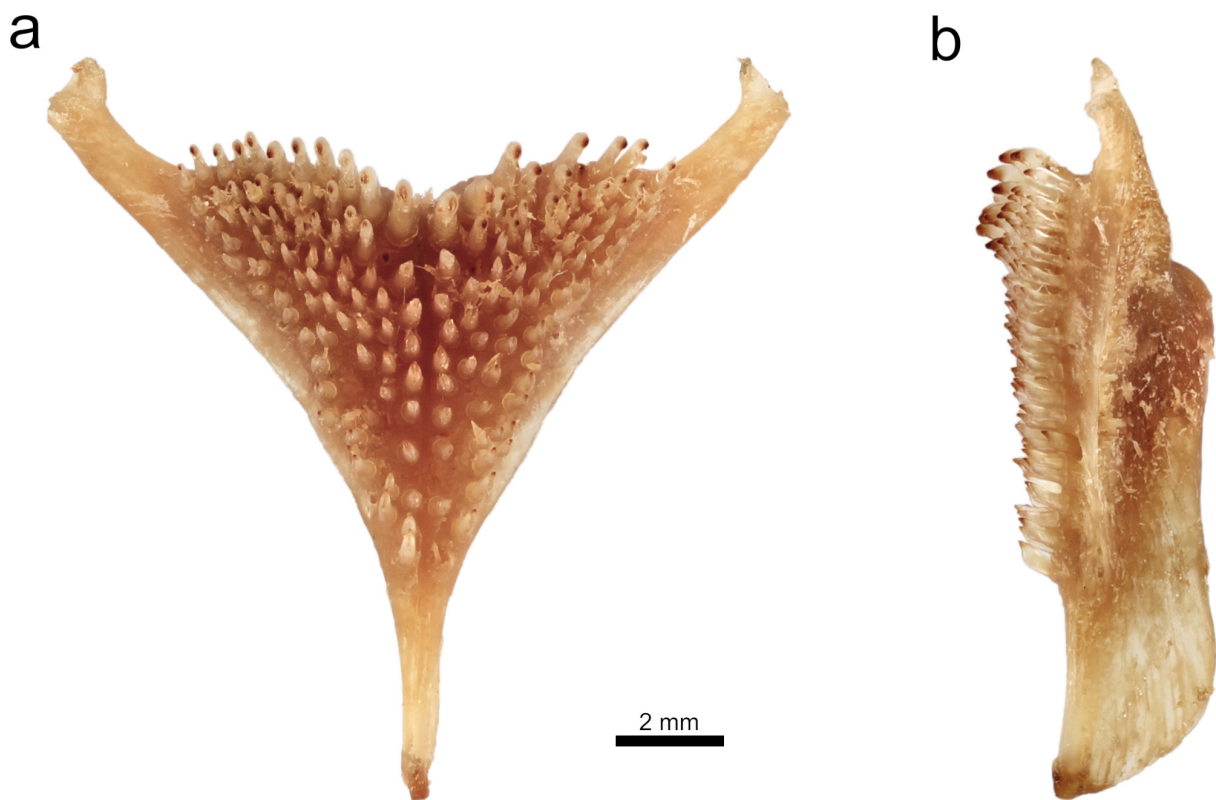


Fig. 25. *Haplochromis kimondo* sp. nov. (RMCA 2018.008.P.0364; 128.1 mm SL). **a.** Dorsal view of the lower pharyngeal jaw. **b.** Lateral view of the lower pharyngeal jaw.

Colouration in life

Dominant males: dorsal parts of both body and head grey; ventral half of body, operculum, cheek, and lips yellow; flank with a blue sheen (Fig. 24c). Lower jaw, preoperculum, and branchiostegal membrane black; belly and chest speckled black; eye with (dark) grey outer ring and silver-yellow inner ring. Flank often with a well-defined mid-lateral band, very faint dorsal-lateral band and 6–7 very faint vertical stripes. Lacrimal stripe broad and well-defined, vertical preopercular stripe well-defined, and nostril and interorbital stripes faint. Pelvic fin black; pectoral fin hyaline. Dorsal fin hyaline and with black lappets; caudal fin dusky dorsally and crimson ventrally; posterior part of dorsal fin and dorsal part of caudal fin maculated crimson. Anal fin crimson and with dusky base and posterior part, black distal border and lappets, and 2–4 small orange egg-spots with dusky rings.

Females and juveniles: dorsal part of body, flank, operculum, cheek, and lips light-grey; ventral part of body, belly, chest and branchiostegal membrane white to yellow; eye with (dark) grey outer ring and silver-yellow inner ring (Fig. 24d). Flank often with a well-defined mid-lateral band and a faint dorsal-lateral band. Snout and lacrimal dusky. Nostril, interorbital, and lacrimal stripes faint, mental blotch present. Pectoral fin yellowish, pelvic fin yellow, dorsal fin hyaline and with black lappets, anal fin yellow and with 1–3 small spots resembling egg-spots, and caudal fin dusky dorsally and yellow ventrally.

Preserved colouration

Dorsal part of body brown; ventral part of body yellowish in females, speckled black in dominant males (Fig. 24a). Cheek light yellow in females, brown in dominant males; lower jaw and preoperculum black in dominant males; snout dusky in all specimens. Flank often with a well-defined mid-lateral band, a faint dorsal-lateral band and 6–7 vertical stripes. Nostril and interorbital stripes faint, lacrimal stripe broad and well-defined, mental blotch present, and vertical preopercular stripes well-defined in dominant males. Pectoral fin hyaline, pelvic fin dusky in females and black in dominant males, dorsal fin dusky and with black lappets and maculated posterior part. Anal fin whitish in females, while hyaline, with dark base and posterior part, and 2–4 small egg-spots in dominant males. Caudal fin with dusky and maculated dorsal part and hyaline ventral part.

Distribution and ecology

Only known from Lake Edward, found over sandy substrates. Based on its morphology, most probably a piscivorous species.

Haplochromis falcatus sp. nov.

[urn:lsid:zoobank.org:act:B780DC12-8C55-4B57-98F1-5799201CD438](https://zoobank.org/act:B780DC12-8C55-4B57-98F1-5799201CD438)

Figs 1–2, 26–28; Table 1

Differential diagnosis

Species with a piscivorous morphology; outer oral teeth many, small, and strongly recurved [UOT 39–51 (median 45)]; dominant males olive-green with an orange-red anterior part of flank and well-defined mid-lateral and dorsal-lateral bands.

Amongst piscivorous species from the Lake Edward system, *H. falcatus* sp. nov. differs from all except *H. curvidens* sp. nov. by strongly recurved vs straight to weakly recurved outer jaw teeth.

It further differs from *H. latifrons* sp. nov., *H. rex* sp. nov., *H. simba* sp. nov., and *H. aquila* sp. nov. by the combination of smaller outer oral teeth and a larger number of outer upper jaw teeth [UOT 39–51 (45) vs 22–42 (27–31)]; further from *H. latifrons* sp. nov., *H. rex* sp. nov., and *H. simba* sp. nov. by a shallower lacrimal [LaD 16.1–18.8 (mean 18.0) vs 18.7–23.0 (19.5–20.8) % HL]; further from *H. rex*

sp. nov., *H. simba* sp. nov., and *H. aquila* sp. nov. by presence vs absence of well-defined mid-lateral and dorsal-lateral bands, and dominant males uniformly olive-green with an orange-red anterior part of flank vs cream-coloured with an orange operculum and light blue snout, uniformly yellow with an orange anterior part of flank, or light grey with a black head, respectively.

It further differs from *H. mentatus* and *H. glaucus* sp. nov. by the combination of a longer pre-dorsal distance [PrD 36.9–41.1 (39.5) vs 33.3–37.0 (35.3–36.1) % SL], a gentler lower jaw side (15–25° vs 30–45°), and presence vs absence of well-defined mid-lateral and dorsal-lateral bands; further from *H. mentatus* by a longer head [HL 36.6–39.6 (38.2) vs 33.4–37.0 (35.1) % SL]; further from *H. glaucus* sp. nov. by dominant males olive-green with an orange-red anterior part of flank vs uniformly light blue.

It further differs from *H. kimondo* sp. nov. by the combination of an oval vs pyriform body, a straight vs convex dorsal outline of head, shallower cheeks [ChD 23.3–27.4 (exceptionally 28.0 in one specimen) (mean 26.0) vs 27.1–35.2 (30.9) % HL], narrower jaws [LJW 40.2–45.6 (42.5) vs 44.7–53.3 (49.3) % L JL], and dominant males olive-green with an orange-red anterior part of flank vs grey dorsally and yellow ventrally.

It differs from *H. curvidens* sp. nov. and further differs from *H. pardus* sp. nov. by the combination of a deeper cheek [ChD 25.1–28.0 (exceptionally 23.3 in one specimen) (mean 26.0) vs 20.8–24.9 (22.5–23.2) % HL] and a longer pre-dorsal distance [PrD 38.2–41.1 (exceptionally 36.9 in one specimen) (mean 39.5) vs 34.1–37.9 (36.0–36.3) % SL]; further from *H. curvidens* sp. nov. by presence vs absence of well-defined mid-lateral and dorsal-lateral bands; further from *H. pardus* sp. nov. by larger adult size (max. 137 vs 96 mm SL) and colour pattern of small specimens (< 100 mm SL) light coloured vs speckled to uniformly black.

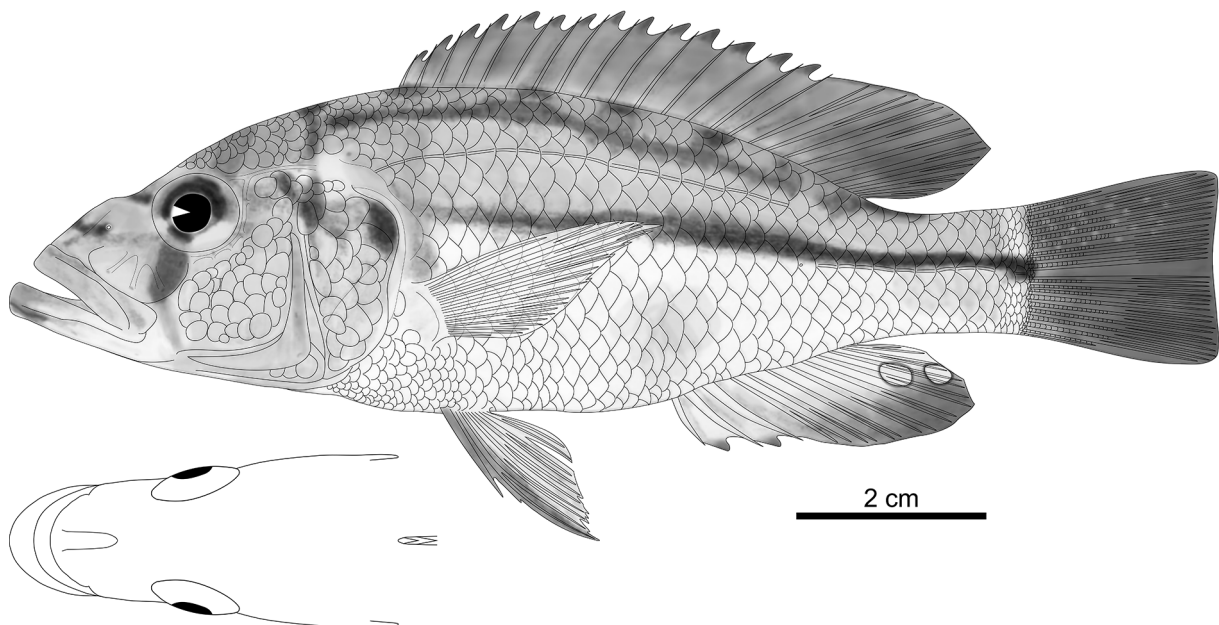


Fig. 26. *Haplochromis falcatus* sp. nov., holotype, ♂, 101.3 mm SL (RMCA 2018.008.P.0401). Drawn by N. Vranken.

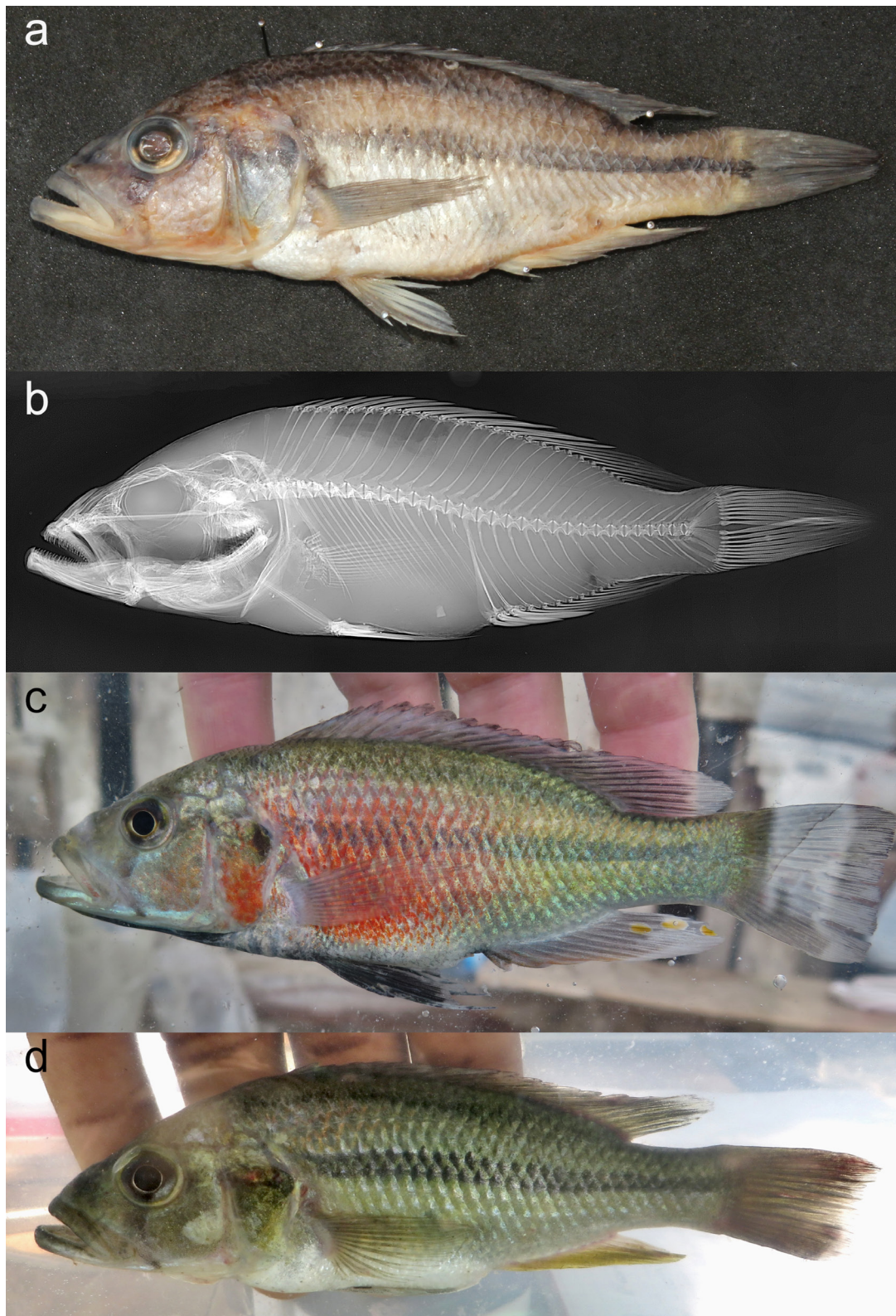


Fig. 27. *Haplochromis falcatus* sp. nov. **a.** Photograph of preserved holotype (RMCA 2018.008.P.0401; 101.3 mm SL). **b.** X-ray image of holotype. **c–d.** Photographs of freshly caught specimens. **c.** Dominant male (RMCA 2017.006.P.0416; 119.1 mm SL). **d.** Female (RMCA 2016.035.P.0257; 112.8 mm SL) to illustrate the live colour patterns. The contrast was slightly enhanced.

It further differs from *H. quasimodo* sp. nov. and *H. squamipinnis* by the combination of a longer head [HL 36.6–39.6 (38.2) vs 33.9–37.2 (35.5–36.0) % SL], a shorter pelvic fin [VL 21.6–25.7 (23.5) vs 25.2–35.4 (28.8–29.4) % SL], and dominant males olive-green with an orange-red anterior part of flank vs light grey dorsally and blue-black ventrally or slate blue, respectively; further from *H. squamipinnis* by absence vs presence of minute scales on proximal parts of dorsal and anal fin.

Etymology

Specific name from the Latin '*falcatus*' for 'sickle-shaped'; referring to acutely pointed sickle-like outer oral teeth.

Material examined

Holotype

UGANDA • ♂, 101.3 mm SL; Lake Edward, Kayanja offshore; 0°05'31.2" S, 29°45'30.3" E; 21 Jan. 2018; HIPE3 exped. leg.; RMCA 2018.008.P.0401.

Paratypes

DEMOCRATIC REPUBLIC OF THE CONGO • 1 ♀, 136.8 mm SL; "Lac Edouard: riv. Luniasenke" [Lake Edward: Luniasenke River]; 0°27'19.2" S, 29°22'08.7" E (inferred); 04 Jan. 1953; KEA exped. leg.; IRSNB 13469 • 1 ♀, 137.1 mm SL; "Lac Edouard: ½h à l'Ouest d'Ishango" [Lake Edward: ½ hour west of Ishango]; 0°08'14" S, 29°38'23" E (inferred); 27 Mar. 1953; KEA exped. leg.; IRSNB 13473.

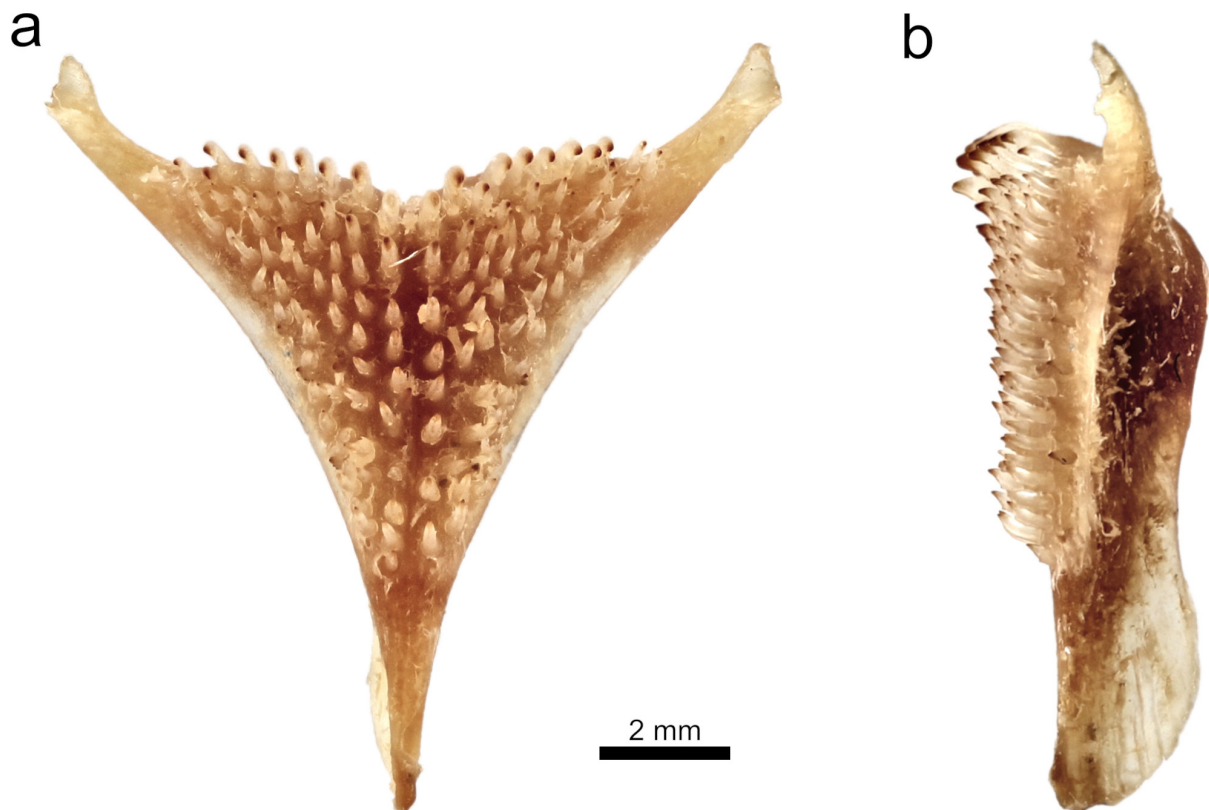


Fig. 28. *Haplochromis falcatus* sp. nov. (RMCA 2018.008.P.0397; 103.3 mm SL). **a.** Dorsal view of the lower pharyngeal jaw. **b.** Lateral view of the lower pharyngeal jaw.

UGANDA – **Lake Edward** • 1 ♂, 2 ♀♀, 98.6–112.8 mm SL; 1 km east of Nyamugasani River; 0°10'22.8" S, 219°50'13.2" E; 22 Oct. 2016; HIPE1 exped. leg.; sand substrate; RMCA 2016.035.P.0256 to 0258 • 1 ♀, 110.8 mm SL; mouth of Kazinga Channel; 0°12'14.4" S, 29°52'37.2" E; 23 Mar. 2017; HIPE2 exped. leg.; hard substrate; RMCA 2017.006.P.0415 • 1 ♂, 1 ♀, 119.1–120.7 mm SL, no morphometrics taken; 0°24'16.0" S, 29°46'24.8" E; 25 Mar. 2017; HIPE2 exped. leg.; bought at Rwenshama landing site; RMCA 2017.006.P.0416 to 0417 • 1 ♀, 81.3 mm SL; Kayanja offshore; 0°05'34.8" S, 29°45'28.8" E; 30 Mar. 2017; HIPE2 exped. leg.; RMCA 2017.006.P.0418 • 2 ♀♀, 81.6, 93.8 mm SL; Kayanja offshore; 0°05'34.8" S, 29°45'28.8" E; 30 Mar. 2017; HIPE2 exped. leg.; RMCA 2017.006.P.0419 to 0420 • 3 ♀♀, 75.0–109.6 mm SL; Kayanja offshore; 0°05'34.8" S, 29°45'28.8" E; 31 Mar. 2017; HIPE2 exped. leg.; RMCA 2017.006.P.0421 to 0423 • 1 ♂, 1 ♀, 88.5–103.3 mm SL; Kayanja, offshore; 0°05'31.2" S, 29°45'30.3" E; 20 Jan. 2018; HIPE3 exped. leg.; RMCA 2018.008.P.0397 to 0398 • 2 ♂♂, 102.1–110.4 mm SL; Kayanja, offshore; 0°05'31.2" S, 29°45'30.3" E; 21 Jan. 2018; HIPE3 exped. leg.; RMCA 2018.008.P.0399 to 0400 • 1 ♀, 93.5 mm SL; same collection data as for preceding; RMCA 2018.008.P.0402 • 2 ♀♀, 110.9–114.2 mm SL; 0°24'16.0" S, 29°46'24.8" E; 24 Jan. 2018; HIPE3 exped. leg.; bought at Rwenshama landing site; RMCA 2018.008.P.0403 to 0404.

Description

Based on 22 specimens (75.0–137.1 mm SL); body shallow (Table 1) and oval (Fig. 26). Head very long, narrow, and with a straight dorsal outline; eye small; interorbital area narrow; cheek and lacrimal average in depth. Snout long, acute, and slopes gently at 35–45°; premaxillary pedicel long and strongly prominent. Jaws isognathous to slightly prognathous, long, slim, narrow, and rounded in dorsal view; gape large and slopes gently at 20–30°; maxilla extends to vertical through pupil. Lower jaw shallow and with a straight ventral outline in lateral view, mental prominence absent, and lower jaw side nearly flat with an inclination of 15–25° to horizontal in anterior view; lower jaw expands slightly laterally halfway its length. Upper jaw weakly expanded anteriorly. Lips and oral mucosa large. Neurocranium shallow, ethmo-vomerine block decurved, preorbital region very shallow (18–22% NL), orbital region shallow (28–30% NL), and supraoccipital crest average in depth and wedge-shaped (Fig. 27b).

Outer oral teeth numerous, unicuspid, and relatively small. Necks stout, conical, and recurved; crowns recurved to strongly recurved, and acutely pointed. Dental arcades rounded, and with anterior half expanded laterally. Outer teeth closely and regularly set with neck-distances of ½–1 neck-width. No enlarged teeth posterior in upper jaw. Inner teeth small, strongly recurved, unicuspid, and acutely pointed. Tooth bands very slender crescent-shaped with 1–2 rows of inner teeth, and narrow posteriorly until only outer row remains past ⅔ lengths of tooth bands. Inner teeth closely and regularly set on ½–1 neck-width from outer row in lower jaw, on 1–2 neck-widths from outer row in upper jaw; implantation recumbent; size uniform throughout tooth band.

Lower pharyngeal bone average in length, triangular, slim, and shallow with a slightly deeper keel (Fig. 28). Pharyngeal teeth relatively large and slender; major cusps acutely pointed; cusp gaps straight; minor cusps and cusp protuberances very small. Teeth in two median longitudinal rows equal in size and form to lateral teeth, 10 in each row. Posterior transverse row with 16–21 teeth, implanted erectly with a lateral inclination; major cusps weakly recurved, bluntly pointed, and laterally compressed; minor cusps mostly absent.

Chest scales small; transition to larger flank scales gradual. Minute scales on proximal half of caudal fin.

Caudal fin subtruncate; dorsal and anal fins reach to vertical through caudal-fin base. Pectoral fin reaches to between genital opening and first anal-fin spine; pelvic fin reaches to between genital opening and first anal-fin spine in females, to first anal fin branched ray in males; first branched pelvic-fin ray elongated in dominant males.

Ceratobranchial gill rakers in outer row of first gill arch very short, stout, and simple; posteriormost rakers weakly anvil-shaped. Epibranchial gill rakers relatively slender and simple.

Colouration in life

Dominant males: body olive-green with yellow sheen; anterior part of flank and operculum bright orange-red; belly and chest speckled black (Fig. 27c). Cheek olive-green with red sheen; snout and lips dusky; lower lip with blue sheen; branchiostegal membrane black; eye with dark silver outer ring and silver to golden inner ring. Flank with well-defined mid-lateral and dorsal-lateral bands; dorsum with 5–7 faint vertical stripes between dorsal-fin base and dorsal-lateral band. Lacrimal, nostril, and interorbital stripes and a mental blotch well defined; supraorbital stripe and nape band faint. Pectoral fin hyaline; pelvic fin black; dorsal fin dusky and with black lappets; anal fin faint orange-red and with dusky base and posterior part, and 3 small yellow egg spots with hyaline rings. Caudal fin with dusky base and hyaline distal part. Non-dominant males: similar to dominant males except for white belly and chest and faint orange-red antero-dorsal part of flank above mid-lateral band.

Females and juveniles: body, operculum, cheek, and lacrimal olive-green yellow; belly, chest, and lower jaw white; eye with dark silver outer ring and silver to golden inner ring (Fig. 27d). Flank with well-defined mid-lateral and dorsal-lateral bands; dorsum with 5–7 faint vertical stripes between dorsal-fin base and dorsal-lateral band. Lacrimal, nostril, and interorbital stripes and a mental blotch well defined; supraorbital stripe and nape band faint. Pectoral and pelvic fins yellowish; dorsal fin dusky and with black lappets; anal fin yellow and with 2–3 small spots resembling egg spots; caudal fin dusky.

Preserved colouration

Dorsal part of body brown; ventral part of body yellowish to white in females; chest and belly speckled black in dominant males (Fig. 27a). Cheek yellowish and snout dusky. Flank with well-defined mid-lateral and dorsal-lateral bands; dorsum with 5–7 faint vertical stripes between dorsal-fin base and dorsal-lateral band. Lacrimal, nostril, and interorbital stripes and a mental blotch well defined; supraorbital stripe and nape band faint. Pectoral fin dusky; pelvic fin dusky in females, black in dominant males; dorsal fin dusky and with black lappets; anal fin with dusky base and posterior part, yellowish distal part, and 1–3 small egg spots; caudal fin dusky and faintly maculated in dorsal part.

Distribution and ecology

Only known from Lake Edward, found over sandy substrates. Based on its morphology, most probably a piscivorous species.

Haplochromis curvidens sp. nov.

[urn:lsid:zoobank.org:act:E11E39DC-0085-4CB5-9E4C-E3EA0C11216F](https://zoobank.org/urn:lsid:zoobank.org:act:E11E39DC-0085-4CB5-9E4C-E3EA0C11216F)

Figs 1–2, 29–31; Table 1

Differential diagnosis

Species with a piscivorous morphology; outer oral teeth many, small, and (strongly) recurved [UOT 45–60 (median 49)]; non-dominant males dusky green with a blue sheen and 5–7 (faint) vertical stripes.

Amongst piscivorous species from the Lake Edward system, *H. curvidens* sp. nov. differs from *H. latifrons* sp. nov., *H. mentatus*, *H. rex* sp. nov., *H. simba* sp. nov., *H. glaucus* sp. nov., and *H. aquila* sp. nov. by small vs large outer oral teeth and a larger number of outer upper jaw teeth [UOT 45–60 (49) vs 22–47 (27–36)]; further from *H. latifrons* sp. nov., *H. mentatus*, *H. rex* sp. nov., *H. simba* sp. nov., and *H. glaucus* sp. nov. by a shallower lacrimal [LaD 16.0–17.8 (mean 16.7) vs 18.0–23.0 (19.5–20.8)]

% HL]; further from *H. rex* sp. nov., *H. simba* sp. nov., *H. glaucus* sp. nov., and *H. aquila* sp. nov. by a shallower cheek [ChD 22.4–24.9 (23.2) vs 26.2–33.5 (28.3–31.1) % HL].

It differs from *H. kimondo* sp. nov., *H. falcatus* sp. nov., and *H. quasimodo* sp. nov. by the combination of a shallower cheek [ChD 22.4–24.9 (23.2) vs 24.8–35.2 (exceptionally 23.3 and 23.7 in one specimen of *H. falcatus* sp. nov. and *H. quasimodo* sp. nov., respectively) (means 26.0–30.9) % HL] and absence vs presence of a well-defined mid-lateral band; further from *H. kimondo* sp. nov. by narrower jaws [LJW 38.5–43.2 (40.8) vs 44.7–53.3 (49.3) % L JL]; further from *H. falcatus* sp. nov. by a shorter pre-dorsal distance [PrD 34.5–37.9 (36.3) vs 38.2–41.1 (exceptionally 36.9 in one specimen) (mean 39.5) % SL]; further from *H. quasimodo* sp. nov. by a shallower body [BD 29.0–32.0 (30.8) vs 33.5–41.7 (37.4) % SL].

It differs from *H. pardus* sp. nov. by the combination of a shorter anal fin base [AFB 17.9–18.6 (18.3) vs 19.2–22.2 (20.5) % SL], a slightly broader interorbital area [IOW 46.4–52.5 (49.1) vs 39.3–48.4 (43.9) % HW], and all specimens faint yellow to dusky green vs speckled to uniformly black.

It differs from *H. squamipinnis* sp. nov. by the combination of a shallower body [BD 29.0–32.0 (30.8) vs 32.4–39.3 (35.7) % SL], a shallower cheek [ChD 22.4–24.9 (23.2) vs 24.9–36.0 (29.0) % HL], and absence vs presence of minute scales on proximal parts of dorsal and anal fins.

Etymology

Specific name from the Latin ‘*curvus*’ for ‘curvature’, and ‘*dentatus*’ for ‘tooth’; referring to strongly recurved oral teeth.

Material examined

Holotype

UGANDA • ♂, 112.0 mm SL; Lake Edward; 0°24'16.0" S, 29°46'24.8" E; 9 Nov. 2016; HIPE1 exped. leg.; bought at Rwenshama landing site; RMCA 2016.035.P.0219.

Paratypes

UGANDA – **Lake Edward** • 1 ♂, 94.8 mm SL; ‘Coral Reef’, hard substrate at mouth of Nyamugasani river; 0°10'08.4" S, 29°49'37.2" E; 21 Oct. 2016; HIPE1 exped. leg.; RMCA 2016.035.P.0215 • 2 ♂♂, 1 ♀, 91.2–102.5 mm SL; Mukutu Kihinga, rocky offshore of Mweya; 0°11'31.2" S, 29°52'26.4" E; 23 Oct. 2016; HIPE1 exped. leg.; RMCA 2016.035.P.0216 to 0218 • 1 ♀, 90.2 mm SL; islands near Katwe; 0°10'04.9" S, 29°52'27.4" E; 18 Jan. 2018; HIPE3 exped. leg.; RMCA 2018.008.P.0340 • 1 ♂, 101.1 mm SL; 0°24'16.0" S, 29°46'24.8" E; 24 Jan. 2018; HIPE3 exped. leg.; bought at Rwenshama landing site; RMCA 2018.008.P.0341 • 1 ♀, 92.3 mm SL, no morphometrics taken; islands near Katwe; 0°10'04.9" S, 29°52'27.4" E; 18 Jan. 2018; HIPE3 exped. leg.; IRSNB 919.

Description

Based on 8 specimens (90.2–112.0 mm SL); body shallow (Table 1) and oval (Fig. 29). Head long, narrow, and with a straight to very gently convex dorsal outline; eye and interorbital area average in width; cheek and lacrimal average in depth. Snout average in length, narrow, acute, and slopes gently at 35–45°; premaxillary pedicel long and strongly prominent. Jaws isognathous to weakly prognathous, long, slim, very narrow, and rounded in dorsal view; gape large and slopes gently at 15–30°; maxilla (almost) extends to vertical through anterior point of pupil. Lower jaw shallow and with a straight ventral outline in lateral view, mental prominence absent, and lower jaw side nearly flat with an inclination of 20–30° to horizontal in anterior view. Upper jaw weakly expanded anteriorly. Lips and oral mucosa thin. Neurocranium shallow, ethmo-vomerine block decurved, preorbital region very shallow (19–21% NL), orbital region shallow (28–31% NL), and supraoccipital crest shallow and wedge-shaped (Fig. 30b).

Outer oral teeth numerous, unicuspid, and small. Necks slender, cylindrical to conical, and weakly recurved; crowns recurved and acutely pointed. Dental arcades rounded. Outer teeth closely and regularly set with neck-distances of $\frac{1}{2}$ neck-width. In upper jaw, 1–3 posteriormost teeth enlarged. Inner teeth small, strongly recurved, unicuspid, and acutely pointed. Tooth bands very slender crescent-shaped with 1–2 rows of inner teeth, and narrow posteriorly until only outer row remains past $\frac{2}{3}$ lengths of tooth bands. Inner teeth closely and regularly set on $\frac{1}{2}$ –1 neck-width from outer row in lower jaw, on 1–2 neck-widths from outer row in upper jaw; implantation recumbent; size uniform throughout tooth band.

Lower pharyngeal bone average in length, narrow, slim, and shallow with a slightly deeper keel (Fig. 31). Pharyngeal teeth relatively large and slender; major cusps acutely pointed; cusp gaps straight; minor cusps and cusp protuberances very small. Teeth in two median longitudinal rows equal in size and form to lateral teeth, 10–11 in each row. Posterior transverse row with 20–22 teeth, implanted erectly with a lateral inclination; major cusps weakly recurved, bluntly pointed, and laterally compressed; minor cusps mostly absent.

Chest scales small; transition to larger flank scales gradual. Minute scales on proximal half of caudal fin.

Caudal fin emarginate; dorsal and anal fins reach to between verticals through caudal-fin base and two scales anterior to this vertical. Pectoral and pelvic fins reach to anal opening, pelvic fin reaches to first anal-fin spine in males; first branched pelvic-fin ray elongated in all specimens.

Ceratobranchial gill rakers in outer row of first gill arch short, stout, and simple; posteriormost rakers anvil-shaped, bi-, or trifold. Epibranchial gill rakers slender and simple.

Colouration in life

Dominant males: colour pattern unknown. Non-dominant males: based on pictures of two recently deceased specimens (Fig. 30c). Dorsal half of body dusky greenish; ventral half of body faint yellow;

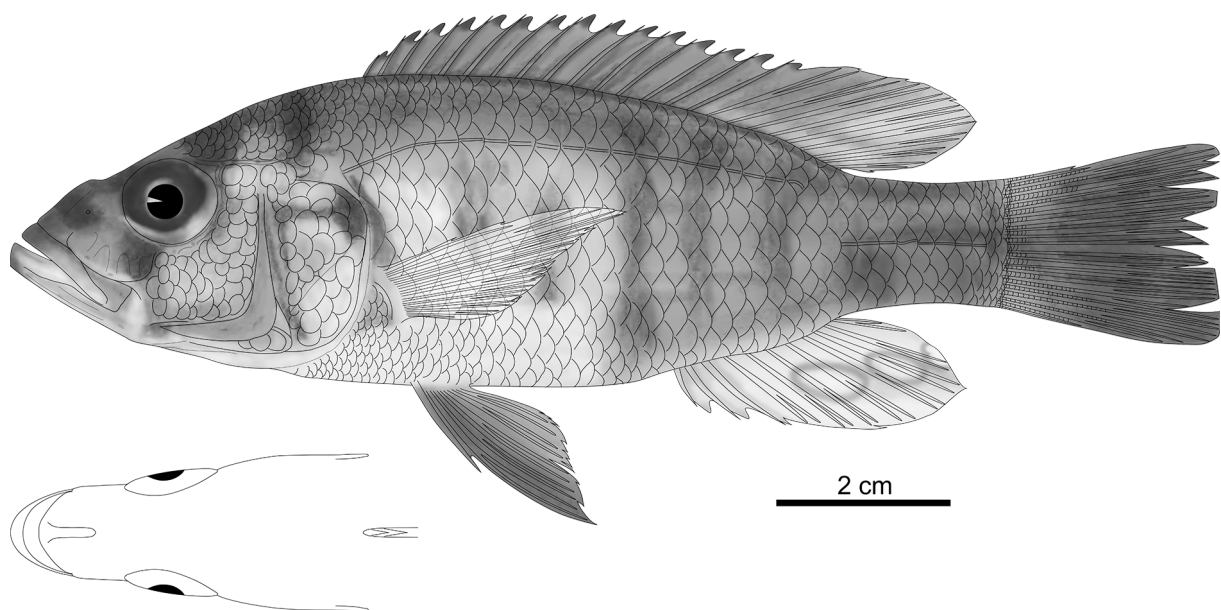


Fig. 29. *Haplochromis curvidens* sp. nov., holotype, ♂, 112.0 mm SL (RMCA 2016.035.P.0219). Drawn by N. Vranken.

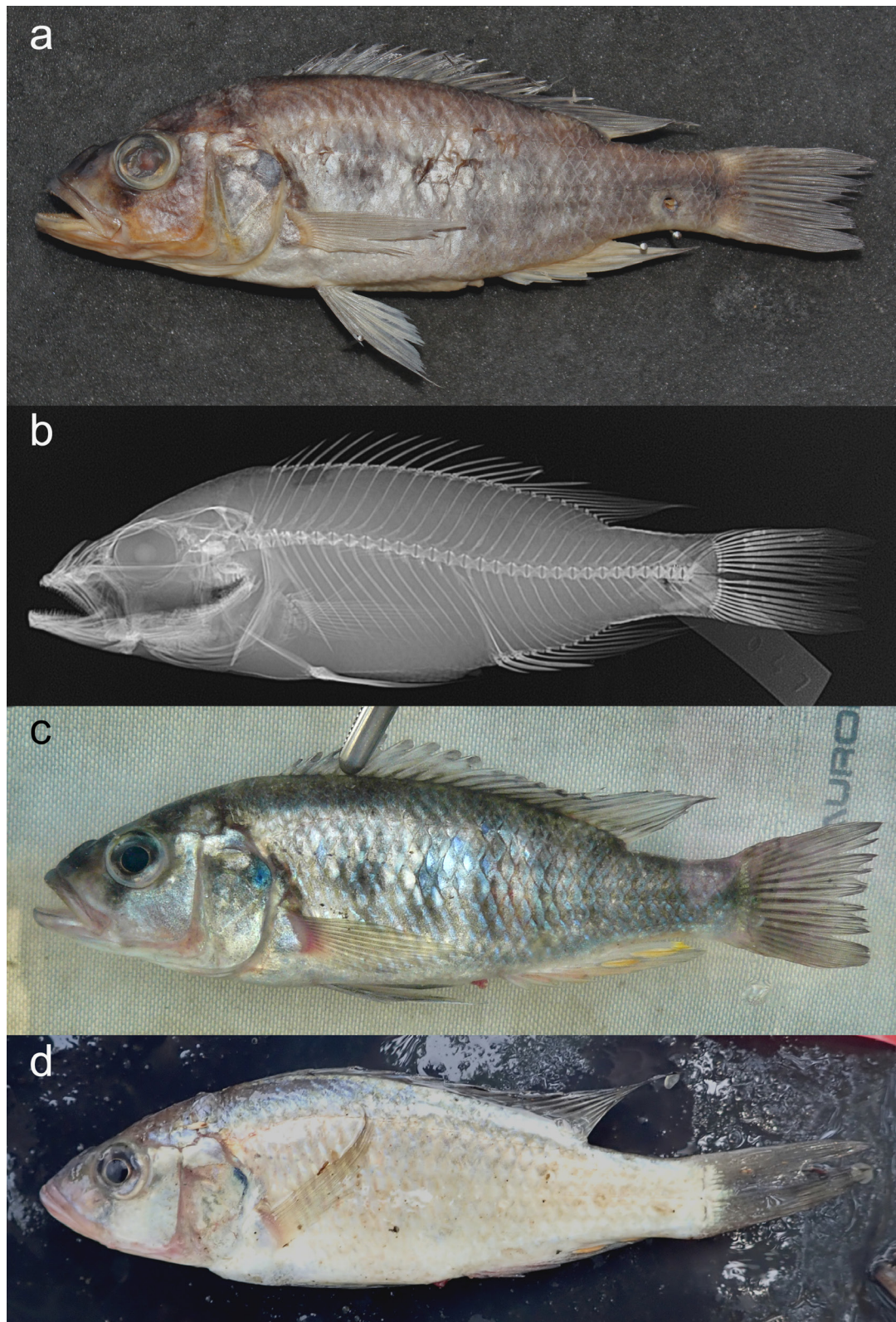


Fig. 30. *Haplochromis curvidens* sp. nov. **a.** Photograph of preserved holotype (RMCA 2016.035.P.0219; 112.0 mm SL). **b.** X-ray image of holotype. **c–d.** Photographs of freshly caught specimens. **c.** Holotype, an adult male. **d.** Female (RMCA 2018.008.P.0340); 90.2 mm SL) to illustrate the live colour patterns. The contrast was slightly enhanced.

transition gradual; flank with blue sheen and 5–7 vertical stripes; belly, chest, and cheek whitish; operculum yellowish; snout dusky; eye with (dark) grey outer ring and silver inner ring. Nostril and lacrimal stripes and nape band present; interorbital and supraorbital stripes faint. Pectoral fin yellowish; pelvic fin black; dorsal fin dusky and with black lappets; anal fin faint orange and with 1–3 relatively large, yellow egg-spots with dusky rings; caudal fin dusky.

Females and juveniles: body faint yellow with a greenish dorsum; belly and chest white; snout dusky; eye with (dark) grey outer ring and silver inner ring (Fig. 30d). Nostril, interorbital, supraorbital, and lacrimal stripes and mental blotch faint. Pectoral and pelvic fin yellowish; dorsal fin dusky and with black lappets; anal fin yellowish and with 2 spots resembling egg-spots; caudal fin dusky.

Preserved colouration

Body brown; dorsum dark brown; chest and belly white; cheek and operculum yellowish; snout dusky (Fig. 30a). Flank with 5–7 (faint) vertical stripes. Nostril and lacrimal stripes and mental blotch present; interorbital and supraorbital stripes faint. Pectoral fin hyaline; pelvic fin yellowish with black first rays in females, black in males; dorsal and caudal fins dusky; dorsal fin with black lappets and posterior sooty part; caudal fin with maculated dorsal part; anal fin yellowish and with dusky distal margin and 1–3 relatively large egg-spots.

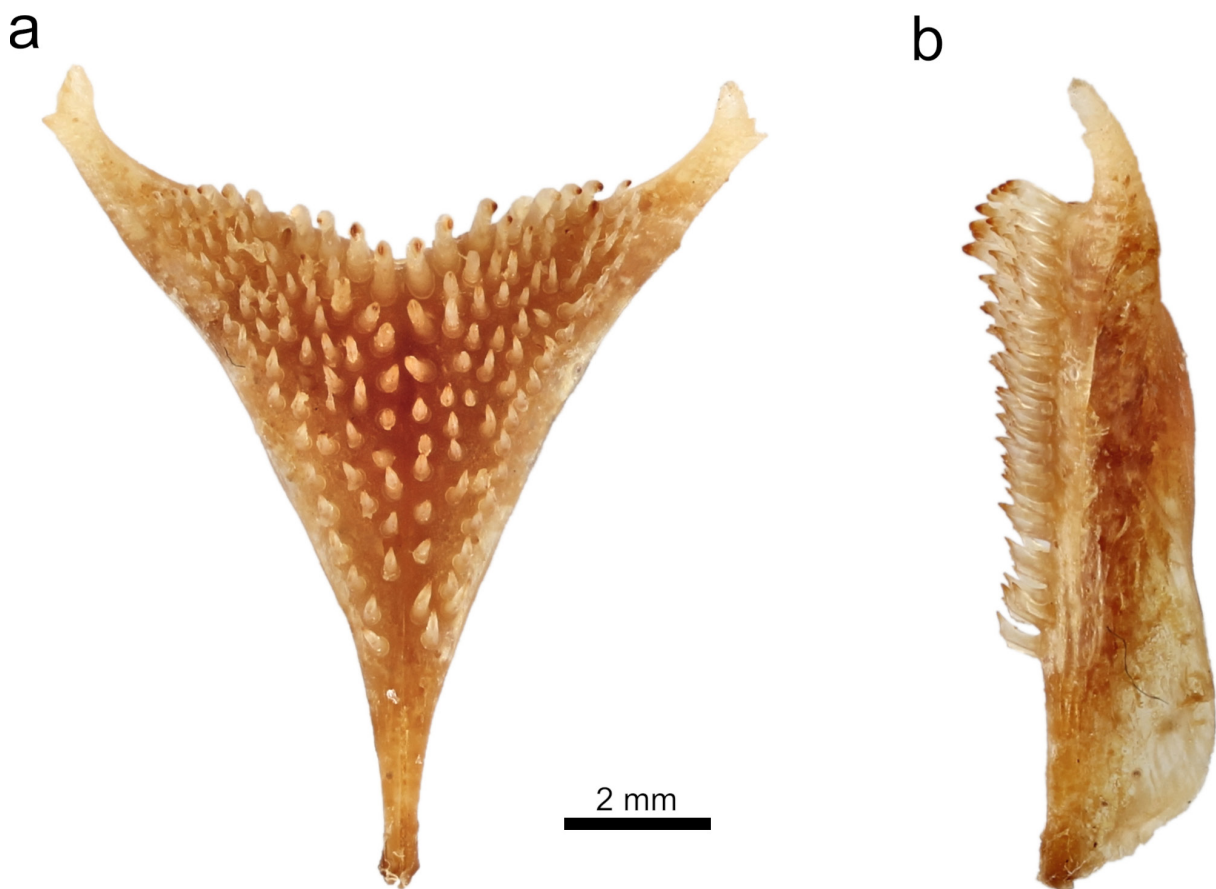


Fig. 31. *Haplochromis curvidens* sp. nov. (RMCA 2016.035.P.0217; 102.5 mm SL). **a.** Dorsal view of the lower pharyngeal jaw. **b.** Lateral view of the lower pharyngeal jaw.

Distribution and ecology

Only known from Lake Edward, found over muddy substrates. Based on its morphology, most probably a piscivorous species.

Haplochromis pardus sp. nov.

[urn:lsid:zoobank.org:act:8DDACAC6-C993-4750-BE1B-1BF4C0312DB7](https://zoobank.org/act:8DDACAC6-C993-4750-BE1B-1BF4C0312DB7)

Figs 1–2, 32–34; Table 1

Differential diagnosis

Species with a piscivorous morphology; adult size small (max. known size 96 mm SL); outer oral teeth many and small [UOT 39–56 (median 58)]; dominant males speckled to uniformly black.

Amongst piscivorous species from the Lake Edward system, *H. pardus* sp. nov. differs from all by the combination of a smaller adult size (max. 96 vs 109–211 mm SL) and colour pattern of small specimens (< 100 mm SL) speckled to uniformly black vs light coloured.

It further differs from *H. latifrons* sp. nov., *H. mentatus*, *H. glaucus* sp. nov., *H. kimondo* sp. nov., and *H. squamipinnis* by the combination of a shallower cheek [ChD 20.8–24.4 (mean 22.5) vs 23.8–36.0 (26.4–30.9) % HL] and a narrower interorbital area [IOW 39.3–48.4 (44.6) vs 48.6–63.3 (51.9–60.0) % HW].

It further differs from *H. rex* sp. nov., *H. simba* sp. nov., and *H. aquila* sp. nov. by the combination of a shallower cheek [ChD 20.8–24.4 (22.5) vs 26.8–33.5 (28.3–31.1) % HL], smaller outer oral teeth, and a larger number of outer upper jaw teeth [UOT 39–51 (45) vs 22–37 (27–31)].

It further differs from *H. falcatus* sp. nov. by the combination of by weakly recurved vs strongly recurved outer jaw teeth, a shallower cheek [ChD 20.8–24.4 (22.5) vs 25.1–28.0 (exceptionally 23.3 in one specimen) (mean 26.0) % HL], and a shorter pre-dorsal distance [PrD 34.1–37.8 (36.0) vs 38.2–41.1 (exceptionally 36.9 in one specimen) (mean 39.5) % SL].

It further differs from *H. curvidens* sp. nov. by the combination of a longer anal-fin base [AFB 19.2–22.2 (20.5) vs 17.9–18.6 (18.3) % SL] and a slightly narrower interorbital area [IOW 39.3–48.4 (44.6) vs 46.4–52.5 (49.1) % HW].

It further differs from *H. quasimodo* sp. nov. by the combination of a shallower cheek [ChD 20.8–24.4 (22.5) vs 23.7–32.9 (27.5) % HL] and a smaller number of caudal peduncle scales (CPS 16, rarely 17 vs 17–20, rarely 16).

Etymology

Specific name from the Latin '*pardus*' for 'leopard'; referring to nearly uniform black to yellow-pink flanks with clear black blotches, i.e., interrupted horizontal and vertical stripes.

Material examined

Holotype

UGANDA • ♂, 89.2 mm SL; Lake Edward, Mukutu Kihinga, rocky offshore of Mweya; 0°11'31.2" S, 29°52'26.4" E; 23 Oct. 2016; HIPE1 exped. leg.; RMCA 2016.035.P.0202.

Paratypes

UGANDA – Lake Edward • 1 ♀, 84.9 mm SL; Mukutu Kihinga, rocky offshore of Mweya; 0°11'31.2" S, 29°52'26.4" E; 23 Oct. 2016; HIPE1 exped. leg.; RMCA 2016.035.P.0203 • 2 ♂♂, 2 ♀♀, 83.6–96.1 mm

SL; mouth of Kazinga Channel; 0°12'32.4" S, 29°53'06.0" E; 24 Oct. 2016; HIPE1 exped. leg.; RMCA 2016.035.P.0204 to 0207 • 1 ♀, 1 ♂, 75.9, 84.7 mm SL; Rwenshama rocky shore; 0°24'05.7" S, 29°46'35.1" E; 26 Mar. 2017; HIPE2 exped. leg.; RMCA 2017.006.P.0342 to 0343 • 3 ♀♀, 67.4–70.5 mm SL; Kayanja offshore; 0°05'34.8" S, 29°45'28.8" E; 30 Mar. 2017; HIPE2 exped. leg.; RMCA 2017.006.P.0346 to 0348 • 1 ♀, 1 ♂, 67.7, 78.1 mm SL; Kayanja offshore; 0°05'34.8" S, 29°45'28.8" E; 30 Mar. 2017; HIPE2 exped. leg.; RMCA 2017.006.P.0344 to 0345 • 1 ♀, 92.4 mm SL; islands near Katwe; 0°10'04.9" S, 29°52'27.4" E; 19 Jan. 2018; HIPE3 exped. leg.; RMCA 2018.008.P.0331 • 1 ♀, 1 ♂, 72.3, 81.7 mm SL; Rwenshama rocky shore; 0°24'05.7" S, 29°46'35.1" E; 24 Jan. 2018; HIPE3 exped. leg.; RMCA 2018.008.P.0332 to 0333 • 2 ♀♀, 2 ♂♂, 71.0–84.9 mm SL; Rwenshama rocky shore; 0°24'05.7" S, 29°46'35.1" E; 26 Mar. 2017; HIPE2 exped. leg.; IRSNB 920 to 922.

Description

Based on 20 specimens (67.4–96.1 mm SL); body shallow (Table 1) and oval to slightly rhomboid (Fig. 32). Head narrow, shallow, and with a straight dorsal outline with a concavity above eye; eye average in size in comparison to generalised *H. elegans* (but large for a piscivorous species); interorbital area very narrow; cheek shallow; lacrimal average in depth. Snout average in length, very acute, and slopes gently at 30–40°; premaxillary pedicel long and prominent. Jaws iso- to slightly prognathous, average in length, narrow, and rounded in dorsal view; gape large and slopes gently at 15–25°; maxilla extends to between verticals through anterior margins of orbit and pupil. Lower jaw shallow and with straight ventral outline in lateral view, mental prominence absent, and lower jaw side nearly flat with an inclination of 15–30° to horizontal in anterior view. Upper jaw weakly expanded anteriorly and ventrally. Lips and oral mucosa large. Neurocranium average in depth, ethmo-vomerine block decurved, preorbital region very shallow (18–22% NL), orbital region average in depth (30–33% NL), and supraoccipital crest shallow and wedge-shaped (Fig. 33b).

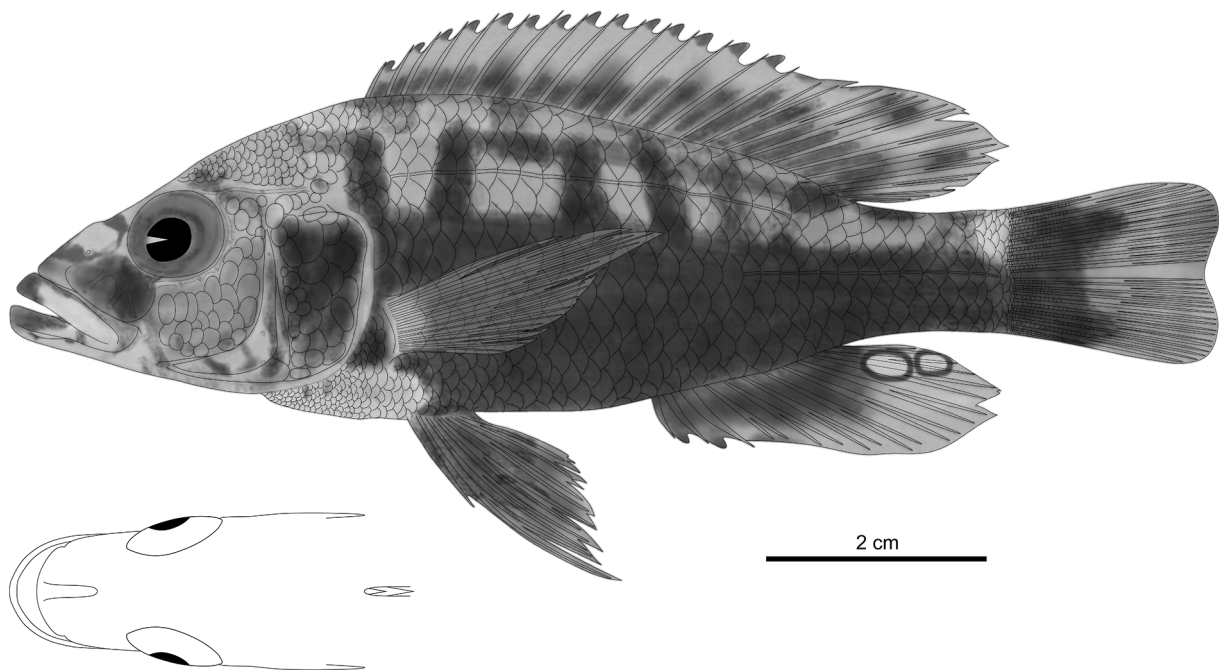


Fig. 32. *Haplochromis pardus* sp. nov., holotype, ♂, 89.2 mm SL (RMCA 2016.035.P.0202). Drawn by N. Vranken.

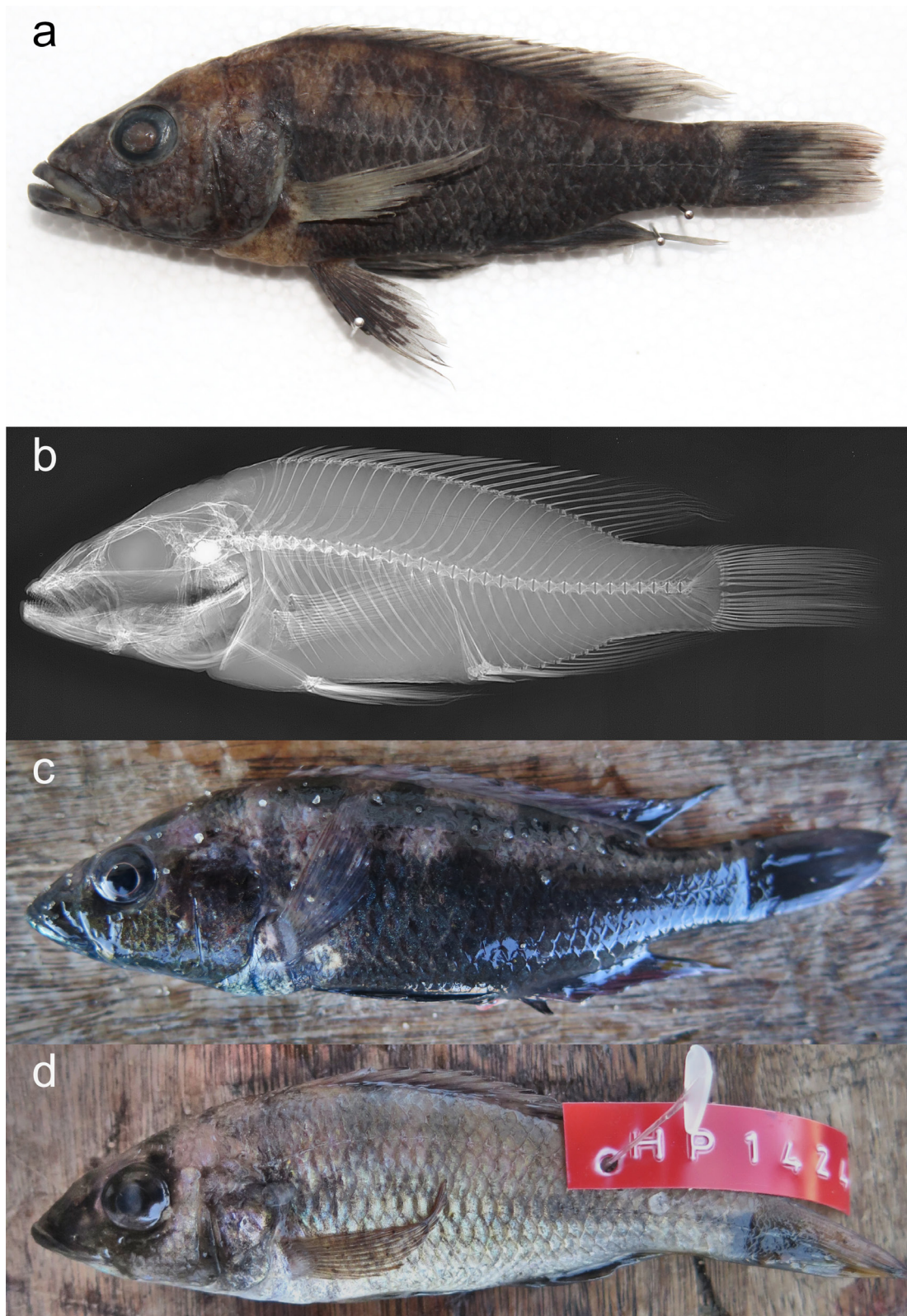


Fig. 33. *Haplochromis pardus* sp. nov. **a.** Photograph of preserved holotype (RMCA 2016.035.P.0202; 89.2 mm SL). **b.** X-ray image of holotype. **c–d.** Photographs of freshly caught specimens. **c.** Dominant male (RMCA 2017.006.P (HP1463); 81.4 mm SL). **d.** Female (RMCA 2017.006.P.0342; 75.9 mm SL) to illustrate the live colour patterns. The contrast was slightly enhanced.

Outer oral teeth numerous, small, and weakly embedded in oral mucosa. Necks stout, cylindrical, and straight; crowns weakly recurved, unicuspid in large specimens (< 80 mm), bicuspid with posteriorly some weakly tricuspid teeth in small specimens (> 70 mm), and acutely pointed in all specimens. Dental arcades rounded and with anterior half weakly expanded laterally. Outer teeth closely and regularly set with neck-distances of $\frac{1}{2}$ neck-width; lateral outer teeth implanted slightly labially. In upper jaw, 1–3 posteriormost teeth enlarged. Inner teeth small, recurved, unicuspid in large specimens (> 80 mm), tricuspid in small specimens (< 70 mm), and acutely pointed in all specimens. Tooth bands very slender crescent-shaped with 2 (rarely 3) rows of inner teeth, and narrow posteriorly until only outer row remains past $\frac{2}{3}$ length of tooth band. Inner rows closely and regularly set on 1 neck-width from outer row in lower jaw, on 1–2 neck-widths from outer row in upper jaw; implantation erect in first row and recumbent in subsequent rows; size uniform throughout tooth band.

Lower pharyngeal bone average in length, narrow, slim, and shallow over entire length (Fig. 34). Pharyngeal teeth small and slender; major cusps acutely pointed; cusp gaps nearly straight; minor cusps and cusp protuberances small. Teeth in two median longitudinal rows equal in size and form to lateral teeth, 11–12 in each row. Posterior transverse row with 22 teeth, implanted erectly with a slight lateral inclination; major cusps weakly recurved, bluntly pointed, and laterally compressed; minor cusps mostly present.

Chest scales small; transition to larger flank scales gradual. Minute scales on proximal half of caudal fin.

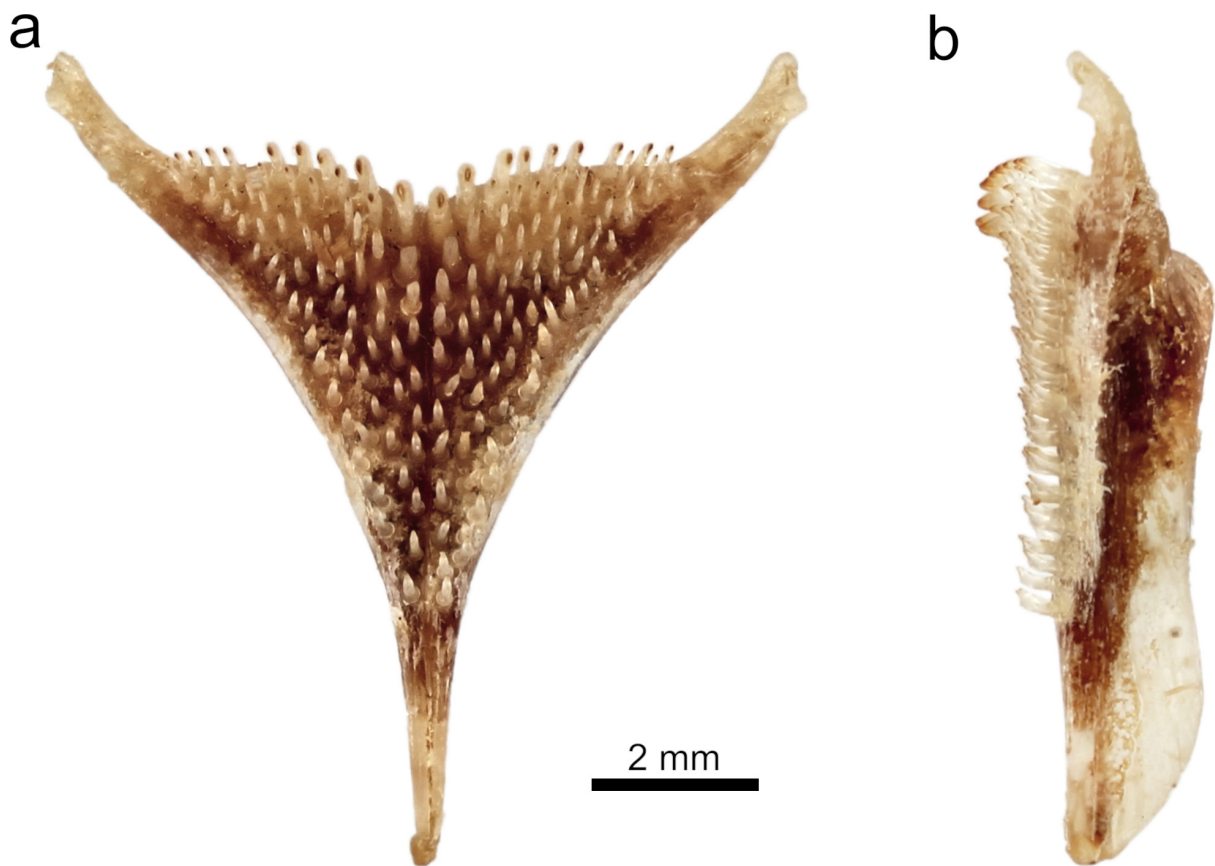


Fig. 34. *Haplochromis pardus* sp. nov. (RMCA 2016.035.P.0207; 96.1 mm SL). **a.** Dorsal view of the lower pharyngeal jaw. **b.** Lateral view of the lower pharyngeal jaw.

Caudal fin emarginate; dorsal and anal fins reach to between verticals through one scale anterior and one scale posterior to caudal-fin base. Pectoral and pelvic fins reach to genital opening; pelvic fin reaches to first anal-fin spine in males; first branched pelvic-fin ray not elongated.

Ceratobranchial gill rakers in outer row of first gill arch short, stout, and simple; posteriormost rakers mostly weakly bifid. Epibranchial gill rakers relatively slender and simple.

Colouration in life

Dominant males: body speckled to uniformly black with a blue sheen; dorsum and dorsal part of head pink to speckled black; chest white; belly, caudal peduncle, operculum, lower jaw, and lips black; cheek, lacrimal, and snout speckled to uniformly black, cheek with yellow sheen; eye with grey to dark outer ring and silver to dark inner ring (Fig. 33c). Flank with dorsal-lateral and mid-lateral bands and 5–6 vertical stripes, all black, broad, well-defined, but interrupted, hereby body seemingly blotched. Nostril, interorbital, supraorbital, lacrimal, vertical preopercular stripes, nape band, mental blotch, and black posterior margin of operculum well-defined. Pectoral, dorsal, and anal fins dusky; lappets, bases, and posterior parts of anal and dorsal fins black; anal fin with faint crimson flush and 1–3 small orange egg-spots with dusky rings. Pelvic and caudal fins black; caudal fin with dusky distal part and a faint crimson flush.

Females and juveniles: body yellowish with a dusky sheen; dorsum and dorsal part of head pink; belly, chest, operculum, and cheek, white; lacrimal speckled black; snout dusky to black; eye with grey to dark outer ring and silver to dark inner ring (Fig. 33d). Flank with dorsal-lateral and mid-lateral bands and 5–6 vertical stripes, all faint and interrupted. Nostril and interorbital stripes faint; supraorbital, lacrimal, vertical preopercular stripes, mental blotch, and nape band well-defined. Pectoral, pelvic, and dorsal fins dusky; anal and caudal fins dusky with yellow sheen; dorsal and anal fins with black lappets and posterodistal part; caudal fin with black base and 1–2 small spots resembling egg-spots.

Preserved colouration

In all specimens, dorsal part of body dark brown to speckled black; ventral part of body dark brown to uniformly black; belly black; chest whitish (Fig. 33a). Flank with faint to well-defined, broad, but interrupted mid-lateral, dorsal-lateral, and dorsal-medial bands and 5–6 vertical stripes. Snout dusky; lips dusky with well-defined black spots; cheek yellowish to black; operculum black. Nostril, interorbital, supraorbital, lacrimal, vertical preopercular stripes, nape band, mental blotch, and black posterior margin of operculum well-defined. Pectoral, dorsal, and anal fins dusky; lappets, bases, and posterior parts of anal and dorsal fins black; anal fin with 1–3 egg-spots. Pelvic and caudal fins dusky to black; caudal fin with blackish distal part.

Distribution and ecology

Only known from Lake Edward; found in inshore areas. Based on its morphology, most probably a piscivorous species.

Haplochromis quasimodo sp. nov.

[urn:lsid:zoobank.org:act:6AE722D9-3BF6-4DD5-8637-55B8400EDD11](https://zoobank.org/act:6AE722D9-3BF6-4DD5-8637-55B8400EDD11)

Figs 1–2, 35–37; Table 1

Differential diagnosis

Species with a piscivorous morphology; body rather deep [BD 33.5–41.7 (mean 37.4) % SL]; interorbital area narrow [IOW 40.5–48.7 (43.9) % HL]; outer oral teeth many and small [UOT 46–71 (median 58)]; dominant males light grey dorsally and blue-black ventrally.

Amongst piscivorous species from the Lake Edward system, *H. quasimodo* sp. nov. differs from *H. latifrons* sp. nov., *H. mentatus*, *H. rex* sp. nov., *H. simba* sp. nov., *H. glaucus* sp. nov., and *H. aquila* sp. nov. by the combination of small vs large outer oral teeth and a larger number of outer upper jaw teeth [UOT 46–71 (58) vs 22–47 (27–36)]; further from *H. mentatus*, *H. rex* sp. nov., *H. simba* sp. nov., *H. glaucus* sp. nov., and *H. aquila* sp. nov. by presence vs absence of a well-defined mid-lateral band.

It further differs from *H. latifrons* sp. nov. and *H. mentatus* by a deeper body [BD 33.5–41.7 (37.4) vs 27.2–32.3 (28.6–31.2) % SL]; further from *H. rex* sp. nov., *H. simba* sp. nov., and *H. glaucus* sp. nov. by a broader head [HW 42.0–48.1 (45.3) vs 36.8–41.6 (39.2–40.8) % HL].

It differs from *H. kimondo* sp. nov. and *H. squamipinnis* by a narrower interorbital area [IOW 40.5–48.7 (43.9) vs 48.6–58.5 (51.9–52.8) % HW]; further from *H. kimondo* sp. nov. by the combination of a rhomboid vs pyriform body, a concave to weakly convex vs convex dorsal outline of head, a gentler sloping snout (30–40° vs 40–50°), and dominant males light grey dorsally and blue-black vs grey dorsally and yellow ventrally; further from *H. squamipinnis* by a gentler gape inclination (20–35° vs 30–45°), a shorter lower jaw [LJL 44.2–49.6 (47.1) vs 47.8–58.6 (52.5) % HL], mostly absence vs presence of minute scales on proximal part of dorsal fin (rarely few rows of 1–4 scales present on dorsal fin in *H. quasimodo* sp. nov.), and dominant males light grey dorsally and blue-black ventrally vs slate blue.

It differs from *H. falcatus* sp. nov. by the combination of a shorter head [HL 33.9–37.2 (35.5) vs 36.6–39.6 (38.2) % SL], a longer pelvic fin [VL 26.2–33.7 (29.4) vs 21.6–25.7 (23.5) % SL], weakly recurved

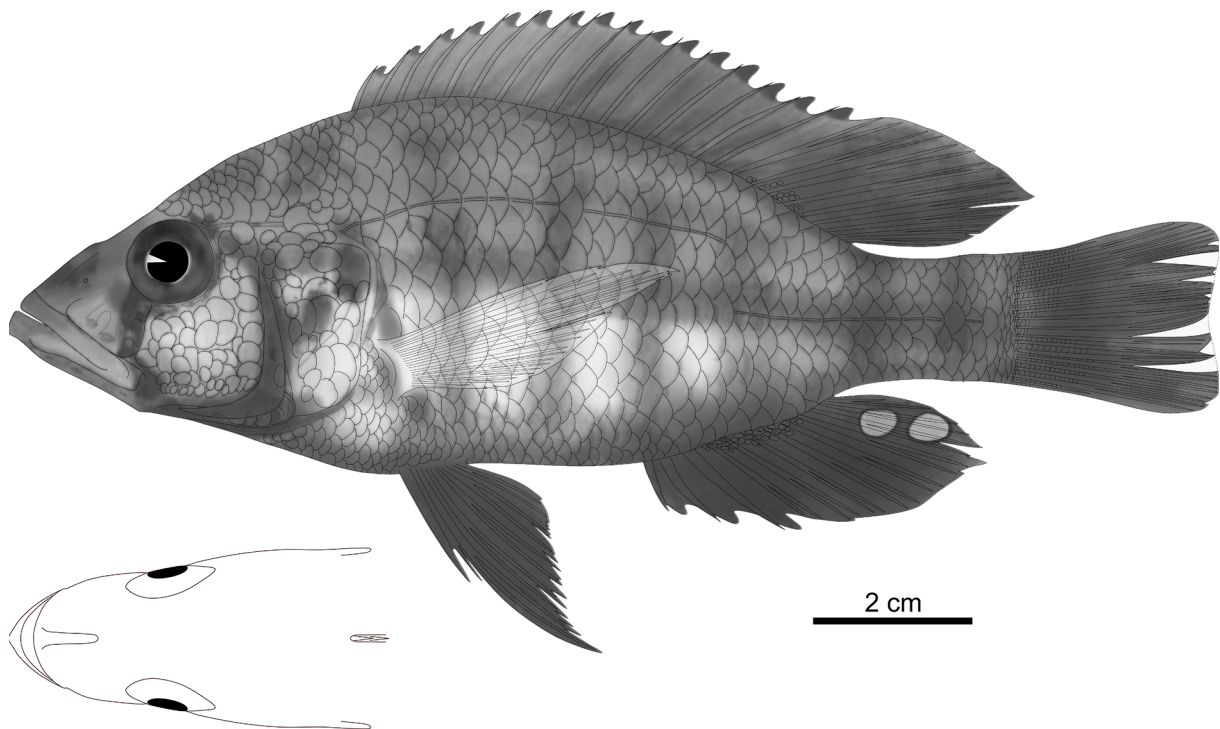


Fig. 35. *Haplochromis quasimodo* sp. nov., holotype, ♂, 120.4 mm SL (RMCA 2018.008.P.0336). Drawn by N. Vranken.

vs strongly recurved outer oral teeth, and dominant males light grey dorsally and blue-black ventrally vs olive-green with an orange-red anterior part of flank.

It differs from *H. curvidens* sp. nov. and *H. pardus* sp. nov. by a deeper cheek [ChD 24.8–32.9 (exceptionally 23.7 in one specimen) (mean 27.5) vs 20.8–24.9 (22.5–23.2) % HL]; further from *H. curvidens* sp. nov. by a deeper body [BD 33.5–41.7 (37.4) vs 29.0–32.0 (30.8) % SL] and presence vs absence of a well-defined mid-lateral band; further from *H. pardus* sp. nov. by a larger number of caudal peduncle scales (CPS 17–20, rarely 16 vs 16, rarely 17), a larger adult size (max. 165 vs 96 mm SL), and colour pattern of small specimens (< 100 mm SL) light coloured vs speckled to uniformly black.

Small specimens (< 90 mm SL) resemble *H. schubotziellus* Greenwood, 1973 in overall habitus and colour pattern. It differs from the holotype of *H. schubotziellus* (NHMUK 1972.6.2.351; ♀, 75.0 mm SL; Lake George, Kankurunga Island) by a smaller eye [ED 26.2–31.8 (29.2) vs 33.7% HL], a longer lower jaw [LJL 44.2–49.6 (47.1) vs 42.6% HL], a deeper cheek [ChD 23.7–32.9 (27.5) vs 24.0% HL], outer oral teeth with no to a small minor cusp vs a well-defined minor cusp, and inner oral teeth set in 1–2 weakly defined rows vs 2 well-defined rows in both jaws.

Etymology

Specific name from Quasimodo, hunchbacked character in Victor Hugo's novel 'Notre-Dame de Paris' (1831); referring to rather shallow head and deep and rhomboid bodies of large specimens.

Material examined

Holotype

UGANDA • ♂, 120.4 mm SL; Lake Edward; 0°21'31.7" S, 29°43'17.7" E; deep catch, open water ± 30 m deep; 1 Feb. 2018; HIPE3 exped. leg.; RMCA 2018.008.P.0336.

Paratypes

DEMOCRATIC REPUBLIC OF THE CONGO • 1 ♀, 147.8 mm SL; "Lac Edouard: 2–3 km ± 500 m au large à l'Ouest de Kiavinionge" [Lake Edward: 2–3 km ± 500 m offshore west of Kiavinionge]; 0°11'39" S, 29°32'31" E (inferred); 1 Jun. 1953; KEA exped. leg.; IRSNB 13480 • 1 ♀, 164.9 mm SL; "Lac Edouard: Kaniatzi (partie N. du lac)" [Lake Edward: Kaniatzi (northern part of Lake)]; 1 Jun. 1953; KEA exped. leg.; IRSNB 13481 • 1 ♂, 147.6 mm SL; "Lac Edouard: 2–3 km à l'Ouest de Kiavinionge" [Lake Edward: 2–3 km west of Kiavinionge]; 0°11'39" S, 29°32'31" E (inferred); 1 Jun. 1953; KEA exped. leg.; IRSNB 13485 • 2 ♀♀, 141.5 mm SL; "Lac Edouard: Vitshumbi (au Nord)" [Lake Edward: north of Vitshumbi]; 0°40'50.6" S, 29°23'22.6" E (inferred); 02 Jul. 1953; KEA exped. leg.; IRSNB 13488.

UGANDA – **Lake Edward** • 2 ♀♀, 2 ♂♂, 92.7–114.3 mm SL; Katoko breeding ground, soft substrate offshore of Katwe; 0°09'43.2" S, 29°53'16.8" E; 20 Oct. 2016; HIPE1 exped. leg.; RMCA 2016.035.P.0208 to 0211 • 2 ♀♀, 83.4, 93.1 mm SL; Mukutu Kihinga, rocky offshore of Mweya; 0°11'31.2" S, 29°52'26.4" E; 23 Oct. 2016; HIPE1 exped. leg.; RMCA 2016.035.P.0213 to 0214 • 1 ♂, 78.9 mm SL; Mukutu Kihinga, rocky offshore of Mweya; 0°11'31.2" S, 29°52'26.4" E; 23 Oct. 2016; HIPE1 exped. leg.; RMCA 2016.035.P.0212 • 3 ♀♀, 79.4–110.1 mm SL; Rwenshama, rocky shore; 0°24'05.7" S, 29°46'35.1" E; 26 Mar. 2017; HIPE2 exped. leg.; RMCA 2017.006.P.0349 to 0351 • 1 ♂, 89.1 mm SL; islands near Katwe; 0°10'04.9" S, 29°52'27.4" E; 18 Jan. 2018; HIPE3 exped. leg.; RMCA 2018.008.P.0334 • 1 ♀, 130.7 mm SL; 0°24'16.0" S, 29°46'24.8" E; 24 Jan. 2018; HIPE3 exped. leg.; bought at Rwenshama landing site; RMCA 2018.008.P.0335 • 1 ♀, 148.8 mm SL; 0°21'31.7" S, 29°43'17.7" E; 1 Feb. 2018; HIPE3 exped. leg.; deep catch, open water ± 30 m deep; RMCA 2018.008.P.0339 • 1 ♀, 1 ♂, 117.9, 126.2 mm SL; 0°21'31.7" S, 29°43'17.7" E; 1 Feb. 2018; HIPE3 exped. leg.; deep catch, open water ± 30 m deep; RMCA 2018.008.P.0337 to 0338.

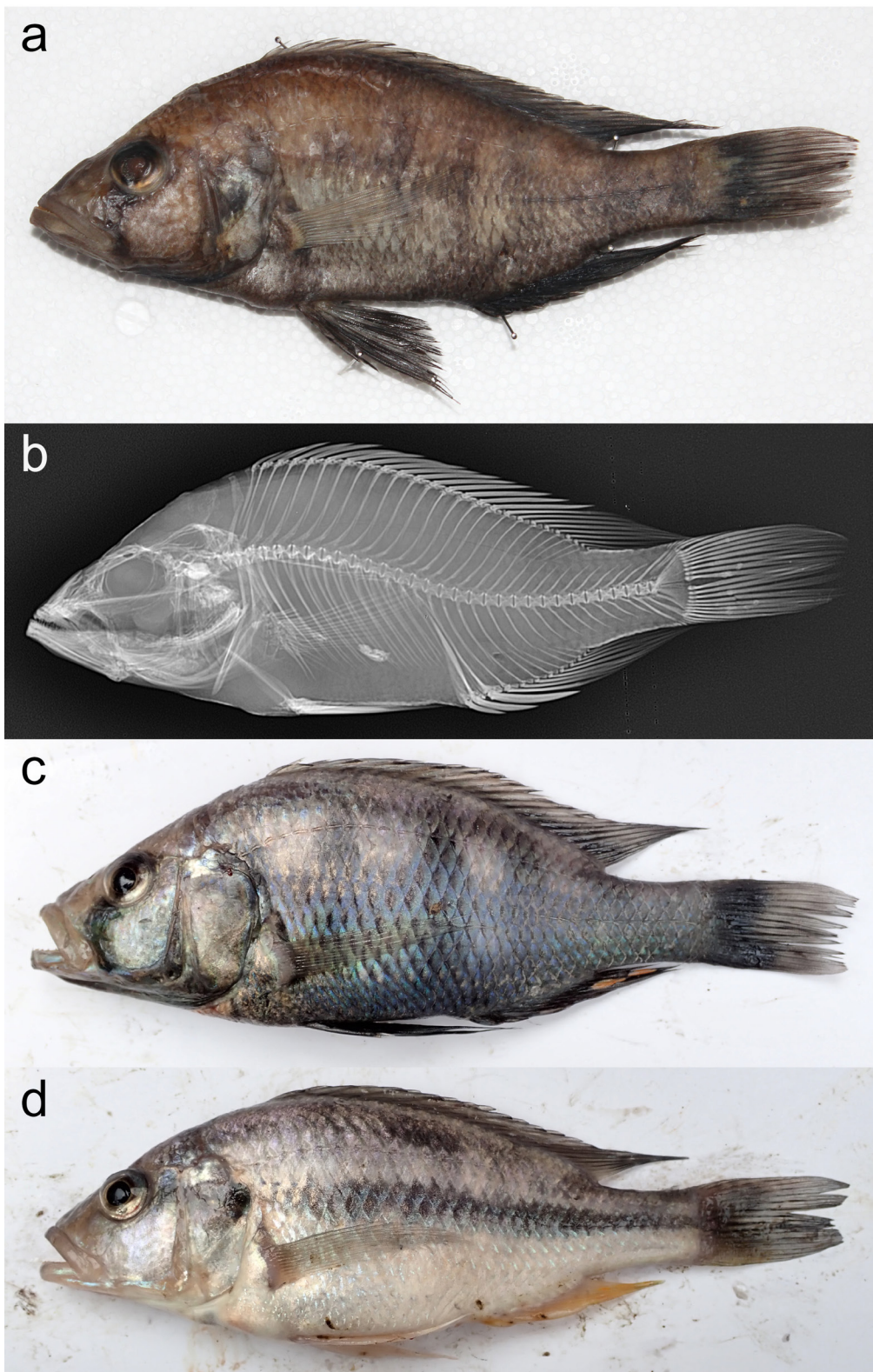


Fig. 36. *Haplochromis quasimodo* sp. nov. **a.** Photograph of preserved holotype (RMCA 2018.008.P.0336; 120.4 mm SL). **b.** X-ray image of holotype. **c–d.** Photographs of freshly caught specimens. **c.** Dominant male (RMCA 2018.008.P(HP3072); 123.7 mm SL). **d.** Female (RMCA 2018.008.P(HP3064); 116.6 mm SL) to illustrate the live colour patterns. The contrast was slightly enhanced.

Description

Based on 21 specimens (78.9–164.9 mm SL); body average in depth in comparison to generalised *H. elegans* (but deep for a piscivorous species; Table 1) and rhomboid (Fig. 35). Head average in width and with a concave to weakly convex dorsal outline; eye small; interorbital area very narrow; cheek and lacrimal deep; lacrimal somewhat convex and hereby protrudes somewhat laterally. Snout average in length, acute, and slopes gently at 30–40°; premaxillary pedicel long and prominent. Jaws isognathous, long, slim, narrow, and rounded in dorsal view; gape large and slopes gently at 20–35°; maxilla extends to between verticals through anterior margins of orbit and pupil. Lower jaw shallow and with a straight ventral outline in lateral view, mental prominence absent or weakly developed, and lower jaw side nearly flat with an inclination of 15–25° to horizontal in anterior view. Upper jaw not expanded. Lips and oral mucosa thin. Neurocranium average in depth, ethmo-vomerine block decurved to horizontally inclined, preorbital region shallow (21–24% NL), orbital region average in depth (30–32% NL), and supraoccipital crest deep and pyramidal or weakly wedge-shaped (Fig. 36b).

Outer oral teeth numerous and very small. Necks stout, conical, and straight; crowns weakly recurved, unicuspid in large specimens (> 80 mm SL), anteriorly unicuspid and posteriorly mostly bi-, weakly bi-, and weakly tricuspid in small specimens (< 80 mm SL), all acutely pointed. Dental arcades rounded. Outer teeth closely and regularly set with neck-distances of $\frac{1}{2}$ –1 neck-width. In upper jaw, 1–3 posteriormost teeth slightly enlarged. Inner teeth small, straight, an admixture of acutely pointed unicuspid and weakly tricuspid. Tooth bands very slender crescent-shaped with 1–2 rows of inner teeth, and narrow posteriorly until only outer row remains past $\frac{2}{3}$ length of tooth band. Inner teeth closely and regularly set on 1– $\frac{3}{2}$ outer neck-widths from outer row; implantation mostly recumbent; size uniform throughout tooth band.

Lower pharyngeal bone average in length, triangular, slim, and shallow over whole length (Fig. 37). Pharyngeal teeth relatively large and slender; major cusps acutely pointed; cusp gaps nearly straight; minor cusps and cusp protuberances mostly absent. Teeth in two median longitudinal rows equal in size and form to lateral teeth, 11–13 in each row. Posterior transverse row with 20–21 teeth, implanted erectly with a lateral inclination; major cusps nearly straight, bluntly pointed, and laterally compressed; minor cusps mostly present.

Chest scales small; transition to larger flank scales gradual. Minute scales on proximal half of caudal fin.

Caudal fin emarginate; dorsal and anal fins reach to between verticals through caudal-fin base and two scales posterior to this vertical. In about half of all specimens (10 of 21 type specimens), some minute, ellipsoid scales present on basal part of membrane of anal fin; between some pairs of fin rays, up to two rows of 1–5 scales extend from body onto fin; scales very variable in distribution and invisible to naked eye (Fig. 35). Dorsal fin rarely with a few isolated rows of 1–4 minute scales (in 3 of 21 type specimens). Pectoral fin long and reaches to between first anal-fin spine and second anal fin branched ray; pelvic fin reaches to between first and second anal-fin spine in females, to second anal fin branched ray in males; first branched pelvic-fin ray elongated in all specimens.

All gill rakers in outer row of first gill arch short, relatively stout, and mostly simple, but sometimes anvil-shaped or weakly bifid.

Colouration in life

Dominant males: body and dorsal part of head light grey with faint yellow sheen; ventral half of body blue-black; belly and chest black; cheek, lower jaw, and lips white; snout dusky; eye with (dark) grey outer ring and silver inner ring (Fig. 36c). Flank with a well-defined mid-lateral band, an interrupted dorsal-lateral band, and 5–6 vertical stripes; lacrimal and vertical preopercular stripes well-defined;

posterior margin of operculum black. Pectoral fin hyaline; pelvic fin black; dorsal fin dusky and with black lappets, base, and posterior part; anal fin black and with 2–7 very large egg spots (i.e., three times distance between rays) with dusky rings; caudal fin dusky and with black base, hyaline distal part, and maculated dorsal part.

Females and juveniles: body and head uniformly white, except for light grey dorsum and dorsal part of head and a dusky snout; eye with (dark) grey outer ring and silver inner ring (Fig. 36d). Flank with faint to well-defined mid-lateral and interrupted dorsal-lateral bands. Pectoral and dorsal fins hyaline; dorsal fin with black lappets and dusky base and distal part; anal and caudal fins yellow; anal fin with 3–5 spots resembling egg spots; caudal fin with a dusky base and a dusky and maculated dorsal part.

Preserved colouration

Body and operculum with yellowish dorsal part, white ventral part; transition gradual; in dominant males, ventral part of body overlain black (Fig. 36a). Flank with mostly mid-lateral and interrupted dorsal-lateral bands; in dominant males, with 5–6 vertical stripes. Cheek yellowish, snout dusky, and lower jaw whitish. Nostril and interorbital stripes and nape band faint in all specimens; lacrimal stripe

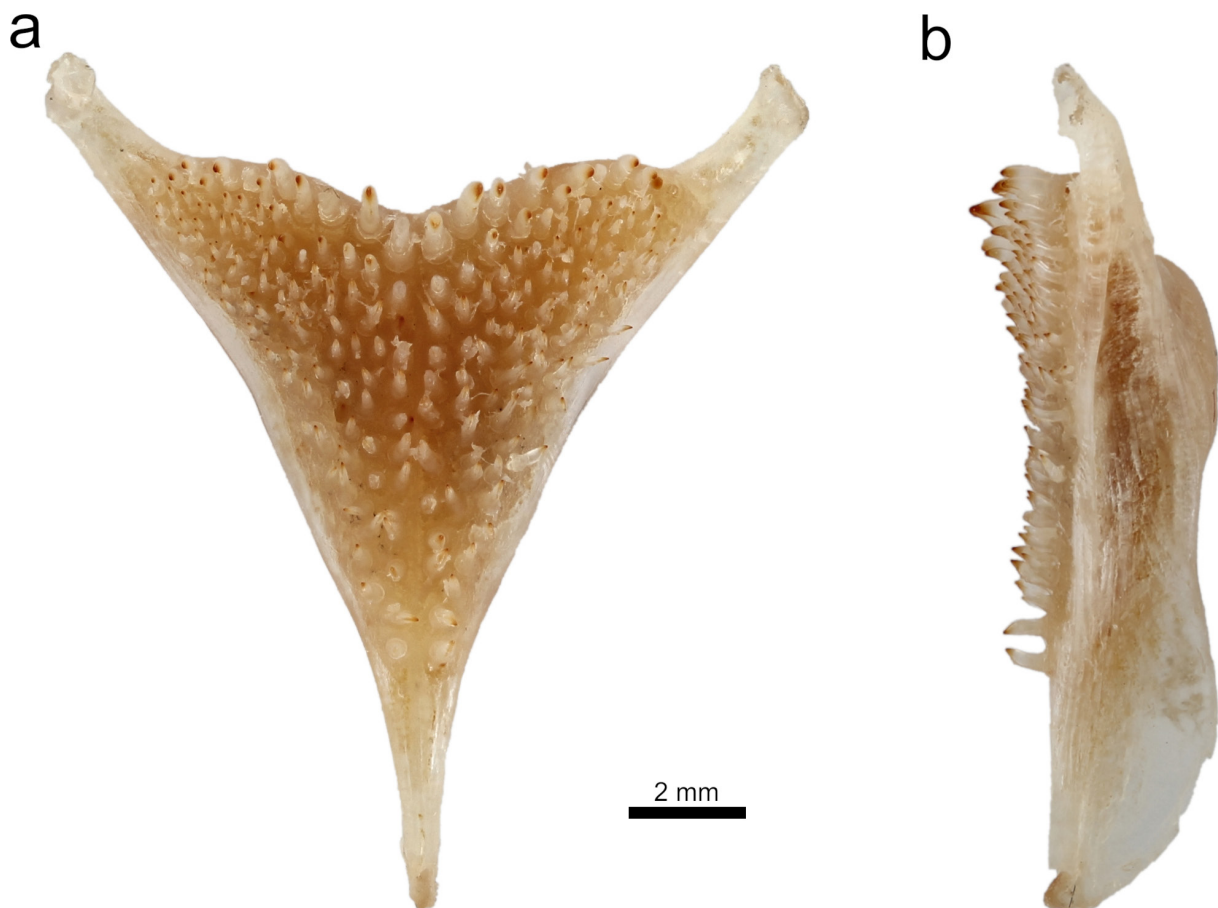


Fig. 37. *Haplochromis quasimodo* sp. nov. (RMCA 2018.008.P.0337; 126.2 mm SL). **a.** Dorsal view of the lower pharyngeal jaw. **b.** Lateral view of the lower pharyngeal jaw.

faint in females, broad and well-defined in males; vertical preopercular stripes well-defined in males. Pectoral fin hyaline; pelvic and anal fins yellowish in females and black in males; anal fin with 2–7 large egg-spots in males. Caudal and dorsal fins dusky and dorsal fin with black lappets; in males, base of caudal fin and posterior part of dorsal fin black.

Distribution and ecology

Endemic to Lake Edward system; found in offshore, benthic areas in shallow and deep waters. Based on its morphology, most probably a piscivorous species.

Haplochromis squamipinnis Regan, 1921

Figs 1–2, 38–40; Table 1

Haplochromis squamipinnis Regan, 1921: 636.

Haplochromis squamipinnis – Trewavas 1933: 338 (redescription). — Greenwood 1973: 204, fig. 31 (redescription).

Harpagochromis squamipinnis – Greenwood 1980: 13.

Differential diagnosis

Species with a piscivorous morphology; body rather deep [BD 32.4–39.3 (mean 35.7) % SL]; oral jaws very long [LJL 47.8–58.6 (52.7) % HL], narrow [LJW 32.6–44.7 (37.2) % LJL], and steep (gape inclination 30–45°); outer oral teeth many and small [UOT 39–79 (median 58)]; dominant males slate blue.

Amongst piscivorous species from the Lake Edward system, *H. squamipinnis* differs from all by presence vs absence of minute scales on proximal part of dorsal fin (rarely few scales present in *H. quasimodo* sp. nov.).

It further differs from *H. latifrons* sp. nov. and *H. mentatus* by the combination of small vs large outer oral teeth, a larger number of outer upper jaw teeth [UOT 39–79 (58) vs 22–47 (27–36)], a steeper gape (30–45° vs 15–30°), and a deeper body [BD 32.4–39.3 (35.7) vs 27.2–32.3 (28.6–31.2) % SL]; from *H. mentatus* by dominant males uniformly slate blue vs yellow-green with a red anterior part of flank.

It further differs from *H. rex* sp. nov., *H. simba* sp. nov., *H. glaucus* sp. nov., and *H. aquila* sp. nov. by the combination of small vs large outer oral teeth, a larger number of outer upper jaw teeth [UOT 39–79 (58) vs 22–47 (27–36)], and dominant males uniformly slate blue vs cream-coloured with an orange operculum, yellow with an orange anterior part of flank, light blue with a dusky to black head, or light grey with a black head, respectively; further from *H. rex* sp. nov., *H. simba* sp. nov., and *H. glaucus* sp. nov. by a steeper gape (30–45° vs 15–30°); further from *H. aquila* sp. nov. by a smaller eye [ED 23.1–29.7 (26.6) vs 30.0–31.5 (30.6) % HL].

It further differs from *H. kimondo* sp. nov. by a concave to straight vs convex dorsal outline of head, a gentler snout inclination (30–40° vs 40–50°), and dominant males slate blue vs grey dorsally and yellow ventrally; further from *H. falcatus* sp. nov. by a shorter head [HL 35.1–36.9 (36.0) vs 36.6–39.6 (38.2) % SL] and dominant males slate blue vs olive-green with an orange-red anterior part of flank; further from *H. curvidens* sp. nov. and *H. pardus* sp. nov. by a deeper cheek [ChD 24.9–36.0 (29.0) vs 20.8–24.9 (22.5–23.2) % HL]; further from *H. pardus* sp. nov. by a larger adult size (max. 211 vs 96 mm SL) and colour pattern of small specimens (< 100 mm SL) light coloured vs speckled to uniformly black.

It differs from *H. quasimodo* sp. nov. by the combination of a broader interorbital area [IOW 48.6–55.6 (51.9) vs 40.5–48.7 (43.9) % HW], a longer lower jaw [LJL 47.8–58.6 (52.5) vs 44.2–49.6 (47.1) % HL], a steeper gape inclination (30–45° vs 20–35°), and dominant males slate blue vs light grey dorsally and blue-black ventrally.

Etymology

Specific name not explained in original description, from the Latin ‘*squamus*’ for ‘scale’, and ‘*pinnis*’ for ‘fin’; probably referring to minute scales on basal parts of dorsal and anal fins.

Material examined

Holotype

DEMOCRATIC REPUBLIC OF THE CONGO (most likely) • 1 ♀, 136.9 mm SL; Lake Edward; 1907–1908; H. Schubotz leg.; NHMUK 1914.4.8.32.

Other material

DEMOCRATIC REPUBLIC OF THE CONGO • 1 ♀, 75.9 mm SL; “Lac Edouard: Bugazia” [Lake Edward: Bugazia]; 0°23′40.8″ S, 29°23′02.0″ E (inferred); 16 May 1935; IRSNB 12939 • 1 ♂, 168.4 mm SL; “Lac Edouard: au large de la riv. Talia” [Lake Edward: offshore Talia River]; 0°31′05″ S, 29°20′26″ E (inferred); 23 Apr. 1953; KEA exped. leg.; IRSNB 13475 • 1 ♀, 167.7 mm SL; “Lac Edouard: au large de la riv. Kigera” [Lake Edward: offshore of the Kigera River]; 0°29′42″ S, 29°38′14″ E (inferred); 25 May 1953; KEA exped. leg.; IRSNB 13477 • 1 ♀, 210.5 mm SL; “Lac Edouard: 2–3 km à l’Ouest de Kiavinionge” [Lake Edward: 2–3 km west of Kiavinionge]; 0°11′39″ S, 29°32′31″ E (inferred); 1 Jun. 1953; KEA exped. leg.; IRSNB 13482.

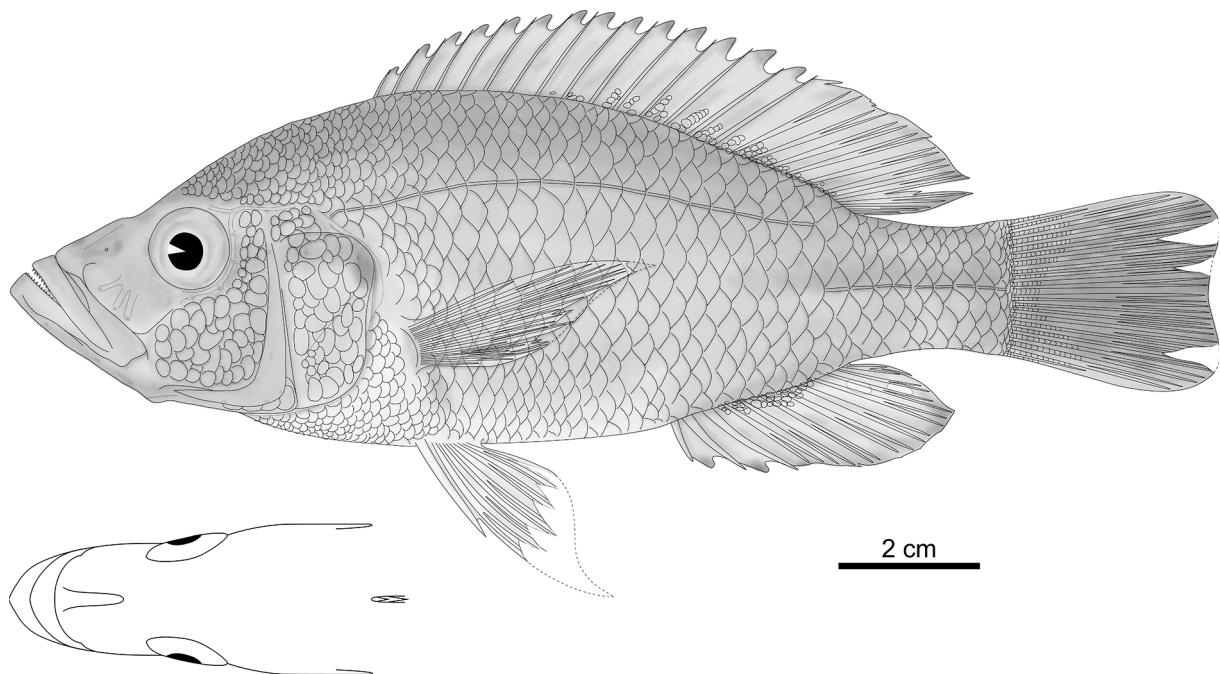


Fig. 38. *Haplochromis squamipinnis* Regan, 1921, holotype, ♀, 136.9 mm SL (NHMUK 1914.4.8.32). Drawn by N. Vranken.

UGANDA – **Lake Edward** • 2 ♀♀, 110.9, 117.4 mm SL; 0°12'00.0" S, 29°47'38.4" E; 23 Oct. 2016; HIPE1 exped. leg.; deep catch, open water ± 20 m deep; RMCA 2016.035.P.0235, 0238 • 2 ♂♂, 182.0, 211.4 mm SL; 0°24'16.0" S, 29°46'24.8" E; 9 Nov. 2016; HIPE1 exped. leg.; bought at Rwenshama landing site; RMCA 2016.035.P.0251, 0254 • 1 ♂, 2 ♀♀, 148.5–177.3 mm SL; mouth of Kazinga Channel, hard substrate; 0°12'14.4" S, 29°52'37.2" E; 23 Mar. 2017; HIPE2 exped. leg.; RMCA 2017.006.P.0375, 0377, 0379 • 1 ♂, 105.4 mm SL; Rwenshama rocky shore; 0°24'05.7" S, 29°46'35.1" E; 25 Mar. 2017; HIPE2 exped. leg.; RMCA 2017.006.P.0385 • 1 ♀, 113.2 mm SL; Kayanja, offshore; 0°05'31.2" S, 29°45'30.3" E; 21 Jan. 2018; HIPE3 exped. leg.; RMCA 2018.008.P.0368. – **Kazinga Channel** • 1 ♂, 111.3 mm SL; near Queen Elisabeth Bush Lodge; 0°08'09.6" S, 30°02'27.6" E; 28 Oct. 2016; HIPE1 exped. leg.; RMCA 2016.035.P.0244. – **Lake George** • 1 ♂, 80.7 mm SL; Akika Island; 0°01'26.7" S, 30°09'38.2" E; 28 Mar. 2017; HIPE2 exped. leg.; RMCA 2017.006.P.0387 • 1 ♀ (90.9 mm SL); Akika Island; 0°01'26.7" S, 30°09'38.2" E; 29 Mar. 2017; HIPE2 exped. leg.; RMCA 2017.006.P.0398 • 1 ♂, 180.1 mm SL; Kashaka bay, north of inlet; 0°04'52.2" S, 30°10'47.3" E; 2 Feb. 2018; HIPE3 exped. leg.; RMCA 2018.008.P.0369 • 2 ♀♀, 77.6, 107.4 mm SL; Kashaka bay, north of inlet; 0°04'52.2" S, 30°10'47.3" E; 2 Feb. 2018; HIPE3 exped. leg.; RMCA 2018.008.P.0371 to 0372.

Description

Based on 20 specimens (75.9–211.4 mm SL); body average in depth in comparison to generalised *H. elegans* (but deep for a piscivorous species; Table 1) and oval to rhomboid (Fig. 38). Head long, narrow, and with a straight to concave dorsal outline; eye small; interorbital area narrow; cheek and lacrimal deep. Snout long, acute, and slopes very gently at 30–35°; premaxillary pedicel very long and prominent. Jaws isognathous to strongly prognathous, slim, very narrow, and rounded in dorsal view; upper jaw long and lower jaw very long; gape large and slopes steeply at 30–45°; maxilla extends to between verticals through anterior margins of orbit and pupil. Lower jaw shallow and with a straight ventral outline in lateral view, mental prominence weakly or strongly developed, and lower jaw side steep with an inclination of 35° to horizontal in anterior view. Upper jaw expanded slightly anteriorly and ventrally. Lips and oral mucosa thin. Neurocranium average in depth, ethmo-vomerine block horizontally inclined, preorbital region shallow (19–25% NL), orbital region average in depth (28–32% NL), and supraoccipital crest deep and pyramidal or weakly wedge-shaped (Fig. 39b).

Outer oral teeth numerous, unicuspid, and small. Necks stout, conical, and straight; crowns weakly recurved in lower jaw, recurved in upper jaw, and acutely pointed. Dental arcades rounded. Outer teeth closely and regularly set with neck-distances of ½–1 neck-width. In upper jaw, 1–3 posteriormost teeth sometimes slightly enlarged. Inner teeth small, weakly recurved, unicuspid in large specimens (> 120 mm SL), tri- to rarely unicuspid in upper jaw and uni- to weakly tricuspid in lower jaw of small specimens (< 120 mm SL), and acutely pointed in acutely pointed in all specimens. Tooth bands very slender crescent-shaped with 1–3 rows of inner teeth, and narrow posteriorly until only outer row remains past ⅔ length of tooth band. Inner teeth closely and regularly set on 1–3/2 outer neck-widths from outer row; implantation recumbent; size uniform throughout tooth band.

Lower pharyngeal bone long, narrow, slim, and shallow with a slightly deeper keel (Fig. 40). Pharyngeal teeth relatively large and slender; major cusps acutely pointed; cusp gaps nearly straight; minor cusps and cusp protuberances small. Teeth in two median longitudinal rows equal in size and form to lateral teeth, 11 in each row. Posterior transverse row with 17–18 teeth, implanted erectly with a lateral inclination; major cusps nearly straight, bluntly pointed, and laterally compressed; minor cusps mostly present.

Chest scales small; transition to larger flank scales gradual. Basal parts of membranes of dorsal and anal fins covered by minute, ellipsoid scales; between some pairs of fin rays, up to two rows of 1–10 scales extend from body onto fin; scales very variable in distribution and density and mostly invisible to naked

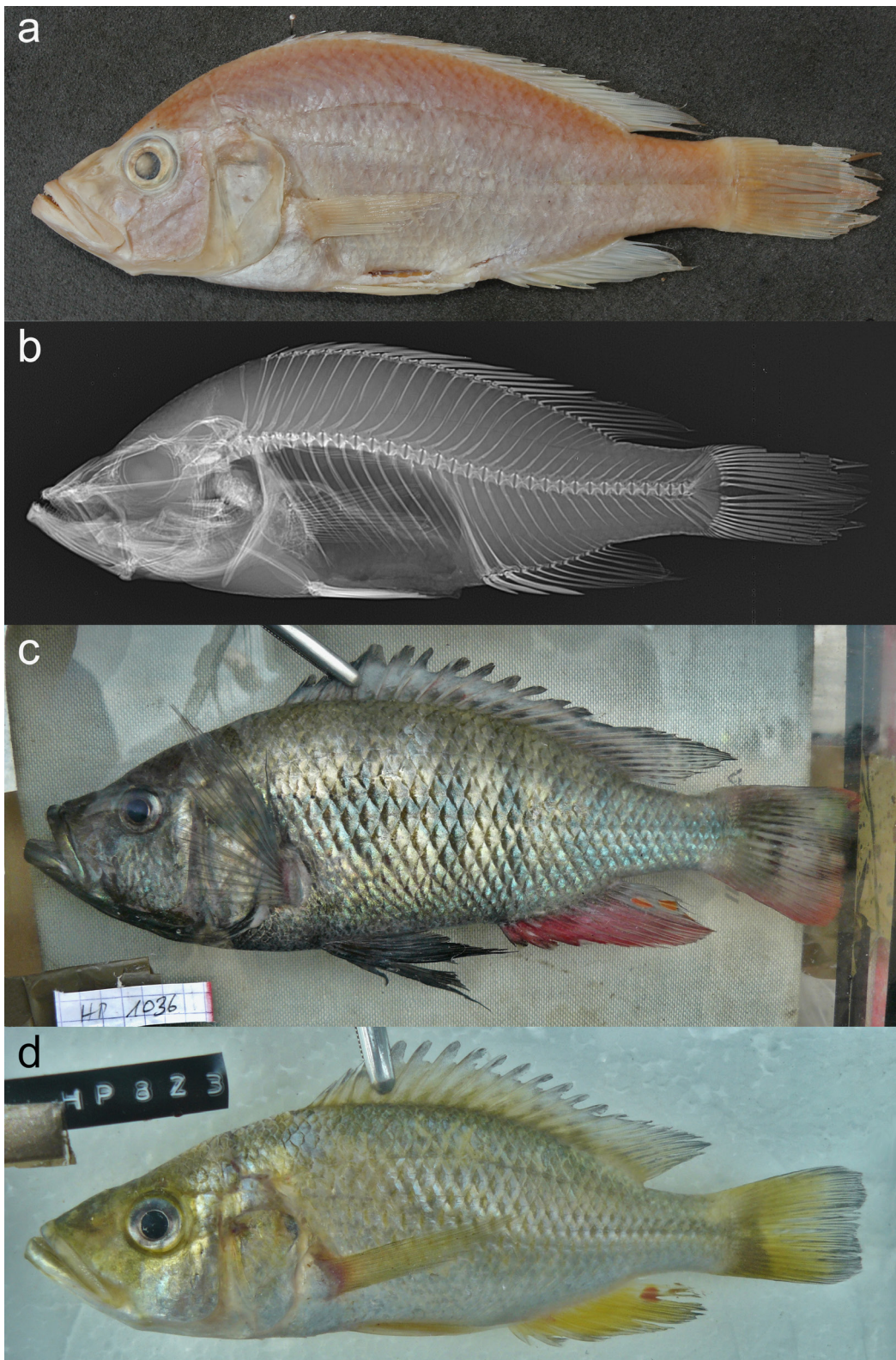


Fig. 39. *Haplochromis squamipinnis* Regan, 1921. **a.** Photograph of preserved holotype (NHMUK 1914.4.8.32; 136.9 mm SL). **b.** X-ray image of holotype. **c–d.** Photographs of freshly caught specimens. **c.** Dominant male (RMCA 2016.035.P.0250; 169.7 mm SL). **d.** Female (RMCA 2016.035.P(HP823); 129.6 mm SL) to illustrate the live colour patterns. The contrast was slightly enhanced.

eye; no scales present anteriorly of fourth dorsal-fin spine (Fig. 38). Minute scales on proximal half of caudal fin.

Caudal fin emarginate to weakly subtruncate; dorsal and anal fins reach to between verticals through caudal-fin base and two scales posterior to this vertical. Pectoral fin reaches to between first and third anal-fin spines; pelvic fin reaches to between first and third anal-fin spine in females, to third anal fin branched ray in males; first branched pelvic-fin ray elongated in all specimens.

Ceratobranchial gill rakers in outer row of first gill arch short, relatively slender, and simple; posteriormost rakers sometimes anvil-shaped or weakly bifid. Epibranchial gill rakers slender and simple.

Colouration in life

Dominant males: body and head uniformly slate blue; belly and chest black; flank with very faint mid-lateral band and 5–7 vertical stripes in some specimens; snout dusky; lacrimal stripe and mental blotch present; eye with (dark) grey outer ring and silver to golden inner ring (Fig. 39c). Pectoral fin dusky; pelvic fin black; caudal fin crimson and with dusky base and maculated dorsal part. Dorsal fin dusky and with black lappets and, in posterior part, maculated crimson; anal fin crimson and with black lappets, a dusky base and posterior part, and 3–4 large orange egg-spots (i.e., twice distance between rays) with hyaline rings. Non-dominant males: body and head yellow-green; chest and belly white.

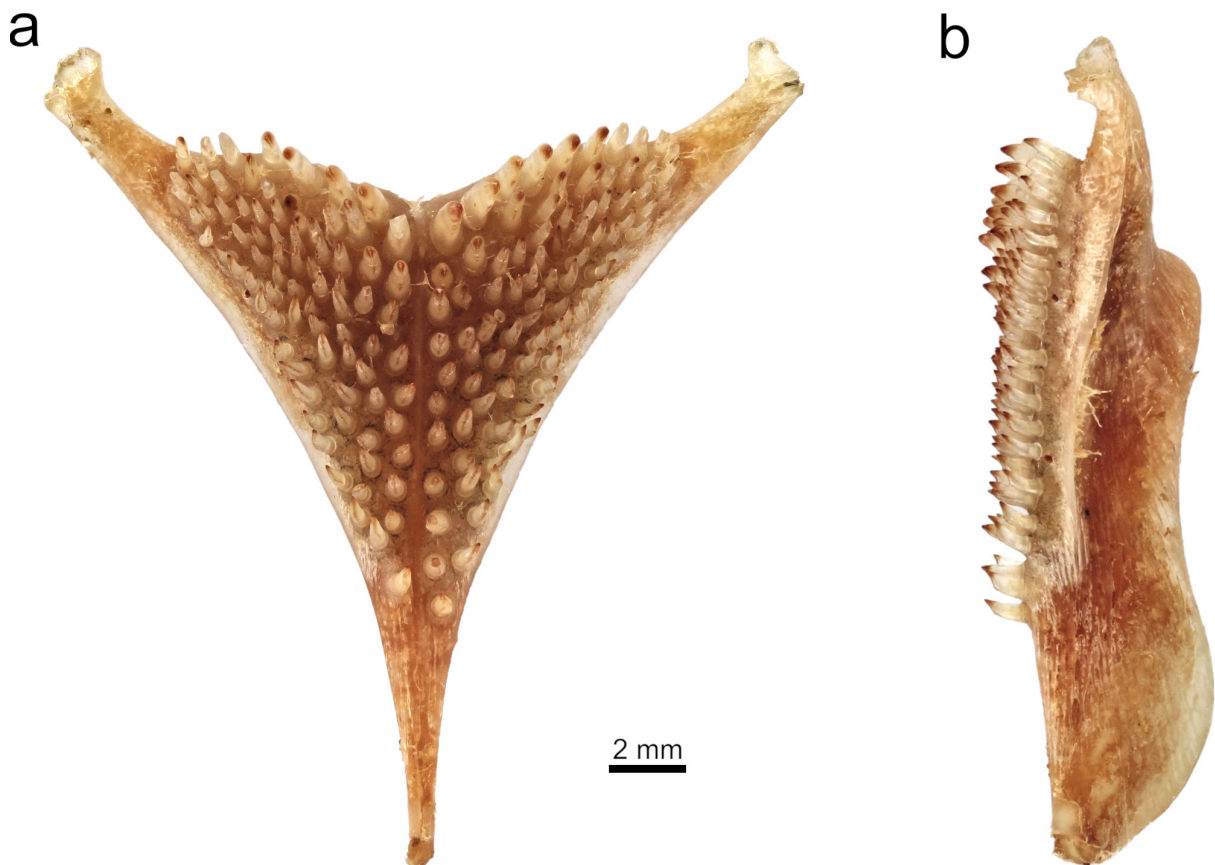


Fig. 40. *Haplochromis squamipinnis* Regan, 1921 (RMCA 2016.035.P.0254; 182.0 mm SL). **a.** Dorsal view of the lower pharyngeal jaw. **b.** Lateral view of the lower pharyngeal jaw.

Females and juveniles: dorsum and dorsal part of head golden; belly, chest, operculum, and cheek white; transition gradual (Fig. 39d). Snout and lower jaw dusky; lacrimal stripe faint, mental blotch present; eye with (dark) grey outer ring and silver to golden inner ring. Flank with a very faint mid-lateral band and 5–7 vertical stripes in some specimens. Pectoral, pelvic, anal, and caudal fin yellowish; anal fin with hyaline base, dusky distal part, and 3–4 spots resembling egg-spots; caudal fin with dusky distal part and maculated dorsal part; dorsal fin dusky and with black lappets.

Preserved colouration

Dorsal part of body dusky brown, ventral part of body white, transition gradual; in dominant males, belly and chest black (Fig. 39a). Flank rarely with a very faint mid-lateral band and very faint 5–7 vertical stripes. Cheek light yellowish; snout dusky. Nostril, interorbital, lacrimal, and vertical opercular stripes faint; mental blotch present; lacrimal stripes present in dominant males. Pectoral fin dusky; pelvic fin yellowish with dusky distal parts in females, black in males; caudal fin dusky and with black distal margin. Dorsal fin dusky and with black lappets and posterodistal margin; anal fin dusky and with a black posterodistal margin, a white base in females, a dark base and 2–3 egg-spots in males.

Distribution and ecology

Endemic to the Lake Edward system; found in offshore benthic areas in mostly shallow and deep waters over muddy substrates. Introduced into Lake Kachira, Lake Victoria drainage, Uganda (Schraml 2004). Piscivorous diet. Diet of Lake George specimens consists mainly of *H. nigripinnis* Regan, 1921 followed by *H. angustifrons* Boulenger, 1914 (Moreau *et al.* 1993); insects and to a lesser degree small fishes and plant fragments contribute to diet in small specimens (< 150 mm SL) (Greenwood 1973; Moriarty *et al.* 1973). Sexual dimorphism in size, as observed by Greenwood (1973), seems absent; both sexes reach > 210 mm SL.

Key to the piscivorous species of *Haplochromis* from the Lake Edward System

This identification key is intended as a practical guide and first step towards the identification of the piscivorous species from the Lake Edward system; in case of doubt, the differential diagnoses in the species' descriptions should be consulted. When identifying live dominant males, the colour patterns are highly diagnostic and should be checked. A simple dichotomous key cannot be compiled as overlap in character states and in the range of values is omnipresent in species of *Haplochromis*, especially when they have a similar ecology (Greenwood 1973; Snoeks 1994). However, the key allows for the identification of most specimens. Within the key, terminology is used in reference to species with a piscivorous morphology (instead of the generalised *Haplochromis* morphology as in the rest of the manuscript).

1. Adult specimens < 100 mm SL; cheek shallow [ChD 20.8–24.4 (mean 22.5) % HL]; anal fin base long [AFB 19.2–22.2 (20.5) % SL]; 16, rarely 17 caudal peduncle scales; body speckled to uniformly black (Fig. 33c–d)..... *H. pardus* sp. nov.
 - Adult specimens > 100 mm SL; specimens < 100 mm SL with cheek deep [ChD 22.4–29.6 (means 22.9–28.5) % SL], anal-fin base short [AFB 16.1–21.7 (14.8–19.8) % SL], 16–20 (medians 17–19) caudal peduncle scales, and body light coloured..... 2
2. Body shallow [BD 27.2–30.1 (28.6) % SL]; anal-fin base short [AFB 14.7–17.3 (15.7) % SL]; interorbital area broad [IOW 57.4–63.3 (60.0) % HW]; 7–8 anal fin branched rays..... *H. latifrons* sp. nov.
 - Body deep [BD 28.4–41.7 (30.8–37.4) % SL]; anal-fin base long [AFB 16.7–21.9 (18.0–19.9) % SL]; interorbital area narrow [IOW 39.3–61.0 (43.9–55.5) % HW]; 8–11 anal fin branched rays... 3

3. Body deep [BD 32.4–39.3 (35.7) % SL]; interorbital area broad [IOW 48.6–55.6 (51.9) % HW]; lower jaw long [LJL 47.8–58.6 (52.7) % HL]; gape steep (30–45°); rows of minute scales on basal part of membranes of both dorsal and anal fins (nearly invisible to naked eye) (Fig. 38); dominant males slate blue (Fig. 39c). *H. squamipinnis*
- Body deep [BD 33.5–41.7 (37.4) % SL]; interorbital area narrow [IOW 40.5–48.7 (43.9) % HW]; lower jaw short [LJL 44.2–49.6 (47.1) % HL]; gape gentle (20–35°); rows of minute scales on basal part of membrane of anal fin in some specimens, rarely few isolated scales on dorsal fin (nearly invisible to naked eye) (Fig. 35); dominant males light grey dorsally and blue-black ventrally (Fig. 36c). *H. quasimodo* sp. nov.
- Body shallow [BD 28.4–36.0 (30.8–33.2) % SL]; interorbital area broad [IOW 39.3–61.0 (44.6–55.5) % HW]; lower jaw short [LJL 42.4–53.1 (44.7–49.5) % HL]; gape gentle (15–35°); minute scales on dorsal or anal fins absent. 4
4. Head broad [HW 40.1–43.7 (42.0) % HL]; eye large [ED 30.0–31.5 (30.6) % HL]; 25–37 (median 31) outer upper jaw teeth; dominant males light grey with black head and bright red anal fin (Fig. 21c). *H. aquila* sp. nov.
- Head narrow [HW 36.8–42.3 (39.2–40.8) % HL]; eye small [ED 22.2–29.9 (24.6–28.3) % HL]; 22–47 (medians 27–36) outer upper jaw teeth. 5
- Head broad [HW 39.9–48.0 (42.9–45.1) % HL]; eye variable [ED 24.6–31.5 (27.5–30.4) % HL]; 39–70 (medians 45–56) outer upper jaw teeth. 8
5. Pre-dorsal distance short [PrD 33.3–37.0 (35.3–36.1) % SL]; interorbital area broad [IOW 50.9–61.0 (53.8–55.5) % SL]; 3–4, rarely 5 infraorbital cheek scales; 25–47 (medians 30–36) outer upper jaw teeth. 6
- Pre-dorsal distance long [PrD 36.1–39.2 (37.3–38.0) % SL]; interorbital area narrow [IOW 44.9–52.7 (48.1–48.9) % SL]; 4–7 infraorbital cheek scales; 22–36 (medians 27–29) outer upper jaw teeth. 7
6. Pre-pectoral distance short [PrP 33.1–38.2 (36.0) % SL]; caudal peduncle long [CPL 15.7–17.5 (16.6) % SL]; head short [HL 33.4–37.0 (35.1) % SL]; dominant males yellow-green with a bright red anterior part of flank (Fig. 9c). *H. mentatus*
- Pre-pectoral distance long [PrP 36.4–39.4 (38.1) % SL]; caudal peduncle short [CPL 13.4–16.1 (14.8) % SL]; head long [HL 35.9–37.9 (36.9) % SL]; dominant males (and females) light blue with black cheek (Fig. 18c). *H. glaucus* sp. nov.
7. Cheek deep [ChD 27.6–33.5 (31.1) % SL]; eye small [ED 22.2–28.3 (24.6) % SL]; 22–27 upper lateral line scales; 12–16 scales between upper lateral line and first anal spine; dominant males cream-coloured with orange operculum and dorsal part of head and light blue snout (Fig. 12c). *H. rex* sp. nov.
- Cheek shallow [ChD 27.0–29.6 (28.3) % SL]; eye large [ED 26.7–29.5 (28.3) % SL]; 19–21 upper lateral line scales; 9–11 scales between upper lateral line and first anal spine; dominant males yellow with an orange anterior part of flank (Fig. 15c). *H. simba* sp. nov.
8. Body pyriform; head convex and broad [HW 42.9–48.0 (45.1) % HL]; cheek deep [ChD 27.1–35.2 (30.9) % HL]; lower jaw broad [LJW 44.7–53.3 (49.3) % LJL]; dominant males grey dorsally and yellow ventrally (Fig. 24c) *H. kimondo* sp. nov.
- Body oval; head straight or slightly convex and narrow [HW 39.9–44.4 (42.6–43.4) % HL]; cheek shallow [ChD 22.4–28.0 (23.2–26.0) % HL]; lower jaw narrow [LJW 38.5–45.5 (40.8–42.5) % LJL]. 9

9. Anal-fin base long [AFB 18.4–20.3 (19.3) % SL]; cheek deep [ChD 23.3–28.0 (26.0) % HL]; dominant males olive-green with an orange-red anterior part of flank and well-defined mid-lateral and dorsal-lateral bands (Fig. 27c). *H. falcatus* sp. nov.
 – Anal-fin base short [AFB 17.9–18.6 (18.3) % SL], cheek shallow [ChD 22.4–24.9 (23.2) % HL]; non-dominant males dusky greenish with 5–7 vertical stripes (Fig. 30c) *H. curvidens* sp. nov.

Discussion

The lacustrine part of the Lake Edward system is inhabited by 12 species of *Haplochromis* with a piscivorous morphology. Prior to this study, the piscivorous species of *Haplochromis* from the system were poorly studied. Only two species were formally described (*H. mentatus* and *H. squamipinnis*) and the validity of *H. mentatus* remained questionable (Trewavas 1933; Greenwood 1973). The species of *Haplochromis* that inhabit the relatively large, deep, and ecologically heterogenous Lake Edward were especially poorly studied, while a taxonomic revision of those from the small, very shallow, and ecologically homogenous Lake George was performed by Greenwood (1973). Greenwood (1973) identified all specimens with a piscivorous morphology from Lake George as *H. squamipinnis*. We found *H. squamipinnis* to be the most abundant piscivorous species in Lake George, but also identified some specimens from this lake as *H. mentatus* and *H. quasimodo* sp. nov. (NHMUK 1987.2.25.148-149). Only three piscivorous species were found in Lake George, while all 12 piscivorous species discussed above are known to inhabit Lake Edward. We hypothesise that the higher species richness of piscivores in Lake Edward results from its larger habitat diversity.

In the large East African cichlid radiations, piscivores consistently represent a species-rich, but non-abundant trophic group that shows a large ecological differentiation in habitat use, feeding behaviour, and food item variety and size in comparison to other trophic groups (Fryer & Iles 1972; van Oijen *et al.* 1981; van Oijen 1982; Witte & van Oijen 1990). Piscivorous species make up 11–30% of the species from the radiations of Lakes Malawi, Tanganyika, and Victoria (Greenwood 1974; Witte & van Oijen 1990; Ronco *et al.* 2020; A. Konings, pers. com.). Comparably, piscivores represent 12–20% of all species in the Lake Edward system (i.e., 12 piscivorous species on a total of 60–100 species; Greenwood 1991; Vranken *et al.* 2019). In contrast to their high species richness, piscivores are relatively rare. In the Mwanza Gulf of Lake Victoria, they represented < 1% of all *Haplochromis* specimens caught before the collapse of the haplochromine cichlids from Lake Victoria during the 1980s (Witte *et al.* 2013; van Oijen *et al.* 1981). Piscivores are also relatively rare in the Lake Edward system. For example, in a night catch using eight gill-nets (mesh sizes 8–40 mm) offshore of Kayanja, Lake Edward (0°05'34.8" S, 29°45'28.8" E) on the 21st March 2019, piscivores represented about 1.4% of all *Haplochromis* specimens caught (57 of ~4079 specimens). In Lakes Malawi and Victoria, the large species richness of piscivores has been attributed to a large ecological differentiation in habitat use, hunting technique, prey species, and/or prey size (Fryer & Iles 1972; van Oijen 1982). Functional morphological research has shown that these ecological specialisations are related to the relatively large morphological differences between species (van Oijen 1982; Barel 1983). Similar morphological differences were also observed between the piscivorous species from the Lake Edward system and, hence, they presumably display a similar degree of ecological specialisation. Thus, the piscivorous cichlid species from the Lake Edward system show a striking resemblance to those of the other large East African cichlid radiations in species richness, species density, and morphological diversity.

The large morphological variation among piscivorous species of *Haplochromis* from the Lake Edward system forms continuous morphoclines in all observed morphological traits. However, a general morphological trend is observed. For habitus and trophic morphology, a distinction can be made between macrodontic species, i.e., *H. latifrons* sp. nov., *H. mentatus*, *H. rex* sp. nov., *H. simba* sp. nov., *H. glaucus* sp. nov., and *H. aquila* sp. nov., and microdontic species, i.e., *H. kimondo* sp. nov., *H. falcatus* sp. nov., *H. curvidens* sp. nov., *H. pardus* sp. nov., *H. quasimodo* sp. nov., and

H. squamipinnis. The macrodontic species differ mostly from the microdontic species by a shallower body [27.2–36.0 (28.6–33.5) vs 29.0–41.7 (30.8–37.4) % SL], a narrower head [36.8–43.7 (39.2–42.0) vs 38.4–48.1 (42.5–45.3) % HL], and more stout jaws set with larger and a smaller number of outer oral teeth [22–47 (median 27–36) vs 39–79 (median 45–58) in the upper jaw]. In piscivorous species from Lake Victoria, the variation in these traits was found to be ecologically relevant (van Oijen 1982; Barel 1983). Species with shallow bodies are generally pursuit hunters, while deep-bodied species are ambush hunters. Species with large and stout teeth are biters and hunt large prey (40–70 mm SL), while species with small teeth are suction feeders that hunt small prey (10–30 mm SL) (van Oijen 1982). Therefore, the morphological distinction between macro- and microdontic piscivores from the Lake Edward system presumably reflects a major ecological separation of the piscivorous species. Macrodontic species might generally be pursuit hunters and biters that hunt large and elusive prey and microdontic species might generally be ambush hunters and suction feeders that hunt small prey. However, within both of these macro- and microdontic piscivores, species show additional morphological traits that suggest further ecological specialisations, as discussed below.

Within the macrodontic piscivores, *H. latifrons* sp. nov. and *H. mentatus* have a very shallow body with a long caudal peduncle and a broad interorbital area. This habitus is similar to that of specialised pursuit hunters in the pelagic waters of Lake Victoria (Barel 1983). These species mainly differ in habitat use: *H. latifrons* sp. nov. has been caught in offshore deep waters and *H. mentatus* has been found in offshore shallow habitats. The remaining four species, *H. rex* sp. nov., *H. simba* sp. nov., *H. glaucus* sp. nov., and *H. aquila* sp. nov. show differences in maximum body size, eye size, and size, stoutness, and curvature of the oral teeth, suggesting that these species also differ in ecology and habitat. *Haplochromis rex* sp. nov. and *H. glaucus* sp. nov. have been caught over sandy substrates, *H. simba* sp. nov. was most abundant over hard substrates, while *H. aquila* sp. nov. was found over muddy substrates. For these four species, the precise catch localities are known for only few specimens (n=5–14), so habitat preferences should be considered with caution.

Within the microdontic piscivores, *H. squamipinnis* and *H. quasimodo* sp. nov. are deep-bodied species with rhomboid-shaped bodies, typical for ambush hunting piscivores (van Oijen 1982). The two species differ mainly in gape inclination. *Haplochromis squamipinnis* probably uses its steep gape to catch prey from below. This could be advantageous over muddy substrates, where small haplochromines seem to stay away from the bottom and inhabit the water column (van Oijen 1981). This hypothesis is supported by its high abundance throughout Lake George, which has almost exclusively muddy substrates. *Haplochromis quasimodo* sp. nov. is a benthic species that occurs over harder substrates. Its gentle gape is probably more effective for catching small haplochromines that also stay in close association with the substrate. The distribution of *H. kimondo* sp. nov. is mostly restricted to sandy substrates. Like *H. kimondo* sp. nov., some sand-dwelling piscivores from Lake Victoria have a decurved head with a gentle gape inclination. This morphology has been hypothesised to be advantageous for ‘digging out’ juvenile haplochromines that take cover in the substrate (van Oijen 1982). *Haplochromis pardus* sp. nov. is characterised by its rather deep body, small size, and mostly dark colour pattern in both sexes. This combination of traits might allow it to ambush small juveniles that seek shelter in the near-shore vegetation.

The remaining two species of microdontic piscivores, *H. falcatus* sp. nov. and *H. curvidens* sp. nov., mostly differ from each other in habitat. While *H. falcatus* sp. nov. is most abundant over sandy substrates, *H. curvidens* sp. nov. inhabits muddy substrates. Morphologically, both species resemble each other in habitus, and both have small and (strongly) recurved outer teeth. This morphology is possibly advantageous in suction feeders that rely on their teeth to ensure that prey is unable to escape the buccal cavity once captured. Notably, both species show a resemblance to the paedophagous *H. paradoxus* (Lippitsch & Kaufman 2003). All three species have an external piscivorous morphology and (strongly)

recurved oral teeth, but the oral teeth of *H. paradoxus* are blunt and almost completely embedded in the oral mucosa (Vranken *et al.* 2019). This difference in trophic morphology presumably reflects their difference in ecology. *Haplochromis paradoxus* feeds on less-mobile eggs and larvae of other species of *Haplochromis* that might be less likely to escape the buccal cavity once captured (Vranken *et al.* 2019). Currently, nothing is known about the relationships between *H. paradoxus* and these piscivorous species.

Small specimens of piscivorous species are known to have opportunistic diets. For example, small specimens of *H. squamipinnis* (< 100 mm SL) from Lake George consume mostly insects and the contribution of fish to their diet increases with size (Moriarty *et al.* 1973). The diet of large specimens (> 200 mm SL) of *H. squamipinnis* may still include a small proportion of insects. From Lake Victoria, some species with a piscivorous morphology are known to include a large proportion of prawns and/or insects into their diets (van Oijen 1982). Adult specimens of these species often have some bi- or tricuspid outer oral teeth. While this tooth shape is absent in all piscivorous species from the Lake Edward system, we cannot exclude that adult specimen of some species might include prawns and/or insects into their diets.

In addition to their trophic morphology, piscivorous species stand out from non-piscivorous species of *Haplochromis* from the Lake Edward system in colour and squamation patterns (Greenwood 1973; Vranken *et al.* 2019, 2020a, 2020b). In colour pattern, nearly all species of *Haplochromis* show a strong sexual dimorphism with dull-coloured females and conspicuously coloured dominant males (Greenwood 1974). Adult females of *H. glaucus* sp. nov., however, have a colour pattern that strongly resembles that of dominant males. In several piscivorous species from Lake Victoria, females also strongly resemble males in live colour pattern, the evolutionary significance of which remains unknown (van Oijen 1991).

Within the Lake Edward system, species of piscivores generally have a larger number of scale rows around the caudal peduncle (16–20 vs 16, very rarely 17) and between the upper lateral line and the first anal spine (11–16 vs 8–12) than non-piscivorous species. *Haplochromis rex* sp. nov. has a larger number of scale rows on the cheeks than other species of *Haplochromis* (4–7 vs 2–5). *Haplochromis squamipinnis* has a smaller number and *H. rex* sp. nov. and *H. glaucus* sp. nov. have a larger number of upper lateral line scales than other species of *Haplochromis* (17–22 and 21–27 vs 19–23, respectively). Similar patterns have been observed in the piscivore from Lake Kivu and some of the piscivores from Lake Victoria. We observed that *H. vittatus* (Boulenger, 1901) (RMCA 1981.055.P.6390 to 91) from Lake Kivu and *H. victorianus* (Pellegrin, 1904) (RMCA 14786); *H. longirostris* (RMCA 1981.030.P.0008); *H. macrognathus* (RMCA 1981.030.P.0010 to 11); *H. argenteus* Regan, 1922 (RMCA 1981.030.P.0003); and *H. cavifrons* Hilgendorf, 1888 (RMCA 14914) from Lake Victoria have many scale rows around the caudal peduncle (16–20) and *H. vittatus* also has many scale rows between the upper lateral line and the first anal-fin spine (12–14). No outstanding squamation or colour patterns were observed in *H. avium* (RMCA 1989.059.P.0295 to 97 and 2002.063.P.0012) from Lake Albert.

Rows of minute scales on the bases of the dorsal and/or anal fins is a rare character that occurs scattered in African cichlids (Lippitsch 1990). Within haplochromine cichlids, it is known to occur in a few non-piscivorous species from Lake Tanganyika, e.g., *Petrochromis macrognathus* Yamaoka, 1983, and from Lake Malawi, e.g., *Protomelas fenestratus* (Trewavas, 1935) and *Melanochromis labrosus* (Trewavas, 1935) (Yamaoka 1983; Lippitsch 1990). We also observed scaled dorsal and anal fins in *H. desfontainii* (Lacepède, 1802) (RMCA 172456 to 0457, 1984.047.P.0031 to 0036), a riverine species from Algeria and Tunisia with a generalised morphology that belongs to a sister clade of the LVRS (Meier *et al.* 2017). Within the LVRS, scaled dorsal and anal fins are only known to occur in some piscivorous species, i.e., *H. squamipinnis* and *H. quasimodo* sp. nov. from the Lake Edward system and *H. howesi* van Oijen, 1992 and an undescribed species (i.e., *H.* sp. ‘orange rock hunter’ sensu Seehausen 1996)

from Lake Victoria (van Oijen 1992; Seehausen 1996). It was proposed that scaled dorsal and anal fins evolved de novo and allowed the fish to swim more efficiently or protect the fin membrane from damage (van Oijen 1992). The occurrence of this trait, however, is very scattered and closely related species with similar behaviours, habitats, and diets lack this trait. Therefore, the functional relevance of this trait seems ambiguous. Recent genomic insights support that the morphological diversity within the LVRS evolved through the segregation of existing ancestral genomic variation (McGee *et al.* 2020). Therefore, within the LVRS, the genetic basis of scaled dorsal and anal fins may be linked to genomic variation associated with a piscivorous morphology.

Greenwood (1980) proposed a classification in which most piscivorous species of *Haplochromis* were placed into two genera: ‘*Harpagochromis*’ and ‘*Prognathochromis*’. These genera were distinguished from each other based on the shallower neurocranium with a shallower supraoccipital crest in the latter genus. However, van Oijen (1991) demonstrated that there is a considerable overlap between both nominal genera. Following Greenwood’s methodology, van Oijen (1991) noticed that his measurements showed deviations from those of Greenwood (1980). Likewise, our measurements of the neurocranium of *H. squamipinnis* deviated from those of both authors, most likely due to a difference in methodology as measurements were taken from radiographs instead of dry skeletal material. Therefore, the neurocranium shape was only compared qualitatively to the genera definitions of ‘*Harpagochromis*’ and ‘*Prognathochromis*’ sensu Greenwood (1980). *Haplochromis latifrons* sp. nov., *H. mentatus*, *H. rex* sp. nov., *H. simba* sp. nov., *H. glaucus* sp. nov., *H. falcatus* sp. nov., and *H. curvidens* sp. nov. have a relatively shallow to very shallow neurocranium with a relatively shallow or shallow supraoccipital crest, hereby corresponding to a ‘*Prognathochromis*’ morphology. The first five of these species deviate from a ‘*Prognathochromis*’ morphology by having a smaller number of outer upper jaw teeth [22–47 (median range 27–36) vs 34–90 (modal range 50–74)]. Additionally, *H. rex* sp. nov. deviates further from a ‘*Prognathochromis*’ morphology by having a larger number of infraorbital cheek scales (4–7 vs 2–6), and *H. rex* sp. nov. and *H. glaucus* sp. nov. by having a larger number of longitudinal line scales (34–38 vs 30–35). *Haplochromis pardus* sp. nov. corresponds to a ‘*Prognathochromis*’ morphology in all traits, except for its generalised instead of shallow neurocranium. *Haplochromis aquila* sp. nov., *H. kimondo* sp. nov., and *H. quasimodo* sp. nov. have a generalised neurocranium, as is characteristic for ‘*Harpagochromis*’, but deviate from the genus’ definition by having a larger number of longitudinal line scales (31–36 vs 30–34). The former two species deviate further from ‘*Harpagochromis*’ by their shallow supraoccipital crest and *H. aquila* sp. nov. by its larger eye [30.5–31.5 (30.6) vs 17–29 (20–24) % HL]. *Haplochromis squamipinnis* corresponds to a ‘*Harpagochromis*’ morphology. In view of the above, it is clear that the distinction between ‘*Harpagochromis*’ and ‘*Prognathochromis*’ as proposed by Greenwood (1980) does not hold for the piscivorous species from the Lake Edward system. We also evaluated how the division in macro- and microdontic species relates to Greenwood’s classification. Small-sized microdontic species (< 140 mm SL; i.e., *H. falcatus* sp. nov., *H. curvidens* sp. nov., and *H. pardus* sp. nov.) and nearly all macrodontic species correspond most to a ‘*Prognathochromis*’ morphology. Large-sized microdontic species (> 140 mm SL; i.e., *H. kimondo* sp. nov., *H. quasimodo* sp. nov., and *H. squamipinnis*) and the macrodontic *H. aquila* sp. nov. correspond most to a ‘*Harpagochromis*’ morphology.

The evolutionary history of the LVRS remains largely unknown. Its fast adaptive radiation coincides with a high degree of hybridisation, incomplete lineage sorting, and morphological convergence in a strongly fluctuating palaeohydrological setting (Verheyen *et al.* 2003; Meier *et al.* 2017, 2019; McGee *et al.* 2020). Collectively, these patterns hamper the induction of evolutionary relationships from both genomic and morphological traits. Nevertheless, hypotheses can be made. Counts seem more evolutionary stable than measurements between closely related species of haplochromine cichlids (Van Steenberge *et al.* 2018). This suggests that the piscivorous species of *Haplochromis*, which show a

relatively large variation in squamation patterns, could have relatively basal positions in the radiation(s) of the LVRS. Similarly, within the cichlid species flocks of both Lakes Malawi and Tanganyika, basal lineages are to a large part made up of piscivores (Malinsky *et al.* 2018; Ronco *et al.* 2021). Our results may contribute to a better understanding of how the LVRS evolved. The exact relationships between the different assemblages of the LVRS remain unknown, but that of the Lake Edward system seems to have a relatively basal position (Meier *et al.* 2017). Further research is necessary to investigate the degree of ecological specialisation and the complex evolutionary relationships of the species of *Haplochromis* with a piscivorous morphology from the Lake Edward system and the LVRS as a whole.

Acknowledgements

This research was conducted within the framework of the BELSPO (Belgian Science Policy) funded BRAIN project “HIPE”: Human impacts on ecosystem health and resources of Lake Edward and an FWO (Research Foundation Flanders) funded PhD fellowship (11E0520N). The fieldwork by NV, MVS, and ED was supported by the FWO and fieldwork by MVS by the King Leopold III Fund for Nature Exploration and Conservation. We thank M. Mbalassa (Université Officielle de Bukavu, DRC), L. Wasswa (Ugandan Fisheries Department), M. Bifamengo (NaFIRRI, Uganda) for their help in collecting specimens, and W. Okello (NaFIRRI, Uganda) for valuable logistic support. We are grateful to M. Parrent (RMCA) and O. Pauwels (IRSNB) for curatorial services and J. Maclaine (NHM) and K.E. Hartel (MCZ) for the loan of the holotypes of *H. squamipinnis* and *H. mentatus*, respectively. Pictures of the lower pharyngeal bones were taken using the digitisation facility of the RMCA in the framework of the BELSPO-funded DIGIT04 project.

References

- Barel C.D.N. 1983. Towards a constructional morphology of cichlid fishes (Teleostei, Perciformes). *Netherlands Journal of Zoology* 33: 357–424. <https://doi.org/10.1163/002829683X00183>
- Barel C.D.N., Witte F. & van Oijen M.J.P. 1976. The shape of the skeletal elements in the head of a generalized *Haplochromis* species: *H. elegans* Trewavas 1933 (Pisces, Cichlidae). *Netherlands Journal of Zoology* 26: 163–265. <https://doi.org/10.1163/002829676X00019>
- Barel C.D.N., van Oijen M.J.P., Witte F. & Witte-Maas E.L.M. 1977. An introduction to the taxonomy and morphology of the haplochromine Cichlidae from Lake Victoria. *Netherlands Journal of Zoology* 27: 333–380.
- de Zeeuw M.P., Westbroek I., van Oijen M.J.P. & Witte F. 2012. Two new species of zooplanktivorous haplochromine cichlids from Lake Victoria, Tanzania. *ZooKeys* 256: 1–34. <https://doi.org/10.3897/zookeys.256.3871>
- Decru E., Vranken N., Bragança P.H.N., Snoeks J. & Van Steenberge M. 2020. Where ichthyofaunal provinces meet: the fish fauna of the Lake Edward system, East Africa. *Journal of Fish Biology* 96: 1186–1201. <https://doi.org/10.1111/jfb.13992>
- Fernald R.D. 2017. Cognitive skills and the evolution of social systems. *The Journal of Experimental Biology* 220: 103–113. <https://doi.org/10.1242/jeb.142430>
- Fryer G. & Iles T.D. 1972. *The Cichlid Fishes of the Great Lakes of Africa. Their Biology and Evolution*. Oliver and Boyd, Edinburgh.
- Genner M.J., Seehausen O., Lunt D.H., Joyce D.A., Shaw P.W., Carvalho G.R. & Turner G.F. 2007. Age of cichlids: new dates for ancient lake fish radiations. *Molecular Biology and Evolution* 24: 1269–1282. <https://doi.org/10.1093/molbev/msm050>

- Greenwood P.H. 1962. A revision of the Lake Victoria *Haplochromis* species (Pisces, Cichlidae), part V. *Bulletin of the British Museum (Natural History) Zoology* 9: 139–214. <https://doi.org/10.5962/bhl.part.16340>
- Greenwood P.H. 1973. A revision of the *Haplochromis* and related species (Pisces: Cichlidae) from Lake George, Uganda. *Bulletin of the British Museum (Natural History) Zoology* 25: 139–242.
- Greenwood P.H. 1974. The cichlid fishes of Lake Victoria, East Africa: the biology and evolution of a species flock. *Bulletin of the British Museum (Natural History) Zoology Supplement* 6: 134. <https://doi.org/10.5962/p.119071>
- Greenwood P.H. 1979. Towards a phyletic classification of the ‘genus’ *Haplochromis* (Pisces, Cichlidae) and related taxa. Part I. *Bulletin of the British Museum (Natural History) Zoology* 35: 265–322. <https://doi.org/10.5962/bhl.part.20455>
- Greenwood P.H. 1980. Towards a phyletic classification of the ‘genus’ *Haplochromis* (Pisces, Cichlidae) and related taxa. Part II. *Bulletin of the British Museum (Natural History) Zoology* 39: 1–101. <https://doi.org/10.5962/bhl.part.13268>
- Greenwood P.H. 1991. Speciation. In: Keenleyside M.H. (ed.) *Cichlid Fishes: Behaviour, Ecology and Evolution*. Fish & Fisheries Series: 86–102. Springer Netherlands.
- Hammer Ø., Harper D.A.T. & Ryan P.D. 2001. PAST: paleontological statistics software package for education and data analysis. *Palaeontologia Electronica* 4: 9.
- Hilgendorf F.M. 1888. Fische aus dem Victoria-Nyanza (Ukerewe-See), gesammelt von dem verstorbenen Dr G.A. Fischer. *Sitzungsberichte der Gesellschaft Naturforschender Freunde zu Berlin* 1888: 75–79.
- Hoogerhoud R.J.C. 1984. A taxonomic reconsideration of the haplochromine genera *Gaurochromis* Greenwood, 1980 and *Labrochromis* Regan, 1920 (Pisces, Cichlidae). *Netherlands Journal of Zoology* 34: 539–565. <https://doi.org/10.1163/002829684X00281>
- Hulot A. 1956. Aperçu sur la question de la pêche industrielle aux lacs Kivu, Edouard et Albert. *Bulletin agricole du Congo Belge* 47: 1–68.
- Lehman J.T. 2002. Application of AVHRR to water balance, mixing dynamics, and water chemistry of Lake Edward, East Africa. In: Odada E.O. & Olago D.O. (eds) *The East African Great Lakes: Limnology, Palaeolimnology, Biodiversity*: 235–260. Kluwer Academic Publishers, Netherlands.
- Lippitsch E. 1990. Scale morphology and squamation patterns in cichlids (Teleostei, Perciformes): a comparative study. *Journal of Fish Biology* 37: 265–291. <https://doi.org/10.1111/j.1095-8649.1990.tb05858.x>
- Lippitsch E. & Kaufman L. 2003. *Pyxichromis paradoxus* (Perciformes: Cichlidae), a new haplochromine species from Lake Edward, East Africa, and reassessment of the genus *Pyxichromis* Greenwood, 1980. *Zeitschrift für Fischkunde* 6: 87–98.
- Malinsky M., Svardal H., Tyers A.M., Miska E.A., Genner M.J., Turner G.F. & Durbin R. 2018. Whole-genome sequences of Malawi cichlids reveal multiple radiations interconnected by gene flow. *Nature Ecology & Evolution* 2: 1940–1955. <https://doi.org/10.1038/s41559-018-0717-x>
- McGee M.D., Borstein S.R., Meier J.I., Marques D.A., Mwaiko S., Taabu A., Kische-Machumu M.A., O’Meara B., Bruggmann R., Excoffier L. & Seehausen O. 2020. The ecological and genomic basis of explosive adaptive radiation. *Nature* 586: 75–79. <https://doi.org/10.1038/s41586-020-2652-7>
- Meier J.I., Marques D.A., Mwaiko S., Wagner C.E., Excoffier L. & Seehausen O. 2017. Ancient hybridization fuels rapid cichlid fish adaptive radiations. *Nature Communications* 8: 14363.

<https://doi.org/10.1038/ncomms14363>

Meier J.I., Stelkens R.B., Joyce D.A., Mwaiko S., Phiri N., Schlieven U.K., Selz O.M., Wagner C.E., Katongo C. & Seehausen O. 2019. The coincidence of ecological opportunity with hybridization explains rapid adaptive radiation in Lake Mweru cichlid fishes. *Nature Communications* 10: 5391.

<https://doi.org/10.1038/s41467-019-13278-z>

Moreau J., Christensen V. & Pauly D. 1993. A trophic ecosystem model of Lake George, Uganda. In: Christensen V. & Pauly D. (eds) *Trophic Models of Aquatic Ecosystems. ICLARM Conference Proceedings* 26: 124–129.

Moriarty D.J.W., Darlington J.P.E.C., Dunn I.G., Moriarty C.M. & Tevlin M.P. 1973. Feeding and grazing in Lake George, Uganda. *Proceedings of the Royal Society B: Biological Sciences* 184: 299–319.

van Oijen M.J.P. 1982. Ecological differentiation among the piscivorous haplochromine cichlids of Lake Victoria (East Africa). *Netherlands Journal of Zoology* 32: 336–363.

<https://doi.org/10.1163/002829681X00374>

van Oijen M.J.P. 1991. A systematic revision of the piscivorous haplochromine Cichlidae (Pisces, Teleostei) of Lake Victoria (East Africa). Part I. *Zoologische Verhandelingen* 272: 1–95.

van Oijen M.J.P. 1992. *Haplochromis howesi* spec. nov., a crab and fish eating cichlid from Lake Victoria. *Zoologische Mededelingen* 66: 561–579.

van Oijen M.J.P. 1996. The generic classification of the haplochromine cichlids of Lake Victoria, East Africa. *Zoologische Verhandelingen* 302: 57–110.

van Oijen M.J.P., Witte F. & Witte-Maas E.L.M. 1981. An introduction to ecological and taxonomic investigations on the haplochromine cichlids from the Mwanza Gulf of Lake Victoria. *Netherlands Journal of Zoology* 31: 149–174.

Poll M. 1939. Poissons. In: *Exploration du Parc National Albert Mission H. Damas (1935-1936)*: 1–73. Institut des Parcs Nationaux du Congo Belge, Bruxelles.

Rasband W.S. 2018. ImageJ. ver.1.52a. National Institutes of Health, Bethesda, Maryland, USA.

Regan C.T. 1921. The Cichlid fishes of Lakes Albert Edward and Kivu. *Annals and Magazine of Natural History* Series 9: 632–639. <https://doi.org/10.1080/00222932108632633>

Regan C.T. 1925. Three new cichlid fishes of the genus *Haplochromis* from Lake Edward, Central Africa. *Occasional Papers of the Boston Society of Natural History* 5: 187–188.

Rice W.R. 1989. Analyzing tables of statistical tests. *Evolution* 43: 223–225.

<https://doi.org/10.1111/j.1558-5646.1989.tb04220.x>

Ronco F., Büscher H.H., Indermaur A. & Salzburger W. 2020. The taxonomic diversity of the cichlid fish fauna of ancient Lake Tanganyika, East Africa. *Journal of Great Lakes Research* 46: 1067–1078. <https://doi.org/10.1016/j.jglr.2019.05.009>

Ronco F., Matschiner M., Böhne A., Boila A., Büscher H.H., Indermaur A., El Taher A., Malinsky M., Ricci V., Kahmen A., Jentoft S. & Salzburger W. 2021. Drivers and dynamics of a massive adaptive radiation in African cichlid fish. *Nature* 589: 76–81. <https://doi.org/10.1038/s41586-020-2930-4>

Salzburger W. 2018. Understanding explosive diversification through cichlid fish genomics. *Nature Reviews Genetics* 19: 705–717. <https://doi.org/10.1038/s41576-018-0043-9>

Schraml E. 2004. Die artenvielfalt der fische in Ugandas gewässern: beiträge zur kenntnis der fischfauna Ugandas. *DCG-Informationen Sonderheft* 3: 2–48.

- Seehausen O. 1996. *Lake Victoria Rock Cichlids: Taxonomy, Ecology, and Distribution*. Verduyn Cichlids, Rotterdam.
- Snoeks J. 1994. *The Haplochromine Fishes (Teleostei, Cichlidae) of Lake Kivu, East Africa: a Taxonomic Revision with Notes on their Ecology*. Royal Museum for Central Africa, Tervuren.
- Svardal H., Salzburger W. & Malinsky M. 2021. Genetic variation and hybridization in evolutionary radiations of cichlid fishes. *Annual reviews* 9: 55–79.
<https://doi.org/10.1146/annurev-animal-061220-023129>
- Van Steenberge M., Raeymaekers J.A.M., Hablützel P.I., Vanhove M.P.M., Koblmüller S. & Snoeks J. 2018. Delineating species along shifting shorelines: *Tropheus* (Teleostei, Cichlidae) from the southern subbasin of Lake Tanganyika. *Frontiers in Zoology* 15: 42. <https://doi.org/10.1186/s12983-018-0287-4>
- Trewavas E. 1933. Scientific results of the Cambridge expedition to the East African Lakes, 1930–1. The cichlid fishes. *Zoological Journal of the Linnean Society* 38: 309–341.
<https://doi.org/10.1111/j.1096-3642.1933.tb00062.x>
- Trewavas E. 1938. Lake Albert fishes of the genus *Haplochromis*. *Annals and Magazine of Natural History* 1: 435–449. <https://doi.org/10.1080/00222933808526788>
- Verheyen E., Salzburger W., Snoeks J. & Meyer A. 2003. Origin of the superflock of cichlid fishes from Lake Victoria, East Africa. *Science* 300: 325–329. <https://doi.org/10.1126/science.1080699>
- Vranken N., Van Steenberge M. & Snoeks J. 2019. Grasping ecological opportunities: not one but five paedophagous species of *Haplochromis* (Teleostei: Cichlidae) in the Lake Edward system. *Hydrobiologia* 832: 105–134. <https://doi.org/10.1007/s10750-018-3742-5>
- Vranken N., Van Steenberge M. & Snoeks J. 2020a. Similar ecology, different morphology: three new species of oral-mollusc shellers from Lake Edward. *Journal of Fish Biology* 96: 1202–1217.
<https://doi.org/10.1111/jfb.14107>
- Vranken N., Van Steenberge M., Kayenbergh A. & Snoeks J. 2020b. The lobed-lipped species of *Haplochromis* (Teleostei, Cichlidae) from Lake Edward, two instead of one. *Journal of Great Lakes Research* 46: 1079–1089. <https://doi.org/10.1016/j.jglr.2019.05.005>
- Vranken N., Van Steenberge M., Balagizi A. & Snoeks J. 2020c. The synonymy of *Haplochromis pharyngalis* and *Haplochromis petronius* (Cichlidae). *Journal of Fish Biology* 97: 1554–1559.
<https://doi.org/10.1111/jfb.14455>
- Wagner C.E., Keller I., Wittwer S., Selz O.M., Mwaiko S., Greuter L., Sivasundar A. & Seehausen O. 2013. Genome-wide RAD sequence data provide unprecedented resolution of species boundaries and relationships in the Lake Victoria cichlid adaptive radiation. *Molecular Ecology* 22: 787–798.
<https://doi.org/10.1111/mec.12023>
- Witte F. & van Oijen M.J.P. 1990. Taxonomy, ecology and fishery of Lake Victoria haplochromine trophic groups. *Zoologische Verhandelingen* 262: 1–47.
- Witte F. & Witte-Maas E.L.M. 1987. Implications for taxonomy and morphology of intra-specific variation in haplochromine cichlids of Lake Victoria. With descriptions of five zooplanktivorous species. In: Witte F. (ed.) *From Form to Fishery*. PhD thesis, Rijksuniversiteit, Leiden.
- Witte F., Seehausen O., Wanink J.H., Kische-Machumu M.A., Rensing M. & Goldschmidt T. 2013. Cichlid species diversity in naturally and anthropogenically turbid habitats of Lake Victoria, East Africa. *Aquatic Sciences* 75: 169–183. <https://doi.org/10.1007/s00027-012-0265-4>
- Yamaoka K. 1983. A revision of the cichlid fish genus *Petrochromis* from Lake Tanganyika, with description of a new species. *Japanese Journal of Ichthyology* 30: 129–141.

Zelditch M.L., Swiderski D.L., Sheets H.D. & Fink W.L. 2004. *Geometric Morphometrics for Biologists: a Primer*. Elsevier Academic Press, London.

Manuscript received: 14 December 2020

Manuscript accepted: 9 January 2022

Published on: 21 April 2022

Topic editors: Rudy Jocqué. Fabio Cianferoni

Section editor: Felipe Polivanov

Desk editor: Marianne Salaiün

Printed versions of all papers are also deposited in the libraries of the institutes that are members of the *EJT* consortium: Muséum national d'histoire naturelle, Paris, France; Meise Botanic Garden, Belgium; Royal Museum for Central Africa, Tervuren, Belgium; Royal Belgian Institute of Natural Sciences, Brussels, Belgium; Natural History Museum of Denmark, Copenhagen, Denmark; Naturalis Biodiversity Center, Leiden, the Netherlands; Museo Nacional de Ciencias Naturales-CSIC, Madrid, Spain; Real Jardín Botánico de Madrid CSIC, Spain; Zoological Research Museum Alexander Koenig, Bonn, Germany; National Museum, Prague, Czech Republic.

Appendices

Table S1. PCA loadings of 21 log-transformed measurements from: *H. latifrons* sp. nov., *H. mentatus*, *H. rex* sp. nov., *H. simba* sp. nov., *H. glaucus* sp. nov., *H. aquila* sp. nov., *H. kimondo* sp. nov., *H. falcatus* sp. nov., *H. curvidens* sp. nov., *H. pardus* sp. nov., *H. quasimodo* sp. nov., and *H. squamipinnis*. Results illustrated in Fig. 3a. Abbreviations: SL = standard length; HL = head length; BD = body depth; PrD = predorsal distance; PrA = preanal distance; PrP = prepectoral distance; PrV = prepelvic distance; DFB = dorsal fin base length; AFB = anal fin base length; CPL = caudal peduncle length; CPD = caudal peduncle depth; HW = head width; ED = eye diameter; IOW = interorbital width; SnL = snout length; LaD = lachrymal depth; ChD = cheek depth; PPL = premaxillary pedicel length; UJL = upper jaw length; LJL = lower jaw length; LJW = lower jaw width.

	PC 1	PC 2	PC 3	PC 4
% variance	96.25	1.10	0.67	0.49
Log(SL)	0.20	0.01	0.19	-0.03
Log(HL)	0.20	0.03	-0.07	-0.06
Log(BD)	0.23	-0.42	0.16	0.01
Log(PrD)	0.20	-0.03	-0.13	-0.04
Log(PrA)	0.20	0.11	0.15	-0.10
Log(PrP)	0.20	0.05	-0.02	-0.12
Log(PrV)	0.21	0.03	0.12	-0.18
Log(DFB)	0.20	-0.14	0.22	0.03
Log(AFB)	0.20	-0.48	0.24	-0.18
Log(CPL)	0.20	0.21	0.55	0.16
Log(CPD)	0.20	-0.24	0.09	-0.02
Log(HW)	0.21	-0.18	-0.12	0.38
Log(ED)	0.14	-0.28	-0.24	0.20
Log(IOW)	0.24	0.35	0.19	0.62
Log(SnL)	0.24	0.27	-0.02	-0.08
Log(LaD)	0.25	0.27	0.02	-0.33
Log(ChD)	0.28	0.22	-0.27	-0.30
Log(PPL)	0.20	-0.13	-0.09	0.04
Log(UJL)	0.25	0.03	-0.20	-0.08
Log(LJL)	0.23	0.02	-0.08	-0.13
Log(LJW)	0.26	0.00	-0.48	0.29

Table S2. PCA loadings of 21 log-transformed measurements from: *H. mentatus*, *H. kimondo* sp. nov., *H. rex* sp. nov., *H. simba* sp. nov., and *H. glaucus* sp. nov. Results illustrated in Fig. 3b. Abbreviations: SL = standard length; HL = head length; BD = body depth; PrD = predorsal distance; PrA = preanal distance; PrP = prepectoral distance; PrV = prepelvic distance; DFB = dorsal fin base length; AFB = anal fin base length; CPL = caudal peduncle length; CPD = caudal peduncle depth; HW = head width; ED = eye diameter; IOW = interorbital width; SnL = snout length; LaD = lachrymal depth; ChD = cheek depth; PPL = premaxillary pedicel length; UJL = upper jaw length; LJL = lower jaw length; LJW = lower jaw width.

	PC 1	PC 2	PC 3
% variance	95.68	1.36	1.13
Log(SL)	0.20	0.14	0.09
Log(HL)	0.20	0.05	-0.08
Log(BD)	0.22	0.00	0.08
Log(PrD)	0.21	-0.01	-0.12
Log(PrA)	0.20	0.21	0.05
Log(PrP)	0.20	0.12	-0.10
Log(PrV)	0.20	0.29	0.00
Log(DFB)	0.21	0.07	0.17
Log(AFB)	0.21	0.28	0.05
Log(CPL)	0.17	0.24	0.49
Log(CPD)	0.20	0.08	0.02
Log(HW)	0.22	-0.36	0.10
Log(ED)	0.15	-0.27	0.02
Log(IOW)	0.22	-0.42	0.59
Log(SnL)	0.25	0.10	0.02
Log(LaD)	0.25	0.24	-0.15
Log(ChD)	0.28	-0.11	-0.43
Log(PPL)	0.21	-0.11	0.07
Log(UJL)	0.24	-0.04	-0.17
Log(LJL)	0.23	0.13	-0.05
Log(LJW)	0.28	-0.46	-0.29

Table S3. PCA loadings of 21 log-transformed measurements from: *H. rex* sp. nov., *H. simba* sp. nov., and *H. glaucus* sp. nov. Results illustrated in Fig. 3c. Abbreviations: SL = standard length; HL = head length; BD = body depth; PrD = predorsal distance; PrA = preanal distance; PrP = prepectoral distance; PrV = prepelvic distance; DFB = dorsal fin base length; AFB = anal fin base length; CPL = caudal peduncle length; CPD = caudal peduncle depth; HW = head width; ED = eye diameter; IOW = interorbital width; SnL = snout length; LaD = lachrymal depth; ChD = cheek depth; PPL = premaxillary pedicel length; UJL = upper jaw length; LJL = lower jaw length; LJW = lower jaw width.

	PC 1	PC 2
% variance	97.43	0.71
Log(SL)	0.20	-0.10
Log(HL)	0.21	-0.03
Log(BD)	0.23	0.35
Log(PrD)	0.21	-0.32
Log(PrA)	0.21	-0.05
Log(PrP)	0.20	0.00
Log(PrV)	0.21	0.10
Log(DFB)	0.21	-0.01
Log(AFB)	0.22	-0.05
Log(CPL)	0.18	-0.12
Log(CPD)	0.21	-0.04
Log(HW)	0.21	0.08
Log(ED)	0.13	0.20
Log(IOW)	0.21	0.65
Log(SnL)	0.25	-0.18
Log (LaD)	0.25	-0.20
Log(ChD)	0.26	-0.31
Log(PPL)	0.21	0.15
Log(UJL)	0.22	0.11
Log(LJL)	0.22	0.17
Log(LJW)	0.26	-0.19

Table S4. PCA loadings of 21 log-transformed measurements from: *H. aquila* sp. nov., *H. falcatus* sp. nov., *H. curvidens* sp. nov., and *H. squamipinnis*. Results illustrated in Fig. 3d. Abbreviations: SL = standard length; HL = head length; BD = body depth; PrD = predorsal distance; PrA = preanal distance; PrP = prepectoral distance; PrV = prepelvic distance; DFB = dorsal fin base length; AFB = anal fin base length; CPL = caudal peduncle length; CPD = caudal peduncle depth; HW = head width; ED = eye diameter; IOW = interorbital width; SnL = snout length; LaD = lachrymal depth; ChD = cheek depth; PPL = premaxillary pedicel length; UJL = upper jaw length; LJL = lower jaw length; LJW = lower jaw width.

	PC 1	PC 2
% variance	97.74	0.80
Log(SL)	0.20	0.17
Log(HL)	0.20	-0.10
Log(BD)	0.24	0.27
Log(PrD)	0.19	-0.13
Log(PrA)	0.20	0.12
Log(PrP)	0.20	-0.03
Log(PrV)	0.21	0.04
Log(DFB)	0.21	0.24
Log(AFB)	0.23	0.20
Log(CPL)	0.21	0.34
Log(CPD)	0.21	0.17
Log(HW)	0.22	-0.20
Log(ED)	0.14	-0.25
Log(IOW)	0.23	0.12
Log(SnL)	0.24	-0.16
Log(LaD)	0.24	0.01
Log(ChD)	0.26	0.07
Log(PPL)	0.20	-0.02
Log(UJL)	0.24	-0.13
Log(LJL)	0.23	-0.08
Log(LJW)	0.25	-0.66

Table S5. PCA loadings of 21 log-transformed measurements from: *H. aquila* sp. nov., *H. falcatus* sp. nov., and *H. curvidens* sp. nov.. Results illustrated in Fig. 3e. Abbreviations: SL = standard length; HL = head length; BD = body depth; PrD = predorsal distance; PrA = preanal distance; PrP = prepectoral distance; PrV = prepelvic distance; DFB = dorsal fin base length; AFB = anal fin base length; CPL = caudal peduncle length; CPD = caudal peduncle depth; HW = head width; ED = eye diameter; IOW = interorbital width; SnL = snout length; LaD = lachrymal depth; ChD = cheek depth; PPL = premaxillary pedicel length; UJL = upper jaw length; LJL = lower jaw length; LJW = lower jaw width.

	PC 1	PC 2	PC 3
% variance	94.10	2.63	1.09
Log(SL)	0.19	0.24	-0.01
Log(HL)	0.21	-0.04	0.05
Log(BD)	0.24	0.11	-0.11
Log(PrD)	0.20	-0.11	0.00
Log(PrA)	0.19	0.22	-0.05
Log(PrP)	0.20	0.02	0.00
Log(PrV)	0.21	0.07	-0.10
Log(DFB)	0.20	0.32	0.01
Log(AFB)	0.21	0.12	0.10
Log(CPL)	0.18	0.57	0.08
Log(CPD)	0.20	0.08	0.05
Log(HW)	0.22	0.00	0.25
Log(ED)	0.16	0.04	-0.04
Log(IOW)	0.24	0.21	0.26
Log(SnL)	0.25	-0.25	0.18
Log (LaD)	0.25	-0.16	-0.29
Log(ChD)	0.25	-0.08	-0.77
Log(PPL)	0.20	-0.29	0.18
Log(UJL)	0.24	-0.19	-0.06
Log(LJL)	0.23	-0.24	0.19
Log(LJW)	0.26	-0.31	0.19

Table S6. PCA loadings of 21 log-transformed measurements from: *H. pardus* sp. nov. and *H. quasimodo* sp. nov.. Results illustrated in Fig. 3f. Abbreviations: SL = standard length; HL = head length; BD = body depth; PrD = predorsal distance; PrA = preanal distance; PrP = prepectoral distance; PrV = prepelvic distance; DFB = dorsal fin base length; AFB = anal fin base length; CPL = caudal peduncle length; CPD = caudal peduncle depth; HW = head width; ED = eye diameter; IOW = interorbital width; SnL = snout length; LaD = lachrymal depth; ChD = cheek depth; PPL = premaxillary pedicel length; UJL = upper jaw length; LJL = lower jaw length; LJW = lower jaw width.

	PC 1	PC 2
% variance	98.15	0.46
Log(SL)	0.19	0.06
Log(HL)	0.20	0.13
Log(BD)	0.26	-0.34
Log(PrD)	0.20	-0.04
Log(PrA)	0.20	-0.12
Log(PrP)	0.20	0.20
Log(PrV)	0.21	0.18
Log(DFB)	0.21	0.10
Log(AFB)	0.19	0.33
Log(CPL)	0.20	-0.37
Log(CPD)	0.21	-0.05
Log(HW)	0.22	-0.06
Log(ED)	0.15	0.36
Log(IOW)	0.23	0.02
Log(SnL)	0.22	0.25
Log (LaD)	0.24	0.10
Log(ChD)	0.28	-0.46
Log(PPL)	0.20	0.24
Log(UJL)	0.24	0.03
Log(LJL)	0.22	0.05
Log(LJW)	0.27	-0.21

Table S7. PCA loadings of 21 counts from: *H. latifrons* sp. nov., *H. mentatus*, *H. rex* sp. nov., *H. simba* sp. nov., *H. glaucus* sp. nov., *H. aquila* sp. nov., *H. kimondo* sp. nov., *H. falcatus* sp. nov., *H. curvidens* sp. nov., *H. pardus* sp. nov., *H. quasimodo* sp. nov., and *H. squamipinnis*. Results illustrated in Fig. 4. Abbreviations: UOT = upper outer teeth; LOT = lower outer teeth; UTR = upper inner tooth rows ; LTR = lower inner tooth rows; GRc = ceratobranchial gill rakers; GRe = epibranchial gill rakers; DFRs = dorsal fin spines; DFRr = dorsal fin branched rays; AFRr = anal fin branched rays; PFR = pectoral fin branched rays; Va = abdominal vertebrae; Vc = caudal vertebrae; LongL = longitudinal line scales; LatLu = upper lateral line scales; LatLl = lower lateral line scales; D-ULL = upper transverse line scales; ULL-A = lower transverse line scales; CPS = caudal peduncle scales; P-V = scales between pectoral and pelvic fins; ChSi = infraorbital cheek scales; ChSp = postorbital cheek scales.

	PC 1	PC 2
% variance	19.42	11.73
UOT	-0.23	0.46
LOT	-0.21	0.44
UTR	-0.05	0.28
LTR	0.00	0.33
GRc	0.17	0.04
GRe	0.01	-0.04
DFRs	-0.15	0.00
DFRr	0.21	-0.02
AFRr	-0.06	0.21
PFR	0.06	0.29
Va	0.20	-0.23
Vc	-0.11	-0.07
LongL	0.36	-0.05
LatLu	0.31	0.00
LatLl	0.01	0.19
D-ULL	0.27	0.29
ULL-A	0.33	0.18
CPS	0.28	0.20
P-V	0.31	0.07
ChSi	0.30	0.06
ChSp	0.25	0.10

Table S8. (continued on the next three pages) Inter-species pairwise comparisons of the species of *Haplochromis* from the Lake Edward system with a piscivorous morphology by means of Mann-Whitney *U* tests. Each pairwise test was performed on subsets of specimens of a similar length class [MWU (SL): $P > 0.5$]. Sequential Bonferroni corrections for multiple tests were performed on each inter-species pair separately for measurements and counts separately. Raw p-values are shown and significance after sequential Bonferroni correction is indicated: $P < 0.1$ +, $P < 0.05$ *, $P < 0.01$ **, $P < 0.001$ ***. Abbreviations: LAT = *H. latifrons* sp. nov.; MEN = *H. mentatus*; REX = *H. rex* sp. nov.; SIM = *H. simba* sp. nov.; GL = *H. glaucus* sp. nov.; AQ = *H. aquila* sp. nov.; KIM = *H. kimondo* sp. nov.; FAL = *H. falcatus* sp. nov.; CUR = *H. curvidens* sp. nov.; PAR = *H. pardus* sp. nov.; QUA = *H. quasimodo* sp. nov.; SQP = *H. squamipinnis*.

Abbr. (n) vs abbr. (n)	SIM (10) vs REX (6)	GL (10) vs REX (11)	GL (8) vs SIM (9)	AQ (8) vs GL (11)	GL (11) vs MEN (20)	LAT (8) vs MEN (17)	AQ (7) vs SIM (10)
SL (mm)	81–128	93–158	90–111	84–158	87–158	75–158	84–118
SL	0.551	0.549	0.665	0.773	0.757	0.503	0.733
HL % SL	0.255	0.193	0.413	0.107	< 0.001 **	0.793	0.022
BD % SL	0.551	0.007	0.163	0.107	0.018	< 0.001 **	0.223
PrD % SL	0.116	0.001 *	0.002 *	0.003 +	0.007 +	0.040	0.661
PrA % SL	0.045	0.062	0.049	0.029	< 0.001 **	0.284	0.961
PrP % SL	0.957	0.193	0.532	0.063	< 0.001 **	0.749	0.057
PrV % SL	0.551	0.010	0.061	0.063	0.002 *	0.051	0.661
DFB % SL	0.957	0.218	0.665	0.773	0.292	< 0.001 **	0.526
AFB % SL	0.255	0.916	0.470	0.231	0.095	< 0.001 **	0.354
CPL % SL	0.026	0.860	0.312	0.773	< 0.001 ***	0.123	0.010
CPD % CPL	0.003 +	0.699	0.112	0.901	< 0.001 **	0.025	0.004 +
HW % HL	0.003 +	0.149	0.014	0.001 *	0.004 *	0.109	0.057
ED % HL	0.026	0.084	0.268	< 0.001 **	0.853	0.001 *	0.001 *
IOW % HL	0.481	< 0.001 **	0.001 *	0.001 *	0.033	0.001 *	0.354
SnL % HL	0.871	0.193	0.810	0.002 *	0.009 +	0.086	0.003 +
LaD % HL	0.143	0.149	0.361	0.007	0.951	0.171	0.004 +
ChD % HL	0.058	0.012	0.268	0.710	0.002 *	0.398	0.407
PPL % HL	0.045	0.170	0.018	0.076	0.496	0.044	0.107
UJL % HL	0.058	0.149	0.136	0.483	0.018	0.580	0.223
LJL % HL	0.011	0.018	0.532	0.052	0.951	0.067	0.057
LJW % LJL	0.143	0.012	0.962	0.173	0.154	0.010	0.306

Table S8. (continued). Inter-species pairwise comparisons of the species of *Haplochromis* from the Lake Edward system with a piscivorous morphology by means of Mann-Whitney *U* tests. Each pairwise test was performed on subsets of specimens of a similar length class [MWU (SL): $P > 0.5$]. Sequential Bonferroni corrections for multiple tests were performed on each inter-species pair separately for measurements and counts separately. Raw p-values are shown and significance after sequential Bonferroni correction is indicated: $P < 0.1$ +, $P < 0.05$ *, $P < 0.01$ **, $P < 0.001$ ***. Abbreviations: LAT = *H. latifrons*; MEN = *H. mentatus*; REX = *H. rex*; SIM = *H. simba*; GL = *H. glaucus*; AQ = *H. aquila*; KIM = *H. kimondo*; FAL = *H. falcatus*; CUR = *H. curvidens*; PAR = *H. pardus*; QUA = *H. quasimodo*; SQP = *H. squamipinnis*.

Abbr. (n) vs abbr. (n)	SIM (10) vs REX (6)	GL (10) vs REX (11)	GL (8) vs SIM (9)	AQ (8) vs GL (11)	GL (11) vs MEN (20)	LAT (8) vs MEN (17)	AQ (7) vs SIM (10)
SL (mm)	81–128	93–158	90–111	84–158	87–158	75–158	84–118
UOT	0.006 +	0.999	0.036	0.836	0.078	0.209	0.007
LOT	0.512	0.569	0.529	0.319	0.071	0.189	0.657
UTR	0.999	0.340	0.999	0.188	0.057	0.403	0.282
LTR	0.001 *	0.018	0.239	0.116	0.488	0.685	0.013
GRe	0.999	0.387	0.304	0.609	0.341	0.657	0.432
GRe	0.252	0.900	0.543	0.280	0.488	0.062	0.825
DFRs	0.690	0.451	0.785	0.773	0.044	0.075	0.761
DFRr	0.220	0.005	0.237	0.116	0.018	0.018	0.424
AFRr	0.947	0.768	0.809	0.669	0.145	0.002 *	0.825
PFR	0.567	0.716	0.663	0.283	0.176	0.196	0.123
Va	0.613	0.391	0.197	0.999	0.456	0.353	0.140
Vc	0.053	0.928	0.020	0.133	< 0.001 **	0.007	0.073
LongL	0.001 *	0.011	0.290	0.898	0.777	0.896	0.081
LatLu	0.002 *	0.020	0.013	0.666	0.059	0.306	0.046
LatLl	0.567	0.799	0.053	0.091	0.462	0.789	0.001 *
D-ULL	0.002 *	0.027	0.018	0.434	0.136	0.201	0.036
ULL-A	0.001 *	0.004 +	0.174	0.059	0.565	0.830	0.001 *
CPS	0.026	0.215	0.256	0.524	0.006	0.089	0.481
V-P	0.002 *	0.156	0.003 +	0.485	0.004 +	0.011	0.001 *
ChSi	0.186	0.001 *	0.005 +	0.810	0.059	0.013	0.065
ChSp	0.281	0.031	0.486	0.826	0.058	0.042	0.999

Table S8. (continued). Inter-species pairwise comparisons of the species of *Haplochromis* from the Lake Edward system with a piscivorous morphology by means of Mann-Whitney *U* tests. Each pairwise test was performed on subsets of specimens of a similar length class [MWU (SL): $P > 0.5$]. Sequential Bonferroni corrections for multiple tests were performed on each inter-species pair separately for measurements and counts separately. Raw p-values are shown and significance after sequential Bonferroni correction is indicated: $P < 0.1$ +, $P < 0.05$ *, $P < 0.01$ **, $P < 0.001$ ***. Abbreviations: LAT = *H. latifrons*; MEN = *H. mentatus*; REX = *H. rex*; SIM = *H. simba*; GL = *H. glaucus*; AQ = *H. aquila*; KIM = *H. kimondo*; FAL = *H. falcatus*; CUR = *H. curvidens*; PAR = *H. pardus*; QUA = *H. quasimodo*; SQP = *H. squamipinnis*.

Abbr. (n) vs abbr. (n)	PAR (11) vs QUA (9)	FAL (19) vs QUA (20)	FAL (19) vs CUR (7)	MEN (20) vs SQP (16)	FAL (20) vs SQP (12)	PAR (9) vs FAL (9)
SL (mm)	78–105	79–149	75–137	76–177	75–149	75–101
SL	0.621	0.509	0.563	0.622	0.546	0.536
HL % SL	0.999	< 0.001 ***	0.002 *	0.002 *	< 0.001 ***	< 0.001 **
BD % SL	0.002 *	< 0.001 ***	0.001 **	< 0.001 ***	0.025	0.427
PrD % SL	0.001 *	< 0.001 ***	< 0.001 **	< 0.001 ***	< 0.001 ***	< 0.001 **
PrA % SL	0.775	< 0.100	0.355	0.066	0.124	0.018
PrP % SL	0.323	< 0.001 ***	0.001 *	0.003 *	< 0.001 ***	< 0.001 **
PrV % SL	0.171	< 0.001 ***	< 0.001 **	0.987	0.009	0.001 *
DFB % SL	0.348	< 0.001 ***	0.094	0.836	0.251	0.030
AFB % SL	0.020	0.025	0.001 **	< 0.001 ***	0.922	0.002 *
CPL % SL	0.002 *	0.002 *	0.005 *	< 0.001 ***	0.115	0.532
CPD % CPL	0.121	0.003 *	0.001 *	< 0.001 ***	0.521	0.229
HW % HL	0.004 +	< 0.001 ***	0.488	0.166	0.005 +	0.377
ED % HL	0.149	0.407	0.021	0.691	0.070	0.022
IOW % HL	0.068	< 0.001 **	0.165	< 0.001 **	< 0.001 **	0.251
SnL % HL	0.171	< 0.001 **	0.001 **	0.015	0.496	0.133
LaD % HL	0.820	0.095	0.001 *	0.209	< 0.001 **	0.999
ChD % HL	< 0.001 **	0.013 +	< 0.001 **	0.037	0.059	0.001 *
PPL % HL	0.224	0.565	< 0.001 **	< 0.001 ***	0.003 *	0.377
UJL % HL	0.058	0.173	0.001 *	0.001 **	0.471	0.001 *
LJL % HL	0.081	< 0.001 ***	0.003 *	< 0.001 ***	0.011	< 0.001 **
LJW % LJL	0.001 *	< 0.001 **	0.064	< 0.001 **	< 0.001 ***	0.930

Table S8. (continued). Inter-species pairwise comparisons of the species of *Haplochromis* from the Lake Edward system with a piscivorous morphology by means of Mann-Whitney *U* tests. Each pairwise test was performed on subsets of specimens of a similar length class [MWU (SL): $P > 0.5$]. Sequential Bonferroni corrections for multiple tests were performed on each inter-species pair separately for measurements and counts separately. Raw p-values are shown and significance after sequential Bonferroni correction is indicated: $P < 0.1$ +, $P < 0.05$ *, $P < 0.01$ **, $P < 0.001$ ***. Abbreviations: LAT = *H. latifrons*; MEN = *H. mentatus*; REX = *H. rex*; SIM = *H. simba*; GL = *H. glaucus*; AQ = *H. aquila*; KIM = *H. kimondo*; FAL = *H. falcatus*; CUR = *H. curvidens*; PAR = *H. pardus*; QUA = *H. quasimodo*; SQP = *H. squamipinnis*.

Abbr. (n) vs abbr. (n)	PAR (11) vs QUA (9)	FAL (19) vs QUA (20)	FAL (19) vs CUR (7)	MEN (20) vs SQP (16)	FAL (20) vs SQP (12)	PAR (9) vs FAL (9)
SL (mm)	78–105	79–149	75–137	76–177	75–149	75–101
UOT	0.381	< 0.001 ***	0.017	< 0.001 ***	0.005 +	0.012
LOT	0.168	< 0.001 ***	0.542	< 0.001 ***	0.292	0.075
UTR	0.087	0.979	0.835	0.005 +	0.115	0.196
LTR	< 0.001 **	0.405	0.132	0.058	0.283	0.076
GRc	0.370	0.025	0.899	0.140	0.983	0.999
GRe	0.999	0.208	0.498	0.058	0.765	0.022
DFRs	0.841	< 0.001 ***	0.025	0.001 *	0.326	0.001 *
DFRr	0.736	0.128	0.132	0.003 *	0.257	0.842
AFRr	0.354	0.705	0.158	0.005 +	0.483	0.426
PFR	0.036	0.855	0.810	0.368	0.007	0.175
Va	0.693	< 0.001 **	0.001 *	< 0.001 ***	0.298	0.076
Vc	0.840	0.108	0.388	< 0.001 **	0.600	0.195
LongL	0.568	0.023	0.407	< 0.001 **	0.230	0.291
LatLu	0.444	0.034	0.089	0.002 *	0.013	0.378
LatLl	0.305	0.509	0.007	0.005 +	0.119	0.337
D-ULL	0.343	0.898	0.324	0.014	< 0.001 **	0.258
ULL-A	0.318	0.093	0.001 *	0.287	0.099	0.002 *
CPS	< 0.001 **	0.768	0.001 *	0.009 +	0.901	< 0.001 **
V-P	0.054	0.230	0.009	< 0.001 ***	< 0.001 ***	0.797
ChSi	0.001 *	0.289	0.085	0.871	0.175	0.001 *
ChSp	0.148	0.457	0.779	0.428	0.004 +	0.044